Government of **Western Australia**
Department of **Mines and Petroleum**

RECORD 2015/4

TECTONITE TYPE: THEIR FORMATION AND SIGNIFICANCE, MAP PRODUCTION, FIELD RELATIONSHIPS AND PETROGRAPHY

by
AE Tomkins

Geological Survey
of Western Australia

MACQUARIE
University
SYDNEY·AUSTRALIA

Government of **Western Australia**
Department of **Mines and Petroleum**

Record 2015/4

TECTONITE TYPE: THEIR FORMATION AND SIGNIFICANCE, MAP PRODUCTION, FIELD RELATIONSHIPS AND PETROGRAPHY

by
AE Tomkins

Perth 2015

Geological Survey of Western Australia

MINISTER FOR MINES AND PETROLEUM
Hon. Bill Marmion MLA

DIRECTOR GENERAL, DEPARTMENT OF MINES AND PETROLEUM
Richard Sellers

EXECUTIVE DIRECTOR, GEOLOGICAL SURVEY OF WESTERN AUSTRALIA
Rick Rogerson

REFERENCE
The recommended reference for this publication is:
Tomkins, AE 2015, Tectonite type: their formation and significance, map production, field relationships and petrography: Geological Survey of Western Australia, Record 2015/4, 113p.

National Library of Australia Card Number and ISBN 978-1-74168-619-7

About this publication
This Record is a Master's thesis researched, written and compiled as part of an ongoing collaborative project between the Geological Survey of Western Australia (GSWA) and Macquarie University, Sydney. Although GSWA has provided field support for this project, the scientific content of the Record, and the drafting of figures, was the responsibility of the author. No editing has been undertaken by GSWA.

Published 2015 by Geological Survey of Western Australia
This Record is published in digital format (PDF) and is available online at **<www.dmp.wa.gov.au/GSWApublications>.**

Further details of geological products and maps produced by the Geological Survey of Western Australia are available from:
Information Centre
Department of Mines and Petroleum
100 Plain Street
EAST PERTH WESTERN AUSTRALIA 6004
Telephone: +61 8 9222 3459 Facsimile: +61 8 9222 3444
www.dmp.wa.gov.au/GSWApublications

Government of **Western Australia**
Department of **Mines and Petroleum**

MACQUARIE University
SYDNEY·AUSTRALIA

Tectonite type: Their formation and significance. Map production, field relationships and petrography.

A.E TOMKINS[1*]

[1] Department of Earth and Planetary Sciences, Building E5A418, Macquarie University NSW 2109, AUSTRALIA.

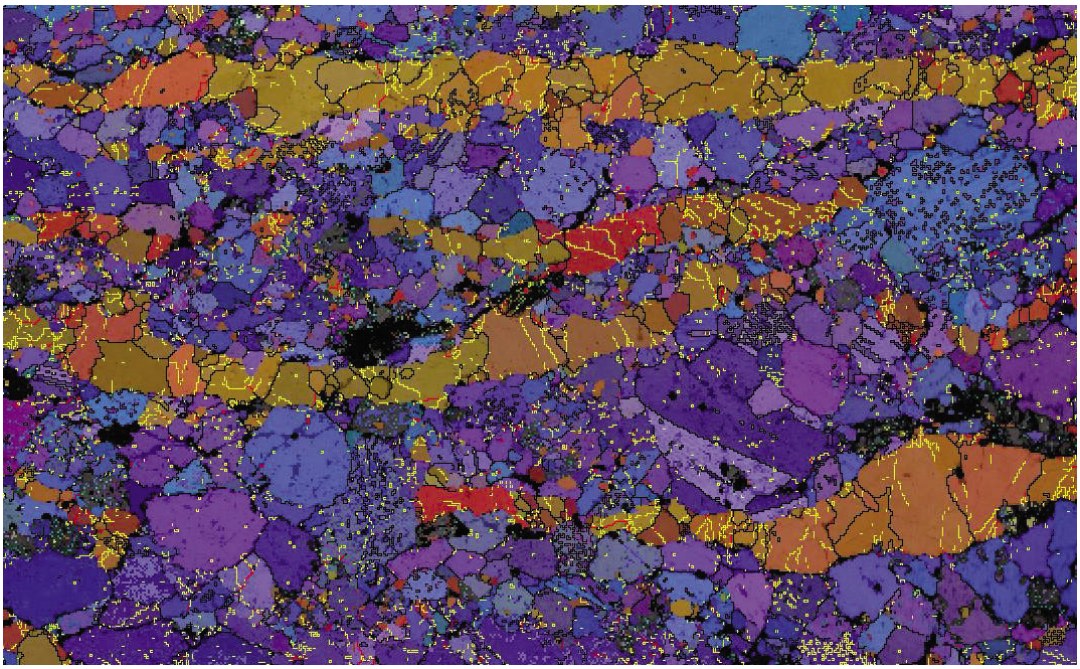

Thesis presented to the Department of Earth and Planetary Sciences for complete fulfillment of the requirements for the degree of

Masters of Geoscience

Macquarie University
2014

STATEMENT OF ORIGINALITY

All the work submitted in this thesis is the original work of the author except where otherwise acknowledged. No part of this thesis has been previously submitted to any other university or institution.

_____ _____

Aaron E. Tomkins Date

Acknowledgments

So I have finally come to the end my time with ‘The Dome’. It was a kind dome, but knew when to bite, usually when you were ‘on the brink of genius’. It was a great year mostly full of good times, and this is where I thank the people that have supported me through those times.

My greatest thanks goes to Sandra, without you Sandra I would have fallen, stumbled and given up. You hooked me on structural geology in 3rd year and found me this awesome project. You kept me on track while in the field, organised while at University and your depth of knowledge and the way you can teach is second to none. Your contribution to my education will not be forgotten. Secondly I would like to thank Ivan, aka ‘Bologna’, thanks for all your time!!! Mainly in the field, but especially after the field work, your help and speedy answers were invaluable, even spanning the distance. Prego.

To old mate Fenny, thanks for being a listening ear, a wealth of knowledge, a good driver, a bank and good conversation. We will always be mates and no doubt business partners.

To Goose, my partner in crime. We were a team, thank you for everything you did from driving, getting bogged, keeping me sane and upbeat, remaining calm (always), liking the same music, carrying 40kg’s of rocks, teaching me French, playing cards and all the rest. I had so much fun with all the laughs, you’re a legend and you will forever be a friend.

Thank you to the Macquarie staff; Dr Steve Craven, for all your help with geochronology and the morning coffees, even if I missed most of them. Cait Stuart, for all your help with my annoying questions, but most importantly putting up with my ridiculous banter, lack of cakes and the rest. Daria for your help with Channel 5, you’re a star. Dr Ed Saunders for having an awesome beard, “CHIPS”. And all the rest I have forgotten.

A huge thank you to my Mum and Dad. You have been stuck with me for many years since my move into Geology, and thank you endlessly for supporting me.

Kate….. The most down to earth, smartest and kind person I know. You kept me sane, in good spirits, you supported me non-stop, and I can't give you enough thanks, I can't wait for Jenolan caves!

Leaving the nearly best till last I want to thank the Schwinger's, Ben Patterson and Ben Thomas. You guys have pushed me, supported me, have been the best mates in the world and have been a great ear to talk to. We will be brothers forever.

Abstract:

Understanding the Yalgoo Batholith is a step further into understanding Archean diapirism. This thesis focuses on the tectonic, field, structural and textural relationships of this metamorphosed granodiorite dome. The dome intrudes through a highly folded, interbedded, meta-banded iron formation, meta-serpentinite schist and meta-peridotite greenstone package. The terrain revealing multiple generation deformation paths, generating non-coaxial oblate and prolate strain dependent tectonites within the Yalgoo meta-granodiorite gneiss. Strain shifts progressively northward within this internal gneissic terrain, ranging from partitioned, constrictional, sub vertical, sheath fold related (greenstone package), elongate L-Tectonites, to a variety of steeply outward dipping, SL and S-Tectonites within the Archean Yalgoo Batholith. Primary D1 deformation is recorded through consistent, highly folded, greenstone packages on the batholith margin, due to nearby subduction and thrust accretion. Secondary D2 deformation is indicated by sub-vertical lineated, downward moving sagducting greenstone packages, non-conformably proximal to upward diapiric doming movement. This movement is recorded in thin section microstructures, primarily in quartz ribbon stretching along the XY plane, co-linear with polymineralic, fine grained, recrystallized quartz and feldspar on the associated ribbon margins. These syn-doming textures conform with reconstructions for rising diapirs through denser crust, holistically part of a larger Yilgarn process initiated from close by dense oceanic crust subducting under buoyant continental crust. Planar fabric abundance within S-tectonites, indicate a transpressional D3 post diapiric event. This late, regional, simple shear related, tectonic deformation creates over printed pervasive planar fabric within SL and S tectonites. Based on field relationships, chemical, textural/microstructural and statistical

analysis we argue that the Yalgoo tectonite formation was through a combination of initial pluton emplacement followed by re-activation of the still hot buoyant pluton tail creating initial lineated fabrics, then followed by multiple tectonic processes resulting in areas of pure L through to pure S tectonites. Multiple successions of doming combined with tectonics may be common throughout the Yilgarn, therefore studies into tectonite formation may hold insights into similar batholiths.

Table of Contents

1. Introduction

1.1 Outline of Project

The Yilgarn craton is one of the oldest remaining crustal blocks in Australia, and is an integral part of Australian Archean tectonics, and therefore gives us an in-depth and reasonably unaltered glimpse into the early earth and its crustal formation. The formation and subsequent ongoing alteration of the craton is an ongoing debate. Early work done by; Sutton (1963), Campbell and Hill (1988) and most recently outlined by Czarnota et al. (2010), Van Kranendonk et al. (2013), show that there has been over 50 years of discussion and that all collective views and existing work done cannot be agreed upon or is eventually proved wrong. However, one particular aspect remains the basis of all past, present and future work, and that is that the formation of the craton consists of multiple events.

The Yilgarn craton is located in the south western corner of Western Australia and is in excess of 60,000km2 making up 10% of the Australian continent. It consists of greenstones, granites, and granitic gneisses ranging from 3730Ma to 2500Ma and is divided into multiple tectono-metamorphic domains and tectonic stratigraphic terranes, each having their own distinct and differing geological histories. The craton is thought to have evolved through arc magmatism, Archean subduction and accretion of terranes, however recent work done by (Van Kranendonk, 2008) and (Van Kronendonk and Ivanic, 2009) outline problems within these theories. Some issues include: rocks assigned to different formations and deformation events in previous schemes, actually belonging to the same unit; rocks that have been grouped together into one lithology actually differ along strike and have differing U-Pb

zircon ages; formations that include differing rock types (greenstone packages and metagranodiorite gneisses) that need separation into distinct classifications.

The Yalgoo dome, a small pluton located within the northern section (Murchison Terrane) of the Yilgarn craton, is an example of a section needing distinct mapping and characterisation. As part of a relatively unmapped area, a holistic research topic was created, incorporating three students that were to provide detailed work within differing sections of the dome. This thesis will analyse information on the North Eastern section of the Yalgoo dome, a complex transect at the contact of the metagranodiorite, greenstone boundary. This thesis will focus on, structural evolution and metamorphic processes, incorporating fieldwork, studies on syn-emplacement and/or syn-crystallisation of structures, synchronised tectonic/contact metamorphism, differentiating of granites and identification of gneisses throughout the area.

The aim of this two part thesis is to firstly characterise L and S Tectonites throughout the Northwest section of the Yalgoo dome, outlining features, microstructures and field relations, and secondly to analyse three tectonites with ranging planar and linear fabrics through statistical analysis and acquiring data from the scanning electron microprobe (SEM), thus correlating all supplied data into a working theory of the formation of the dome. Data will be analysed to identify if the Yalgoo batholith is; a dome; or a result of deformation interference patterns, created through tectono-magmatic processes. The S and L tectonites will be analysed via SEM, viewing their backscatter diagrams, with a primary view of identifying quartz CPO, deformation mechanisms and metamorphic grade. A brief outline of the regional geology, formation of the Yilgarn Craton and the Murchison Terrane will also be provided. Along with the latest research by Foley (1997) and Caudery (2013) on the Yalgoo dome, comparing their results and incorporating existing work throughout the world.

2. Regional Geology and Open Questions

Due to the Yilgarns complicated evolution and history, the area has been grouped into 3 super terranes and subdivided within those 3 into terranes and domains. The main super terranes outlined by (Cassidy et al., 2006) and (Myers, 1995) are as follows (Fig1):

1. West Super terrane, comprising of the Narryer, Murchison, Balingup, Boddington, Dumbleyung and Hyden terranes.
2. Central Super terrane, comprising of the Barlee and Yellowdine terranes.
3. East Yilgarn Super terrane, comprising of the Karlgoorlie, Kurnalpi, Laverton, Gindalbie, Jubilee, Pinjin and Norseman terranes.

These super terranes each exhibit their own deformation histories and are theorised through multiple journals, (Myers, 1995; Czarnota et al., 2010; Sutton, 1963; Van Kranendonk et al., 2013) to name a few.

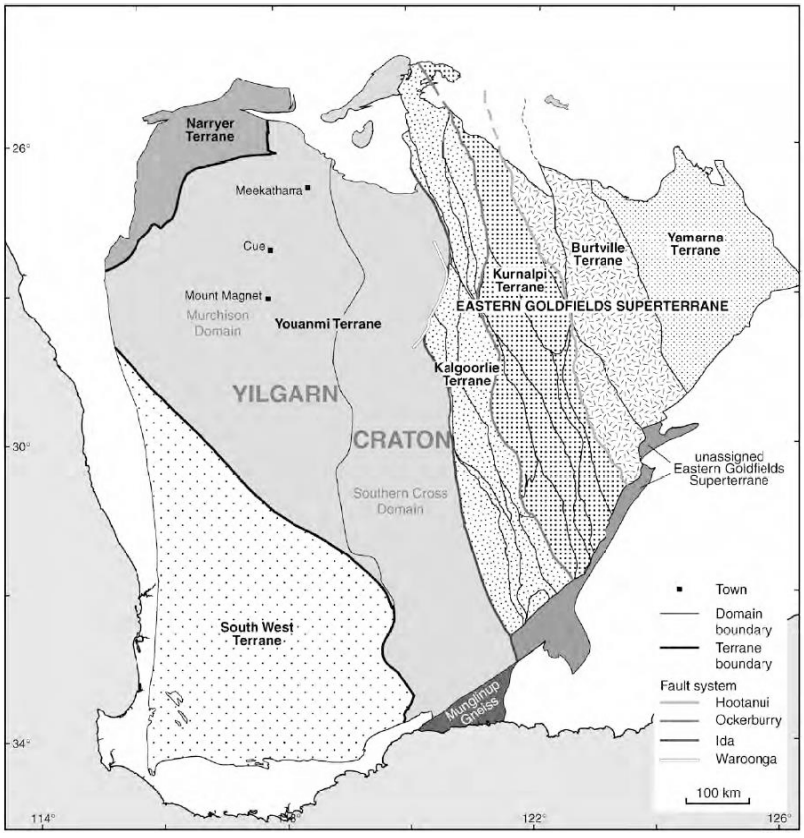

Fig1. Showing multiple terranes of the Yilgarn Craton, separated into super terranes, terranes and smaller domains. (Myers, 1995)

The Archean Yilgarn Craton is made up of volumetrically dominant granites and granitic gneiss (>80%) and is predominantly surrounded by greenstone boundaries of ultra-mafic schists, slates and banded iron formations (Zibra, 2012). This terrane represents a natural laboratory to study one of the oldest known crustal fragments in the world, with one of the best average outcrops in the world.

Regional-scale, roughly N-S trending anastomosing shear zone networks are prolific throughout the craton, with a centrally dominating highly mineralised zone toward the central-east of the Yilgarn Craton (eastern goldfields).

As described by (Myers, 1995), the craton appears to be a remnant of a formerly larger late Archean continent that collided and accreted with other various terranes up until 2500Ma. This process and collision was accompanied with widespread volcanism, granite emplacement and metamorphic deformation, creating the individual super terranes and domains within. Economic mineralisation is substantial throughout, with Au deposits dominating in the south east (Eastern goldfields) and North West (Murchison province). These deposits have multiple formation theories (Sharpe and Gemmell, 2001) and (Wang et al., 1998) and were exploited in multiple 1900's gold rushes. Volcanism throughout the region ranges from felsic granodiorite intrusions, creating highly folded strains zones in overlying greenstones belts, to multiple successions of underwater mafic dominated basaltic lavas creating layered pillows and invasive komatiitic flows (Beresford and Cas, 2001). Contact margins of the large scale regional geology show intruding granites into greenstones with ranging ages around 2900Ma indicating subduction processes at work. (Fig2)

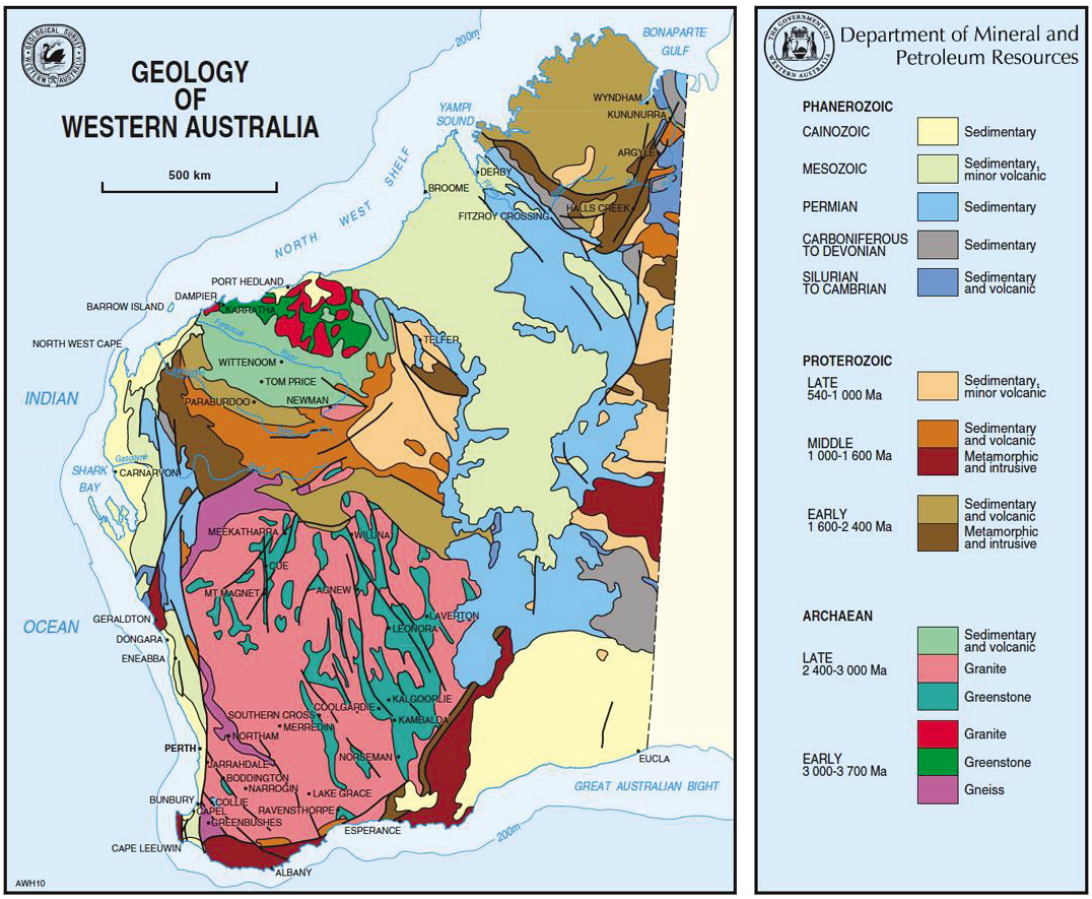

Fig2 – Map from the Department of Minerals and Petroleum outlining, co planar elongate greenstone belts, indicating formation before craton deformation. The pink area in the south west is the Yilgarn craton. (GSWA, DMP)

The current theory of craton-scale distribution of greenstone belts, is largely related to shear zone patterns, with a close spatial and temporal relationship between pluton emplacement and shear zones that has been documented in various geological settings (Rosenberg, 2004) and (Weinberg et al., 2004). Greenstone belts throughout the craton show multiple trending directions but most are elongate and co planar with shear zone directions. This is consistent with the current theory of greenstone formation before large scale deformation. (Champion and Sheraton, 1997) (Fig2)

Shear-zone surfaces may have provide unimpeded pathways necessary for magma ascent through the associated greenstone overlying structures. This in conjunction with pure and simple shear strain from continental collision, creating polyphase deformation, which then

gives way to the dome and basin theories throughout the Yilgarn craton and Murchison terrane put forward by (Myers and Watkins, 1985) and (Myers, 1990) (Fig3).The Yilgarn Craton granitic plutons, display a wide variety of shapes and internal structural features that are closely related to their local and regional structural evolution (Fig3). During regional deformation, pre-tectonic plutons are inferred to react as rigid bodies in dramatic upward ascent creating brittle and ductile deformation against rheologically weaker greenstone belts. Thus creating a differential contrast along strike of the greenstone belts, shown by in situ pervasive fabrics of intrusive ultra-mafic schists affected by brittle shearing, local folding and remelting. This occurs in succession throughout the Murchison terrane, as outlined by (Van Kranendonk et al., 2013).

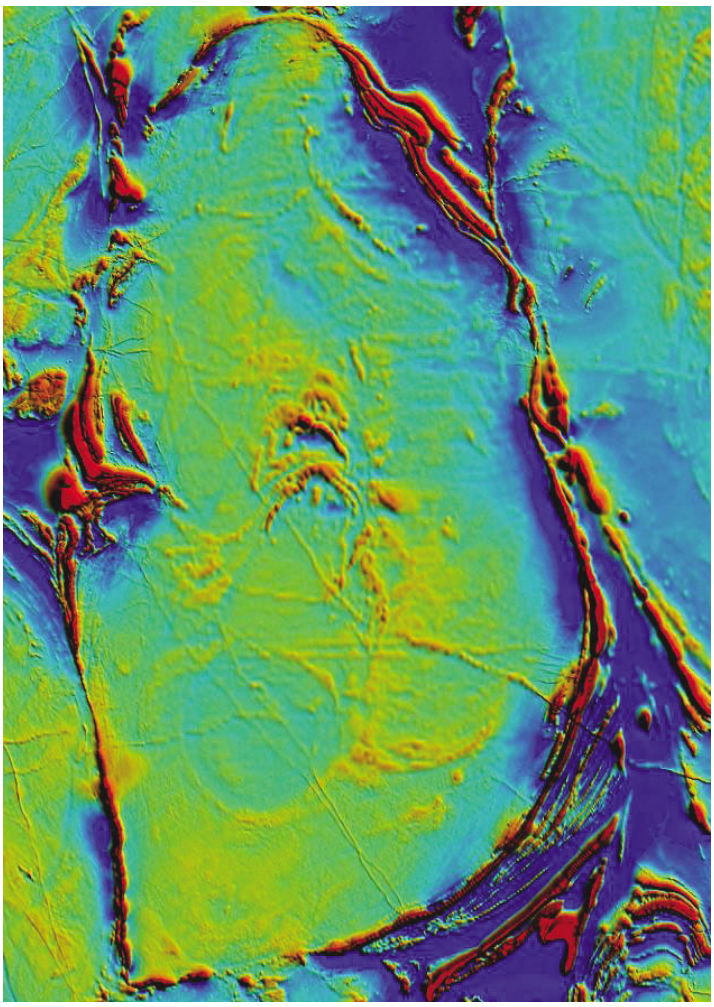

Fig3 – Yalgoo Dome of the Murchison Terrane. The red ring surrounding the dome is original deposited greenstones belts of sequential Algoma type deposit BIF, Serpentinite schist, slates, and Mg rich clastic basalts. Two sequences of granites are within the centre of the dome. The first being a tonalitic intrusion creating initial doming and sheath folding toward the greenstone boundaries and the second being a more mafic intrusion creating migmatites in the core of the dome while being effected by regional scale faulting shown by elongation, a small amount of rotation of the dome and large scale dyking and exploitation of weaker fabrics. (GSWA, DMP)

2.1 Murchison Terrane

There has been minimal work done since initial mapping by the Department of Minerals and Petroleum in 1960 on the Murchison Terrane, with two current theories outstanding. Myers and Watkins touched on the granite greenstone patterns in 1985 and outlined that the Murchison Province displays a classical granite-greenstone association, with N-S elongated granatoid domes separated by synformal graben type structures of greenstone sequences. The fold interference model was then proposed by (Myers and Watkins, 1985) using a basis of the earliest work done by Ramsay (1960), to explain the dome-and-basin patterns (Fig4a). This model was based on the assumption that the NS-trending regional foliation, cross cuts an older EW-trending foliation through regional stresses. (Fig4b)

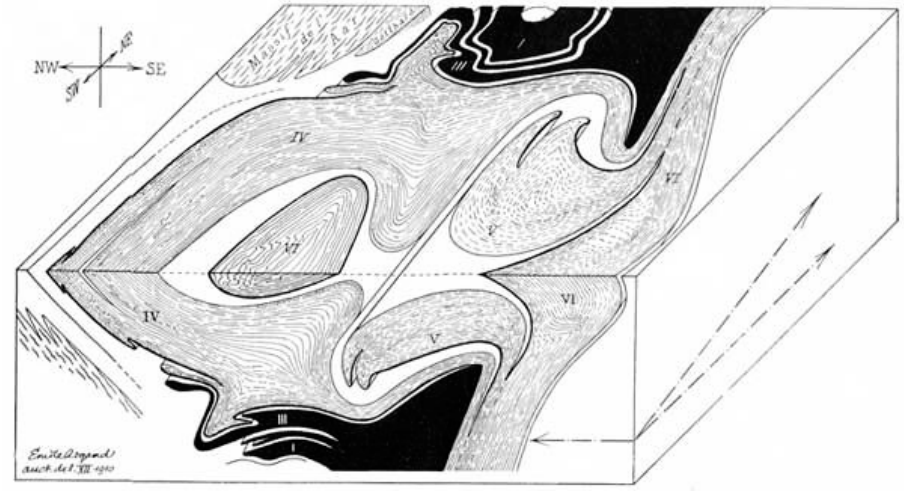

Fig4a – One of the earliest block diagrams from Ramsay (1960) illustration the mechanisms of polyphase deformation. Stresses are indicated by the arrows on the right of the image, creating complex structures within the affected area.

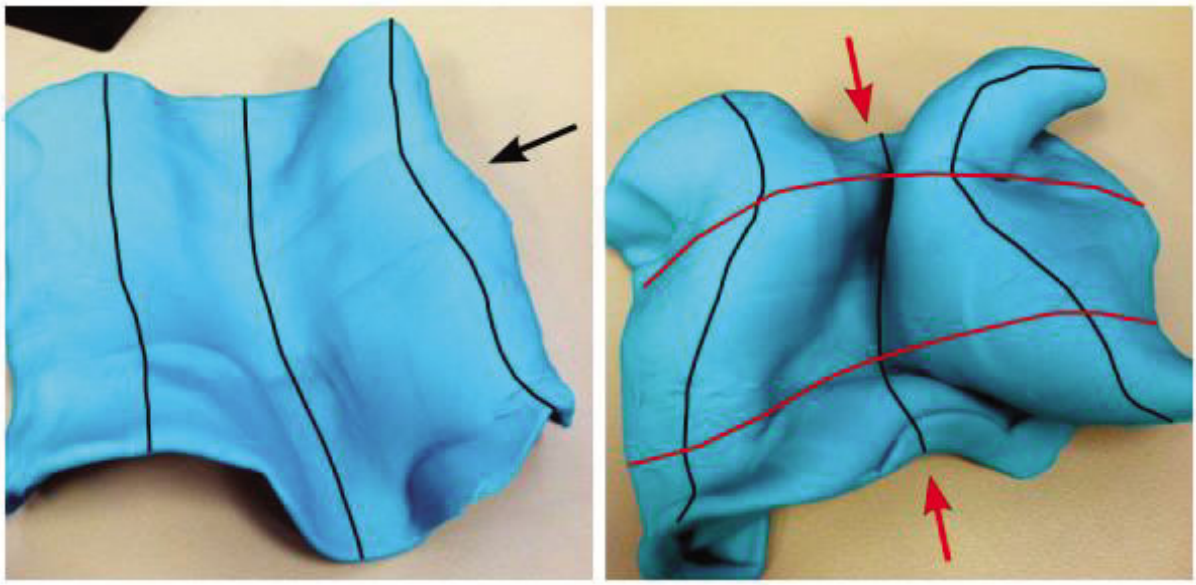

Fig4b – Polyphase deformation from east/west and north/south mechanisms (based off Ramsay), creating dome and basin structures using mouldable putty. (Maitri, 2011)

Alternatively, studies by Rey in the last 20 years introduce a new theory and emphasize that the regional strain field pattern observed in the Murchison Province was likely produced during a single event of progressive deformation, rather than during multiple folding events of regional deformation. This is outlined by Rey, 1998 at an AGU international conference, and also by collaborative work between Rey and Philippot in 2006, where single, steeply dipping, regional foliation is present that delineates the domes and basins. Foliations are seen in the greenstones that wrap around hinges of synforms and trends parallel to the granatoid/greenstone contacts, separate from highly migmitised areas in the centre of the dome. The granatoid foliation underlines the shape of the domes, and the fabric varies from magmatic to solid state towards the contact with the greenstones. Kinematic indicators show upward trends within the granatoid outcrops and downward displacement of the greenstones, which alternatively fall in line with (Myers and Watkins, 1985) dome and basin formations. Rey also outlined that, fold interference patterns used by (Myers and Watkins, 1985) as evidence for multiple events of regional deformation, but they only occur at

foliation triple junction points within the greenstone synforms, or in banded magmatic gneisses located in the core of the domes.

Similar structural features that Rey outlines above are described in other Archaean cratons, like the Dharwar in India, and are compatible with the emplacement of multiple granitic domes. Rey finishes with proposing the dome-and-basin patterns outlined by (Myers and Watkins, 1985) and observed in the Murchison Province reflects emplacement of buoyant granatoids, which in turn disturbed the regional strain field dominated by N-S stretching.

Since Rey, studies have been done on geochronology and geochemistry of the granites and a three stage theory has been proposed below by (Blewett et al., 2009) and in conjunction with the Integrated Terrane Analysis Research centre.

This theory incorporates an initial plume related ingestion of surrounding material along with subduction of surrounding felsic crust, injecting the plume with felsic material and subsequently creating a tonalitic composition. (Fig5)

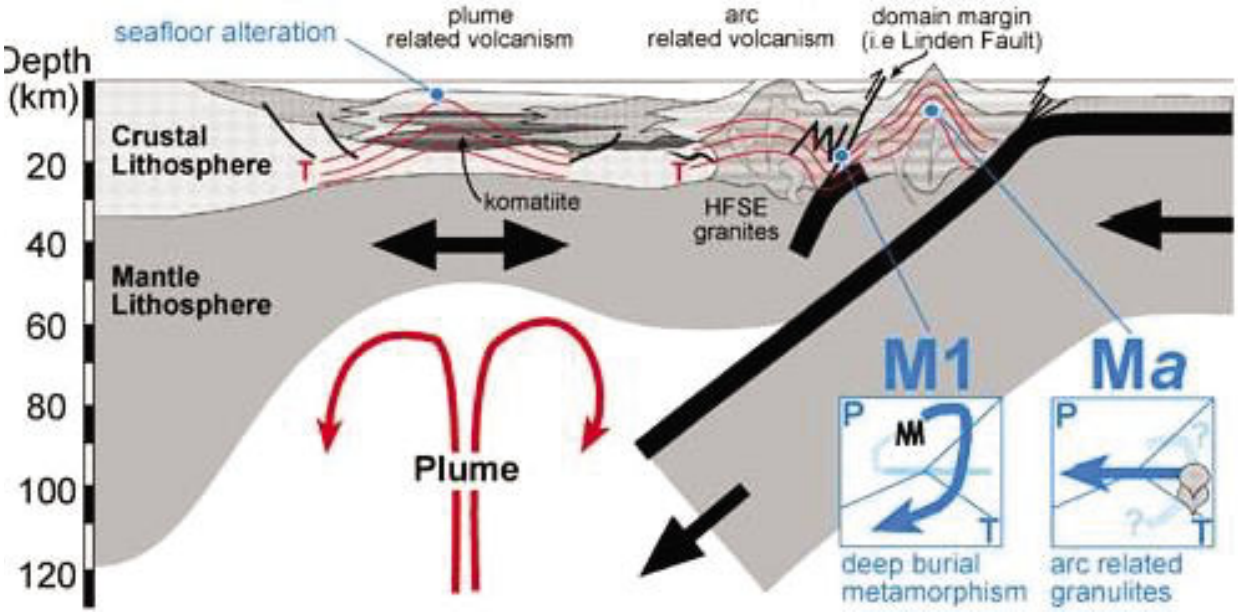

Fig5 – Plume related formation of the initial tonalite intrusion, creating the dome itself through extension and subsequent stretching and sinking through isostasy of the overlying material. (ITARC)

Above is followed by granatoid formation with rapid upward decompression creating multiple dome structures. This type of doming is found throughout the Murchison area and is said to be in conjunction with compression and transpression stress from continental pressures (Fig6). This event would produce a dominant D1 lineated fabric throughout the area.

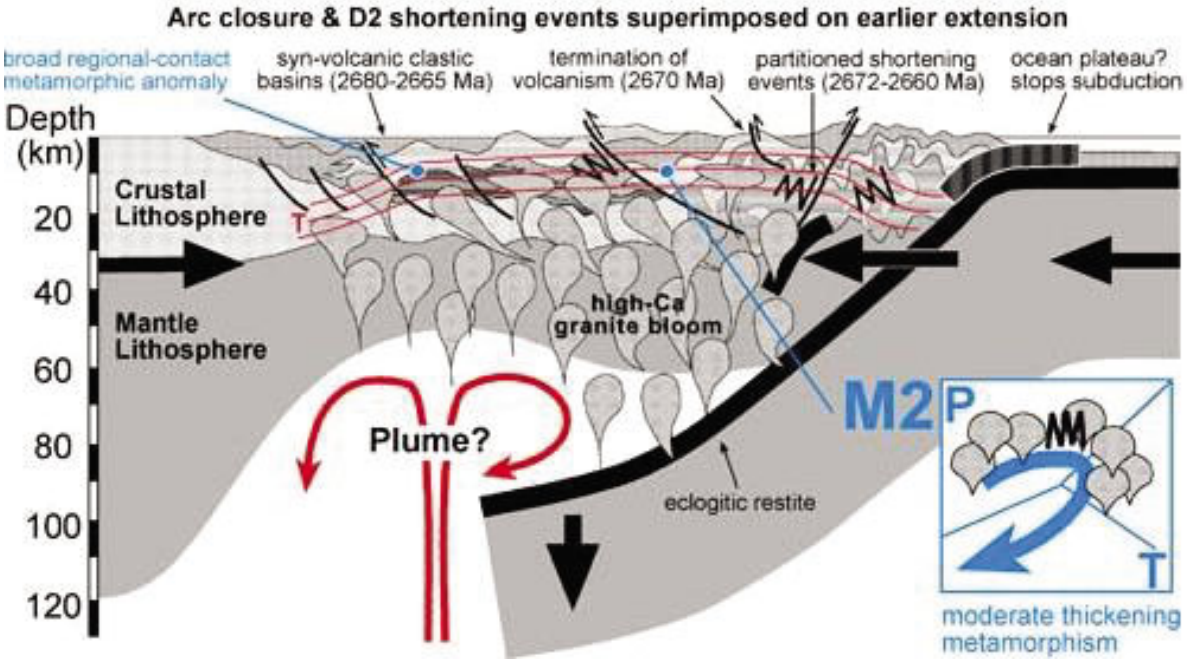

Fig6 – Granitoid pluton formation and uplift due to rapid decompression and cooling of surrounding rock. (ITARC)

Finally, mafic melt due to thermochemical magma differentiation would follow, this is theorized by Ballmer and his work in Hawaii, and is due to magma ponding, development and evolution of the pluton. Mafic melt upwelling continues in conjunction with local and regional scale extensional rifting, creating multiple generations of pluton mixing, forming elongate schlieren, areas of high stress/strain and potentially creating migmatites with a leucocratic and melanocratic nature. (Ballmer et al., 2013)

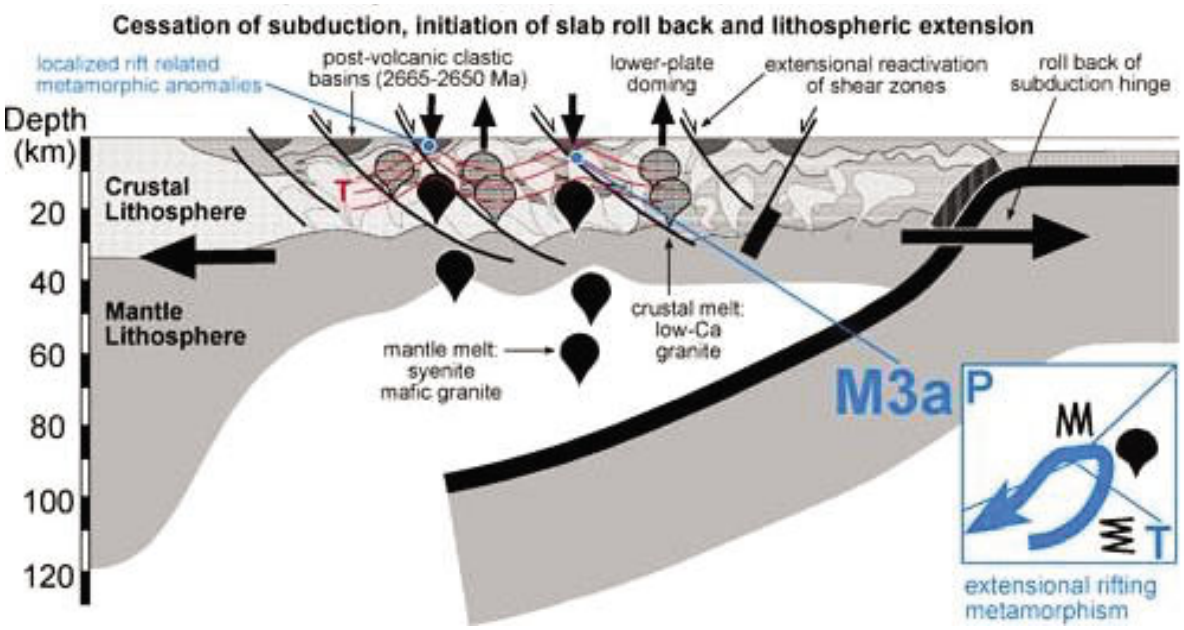

Fig7 – Multiple pluton mixing, syn-deforming with regional and local extension. (ITARC)

This third and combining theory along with current field work, geochemistry and mapping of the Murchison and Yalgoo area creates a combination of Myers and Reys work. Recently Ivanic and Van Kranendonk have ongoing work in the Murchison Domain and have said that the craton was void of volcanic activity and is well preserved from 4.0 to 3.0 Ga. This is directly followed by the eruption of the first widespread greenstones (mafic underwater extrusives) and associated intrusive granites at 2.95GA. This is connected with continental collision and subsequent accretion of surrounding terranes. There was then an 110Ma pause in magmatism, followed by a series of nearly continuous contemporaneous magmatic events (underwater mafic volcanism and felsic plutonism) over an interval of at least 220Ma from 2820 to 2600 Ma, thus leading to a thick, indigenous greenstone succession and widespread crustal growth through in situ recycling of surrounding older crust.

An onset of magmatic events at 2820–2790Ma occurred and was initiated by large volume mantle melting, including the eruption of komatiitic melts derived from a deep mantle

plume (Barley et al., 2000). At this time mafic-ultramafic magmatism across much of the Yilgarn Craton was occurring and suggests the possibility that the craton had homogenous borders and subsequently was split into narrow crustal ribbons through N/S rifting and volcanism. The Murchison Terrane shares a large amount of common history with the rest of the craton, including 2720Ma ultramafic volcanism, the widespread emplacement of crust derived granitic rocks at 2690–2640 Ma, ductile shearing, gold mineralisation at 2660–2630 Ma, and intrusion of post and syn-tectonic granites at 2630–2600 Ma. The work presented by (Van Kranendonk et al., 2013) identifies that the currently preferred model of craton formation through arc magmatism and terrane accretion is wrong and the structural information within Murchison Domain proves this and needs review. They go on to suggest a new alternative model of crust formation through one or more significant mantle plume events which needs developing. This may account for the multiple successions of greenstones and granites.

2.2 Working models for the Yalgoo Dome:

The Yalgoo dome is situated 200kms east of Geraldton and directly south of the township of Yalgoo. The dome is discernable from aero photos and is approximately 56kms x 90kms (Fig 8)

Fig8 – Yalgoo Dome from Google Earth within the black ellipse. The yellow star indicates where Caudery mapped in 2013. The dome is very large with only limited amounts of outcrop to be observed.

There has been very little work done on the Yalgoo gneiss dome in the past, with only two thesis papers produced along with regional scale mapping, and very recently seismic and aero magnetics on the area. Foley (1997) originally mapped out and theorized the formation of the dome in which Caudery (2013) then re-mapped out a specific section (Fig8) of the core area within the inner dome. The mapping from Foley and Caudery included three areas within the main magmatic area of the core. From mapping just this specific area, they established two differing magmatic-solid state dome and basin hypotheses for the whole dome formation. The following is summarised:

2.2.1 Foley, 1997 – Solid state dome and basin

Foleys model followed the same principals as (Gee et al., 1981) originally addressing this theory by outlining that the melt had formed at minimal depth, thus not being influenced by the underlying mantle (above 30kms) or subsequent co-event basaltic surface eruptions. Foley then added the development of the greenstone belts and granite domes throughout the area, forming through a singular tectono-thermal event (volcanism, sedimentation, metamorphism and deformation) over a small time window between 2.8 and 2.6 Ga. The event was a syn-tectonic/plutonic event where felsic plutons underwent rapid uplift and intrusion into the over lying sialic crust. Upwelling then stopped at 2.6Ga and the associated migmatites formed through metamorphic differentiation and partial melting at intermediate and lower levels in the crust. (High temperatures can be experienced in the crust for this kind of formation, with the subsequent addition of granulite facies rocks leading to granitic melts). As Foley expanded on the original theory he then proposed a new four stage structural and tectonic model (not including original pluton formation). Stages:

1. A density difference between the dense greenstone sequences and the underlying granatoids resulting in granatoid material intruding overlying greenstones in a diapiric mechanism. These plutons most likely evolved by a process of amalgamation of smaller plutons that intrude separately during one major progressive emplacement.
2. As the granatoids intruded, the overlying sequences are heated and become ductile, consequently sagging due to the density differences. (Fig 9 – Foley 1997)

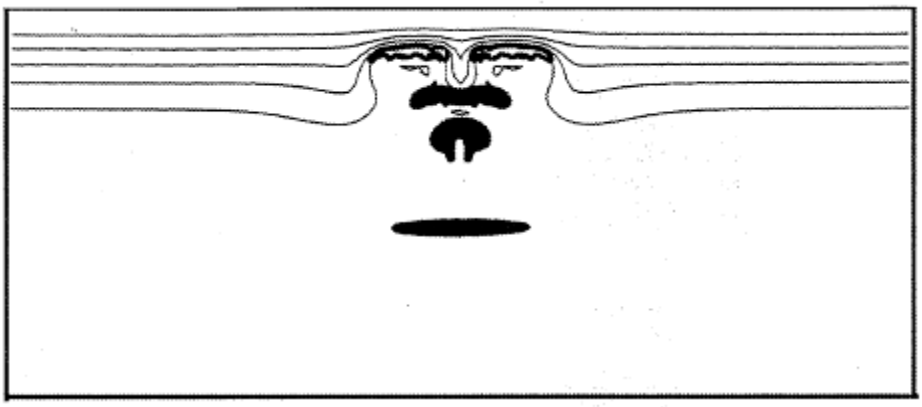

Fig 9 – Multiple emplacement of granitoid plutons, emplacing separately and progressively. As the plutons rise, they meet discontinuities, differentiate and exploit fabrics of least resistance.

3. Granitoid outer margins start to lithify, and are affected in specific areas by sharp contacts and overprinting fabrics. Possibly through nested diapirism; continual injections of different magmas into the magma chamber, and ballooning; where lithification and solidification would occur to the outer most parts of the pluton, with continual crystallisation occurring of the single parent magma. The hotter tail, still buoyant, would then continue to rise into the central part of the pluton, increasing strain to the outer rim of the main dome creating linear and foliated fabrics in different areas depending on strain.
4. At the end of the granitoid emplacement and greenstone sagduction, regional stress's occurred from tectonic activity and brittle deformation effected the area.

2.2.2 Caudery, 2013 – Single stage, multiple pluton emplacement

Caudery mapped a more specific area in 2013 and aimed to expand on Foley's singular emplacement theory and disprove Myers and Watkins multiple stage pluton emplacement theory from 1985. Caudery outlined this by giving detailed deformation events as follows.

1. The Archean greenstone belt surrounding the dome, is also found in outcrops throughout the dome and is interpreted to be laid down through volcanism and sedimentation prior to 2960Ma.
2. D1: At 2960, a tonalite intrusion intruded the greenstones, forming the S1 metamorphic foliation. Multiple small domes consequently form in conjunction with the main event. Melting and migmatisation occurs, melting both the tonalite and the amphibolite. Leucosomes and felsic melt bands respectively, form sub-parallel to the S_1 foliation. Various pegmatite dykes also intrude through the area at around this time.
3. D2: F2 isoclinal and sheath folds occur, folding the S1 foliation. It is most likely that this event involved a component of N-S shortening due to typical E-W trending F2 folds. S2 forms parallel to S1.
4. D3: N-S trending upright F3 open folds occur, resulting from E-W shortening, forming the S3 foliation. This event overprints the previous foliations. This phase is associated with melting found in axial planar foliations and fold hinges.
5. D4: At 2752 Ma, various granitic intrusions occur, intruding into the same area, and melting of older rock types at the exposed level had stopped. These granitic intrusions eroded and entrained xenoliths of the central tonalite. Pegmatite dykes, oriented approximately E-W intruded the entire region also at this time. The granitic intrusions increased the size of the dome to be what it is today.

6. D2+: A late crenulation cleavage occurred, and is recorded only in the weakest units of the greenstones on the boundary of the dome. We cannot determine the relative age of this event due to lack of overprinting relationships, except to say it was post D2. It is most likely a local and minor event.

The detailed mapping Caudery completed of the small inner dome, along with evidence of sheath folds developed in D2, argues against the superposed fold model proposed by Myers and Watkins (1985). Caudery outlines the granitoids of the Yalgoo Dome were emplaced through smaller domes, progressively intruding in single events developed and recorded by large scale sheath folds and domes.

2.3 The use of Tectonites in the study of deformed terrains

As outlined in the introduction, one of my aims is to provide a current formation theory of L to S Tectonites through my specific mapped area outlining features and field relations. By analysing this information of field relationships within outcrop and boundaries of L to S Tectonites, an understanding of deformation mechanisms and formation of different fabrics through differing processes will be provided. This information can then create a working hypotheses for the structural emplacement of the mapped section of the dome. From these results I will then be able to discuss theories from the previous work of Foley and Caudery and identify if there is another mechanism at work.

Sullivan (2009), Sullivan (2006) and importantly Sullivan (2013), outline the classic theory of L through to S tectonite formation, depending on constriction or flattening strain during a single event. Sullivans work with Tectonite formation will become a basis for the Yalgoo tectonite formation and consequently the evolution of strain dependant fabrics.

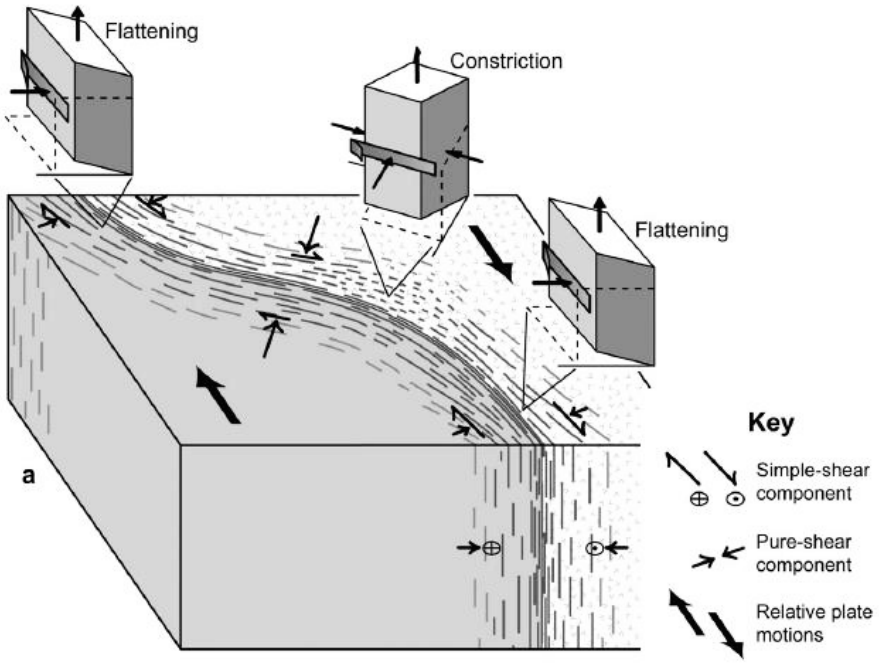

Figure 10a: An environment similar to Yalgoo dome where a combination of pure and simple shear is affecting S and L tectonite formation. Adding successive events to this or a two stage pluton emplacement can then favour the final event to overprint existing structures. (Sullivan, 2013)

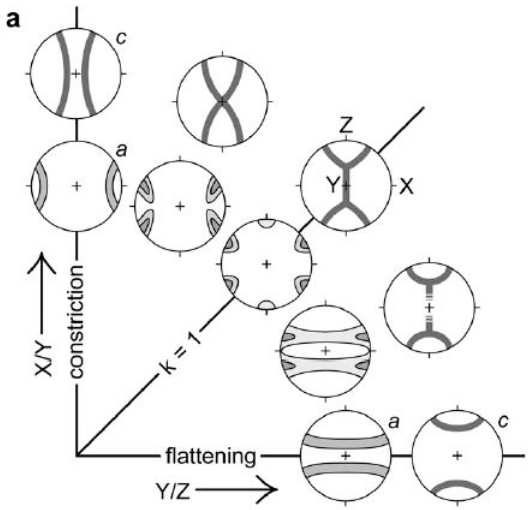

Figure 10b: Quartz crystallographic fabric geometries predicted for coaxial deformation under greenschist-facies conditions. X, Y, and Z are the maximum, intermediate, and minimum axes of the finite strain ellipsoid respectively. (Sullivan, 2013)

A main question of tectonite formation is if lineations are strain dependant, consequently being overprinted when strain increases or another event occurs. Answering these questions will be done by observing a kinematic sequence of overprinting by showing mineral and clast stress rotation directions trending throughout the research area from pure L tectonites to pure S tectonites. Meaning most tectonites were initially S or L tectonites followed by varying stresses on specific area's creating a variety of foliated and lineated areas. Toy., et al (2012) touches on transpressive lineation formation in New Zealand and outlines this type of original formation followed by specific strain changes within the same package, consequently creating a direct relation to a foliation or lineation dominant fabric.

2.4 Set-up of Thesis

The thesis was set up with two components, within a larger project for the Geological Survey of Western Australia (GSWA). The first component was a 5 week field expedition to Yalgoo mapping the greenstones and granites on the margin of the pluton. This was to create a map, outline field relationships of each unit, identify varying tectonites along the north east transect and to create field report outlining each rock type. The second component was to analyse collected data, creating a working model of the processes affecting dome formation, and to decipher if there are multiple events forming foliated and lineated fabrics within the tectonites from the area. This is aimed to answer the question of; are the lineations seen due to A) an emplacement mechanisms (solid state vs crystal lattice deformation), B) later tectonic overprinting (transpression and simple shearing in specific locations defining margin shape), C) multiple overprinting relationships which affect different areas to different degrees, therefore causing L,LS and S tectonites to occur.

3. Part 1 - Geological Mapping, NE border of the Yalgoo Dome

3.1 Mapping Context:

Mapping of the Yilgarn craton has been increasing over the last decade with contributions from the Department of Minerals and Petroleum (DMP) and the Western Australian Government. The Yalgoo Dome has been focussed on as it is an integral part of Archean tectonics, and gives us an in-depth and reasonably unaltered glimpse into the early earth and its crustal formation. A mapping expedition was initiated, with collaborations between the Western Australian Government, Macquarie University and Monash University. The latter focussed on mapping the internal section of the dome (Fenwick, 2014). Macquarie focussed on mapping the north eastern limb of the granite greenstone contact, looking

closely at deformation mechanisms and tectonic relationships. A 6km x 16km map was produced outcrop and structure descriptions, each with a quantitative age relationship observed from any outcropping unit. The information was gathered over a two month period from April to May 2014, forming the basis of this thesis.

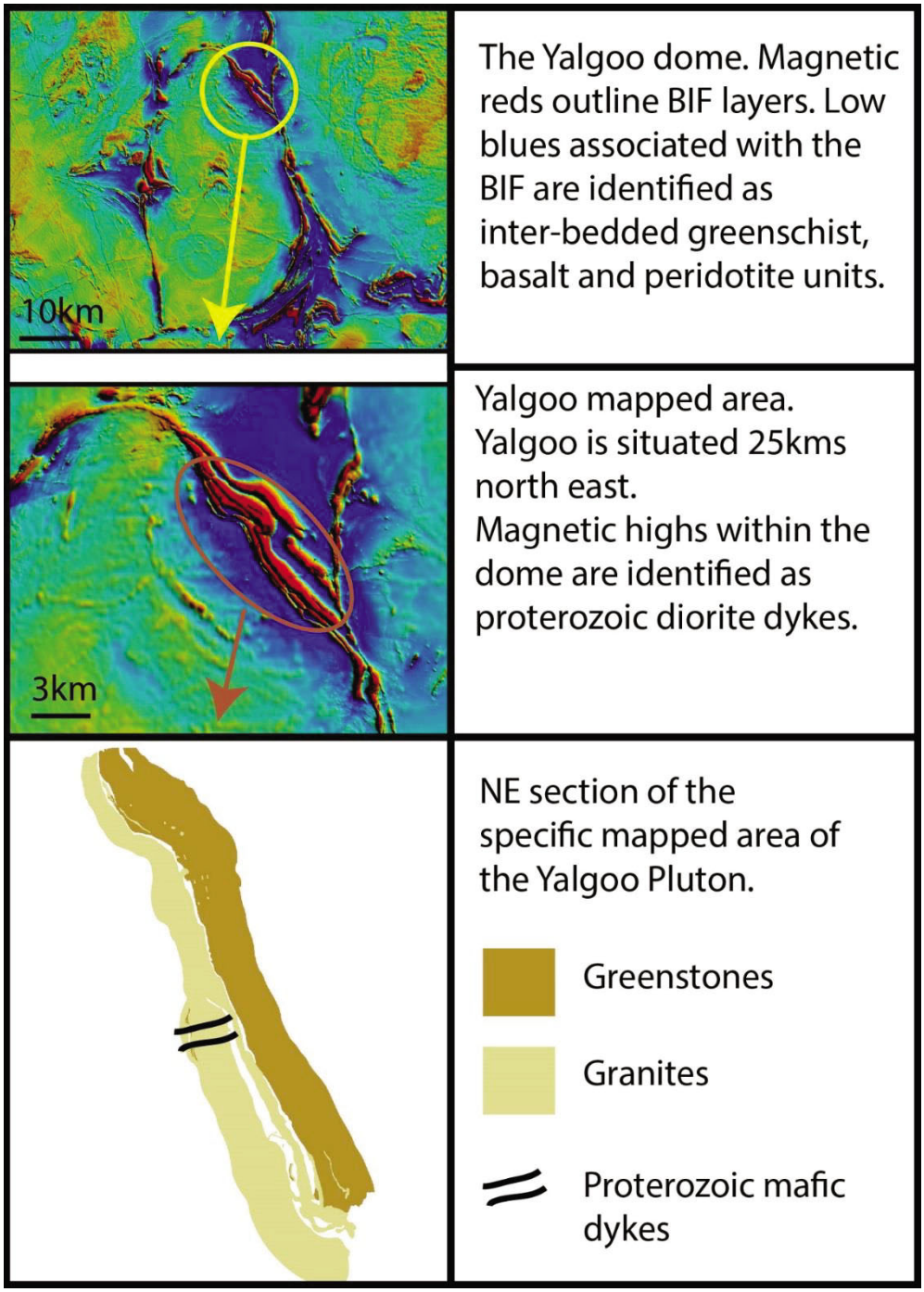

Fig10c – Magnetics map courtesy of GSWA of the Yalgoo dome. Zoomed in section of the mapped area. Illustrated map of the boundary between the greenstones and granites.

3.2 Field area

The north eastern flank (fig 10c) was mapped by myself in conjunction with Piazolo and Zibra. This field work predominantly concentrated on the greenstone/gneiss boundary within the stratigraphic sequences, kinematic indicators, dykes and S or L tectonites. The study consisted of traverses over known areas of outcrops as well as new exploration areas where no mapping had occurred previously. The area was a 6km x 25km section over BIF's, greenstones, dykes and tectonites. GPS co-ordinates from 50J – 481582 – 6842439 to 50J – 471930 – 6855287. Terrain was predominantly flat with some areas of high relief. Lateritic BIF and colluvium dominated up to 70% of the area.

3.3 Methods:

3.3.1 Field Work

Mobilisation occurred in late April and consisted of driving Toyota Landcruisers North to Yalgoo. A base camp in the southern mapped section (Badja), was set up in the first few days where all students and lecturers could start from to observe good field outcrops. After theses few days past, all students split up to study their allocated areas. A field assistant was allocated and mapping commenced on the Northeast section of the dome. Mapping concluded in early June and all persons demobilised back to Perth. Time in the first week of June, was allocated to be used in GSWA's laboratory. Tasks completed included, cutting of rocks for thin sections and geochemistry.

Total days in the field	36 days
Total days at Perth base	4 days
Total rain days	7 days

3.3.2 Planes

The thesis will be described using planes. The following illustration outlines each plane.

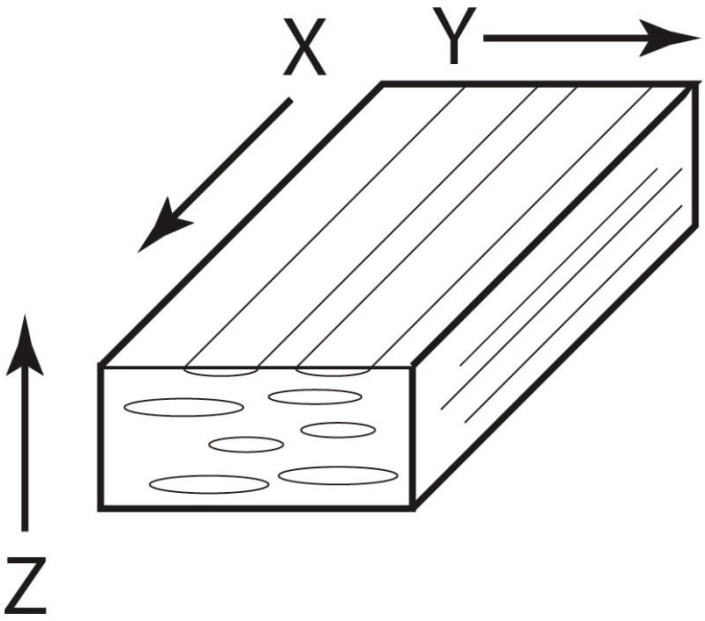

Figure 11: Representation of planes via a rectangle. Lineations seen on the XY plane. Foliations are seen on the ZY plane.

4. Field results

4.1 General outline of the geology of the mapping area:

The area consisted of 2 main groups being greenstones and granites. These were split into subgroups: Greenstones consisting of BIF's, schists, and mafic units. Granites consisting mainly of meta-granodiorite gneiss with tectonite fabrics ranging from S to L tectonites. All units followed a regional trend at North West. Main pervasive fabrics of the units were generally co-planar with this strike. F1 and F2 fold generations were co planar with the pervasive S1/S2. A F3 perpendicular NE/SW regional fold truncates all deformation and is interpreted to be the last event. The units generally see an increase in contact metamorphism with proximity to the boundary. The greenstones see compression of minerals and a combination of dynamic and static recrystallisation with proximity to the boundary of the pluton. Granites, unaffected by folding, see a combination of pure and simple shear with metamorphic fabrics present and a combination of foliated and lineated textures. Units were mapped across a perpendicular strike traverse.

4.2 Lithological units mapped:

Greenstones: Interbedded BIF, meta-basalts and schists (serpentinite to peridotite).

4.2.1 BIF – Meta-Banded Iron Formation, field appearance and field relationships

- The BIF's ranged from foliated layers of quartz (50%) and hematite/magnetite (50%), (except in isoclinal folds where felsic silicic quartz showed in the axial plane), to areas of high strain where folds and layering were not discernible and hence called areas of high strain. The quartz that is interbedded with the hematite has a mafic, sugary, smooth texture with no visible clasts and is extensively fractured. It showed millimetre scale felsic banding that was parallel to the F1 fold axis. The BIF exhibited multiple folding generations seen in high strain zones in millimetre, decimetre and meter scale. These included F1 isoclinal folds that had steeply inclined to upright axial planes and steeply plunging to sub vertical fold axis, striking 110. Vertical mineral elongation was noted on the siliceous faces parallel to the axial plane of F1. An intersection lineation was striking perpendicular to the axial plane of F1 and parallel to the axial plane of F2. The F1 and F2 folds were both cleaved at the nose of the folds. The BIF showed evidence of sheath folding and polyphase deformation with the plunge of the fold axis parallel to the intersection lineation.

  Throughout the outcrop along strike, into the northern sector of Yalgoo, the BIF exhibited the same F1 Isoclinal folding with interference from a F2 fold perpendicular to this F1. The BIF ranged from unaltered on the outskirts of the boundary to highly altered, with extremely foliated beds and higher percentage quartz moving toward contact and into the dome.

Fig12a – Above - High strain zone within the hinge of a regional open fold visible on air photo. Small donuts can be seen within the BIF indicating polyphase deformation.
Figure 12b Below – An illustration of folding with axial trace lines within a high strain BIF unit. 3 Generations of folding is seen. Typically characteristic of sheath folding and interference patterns.

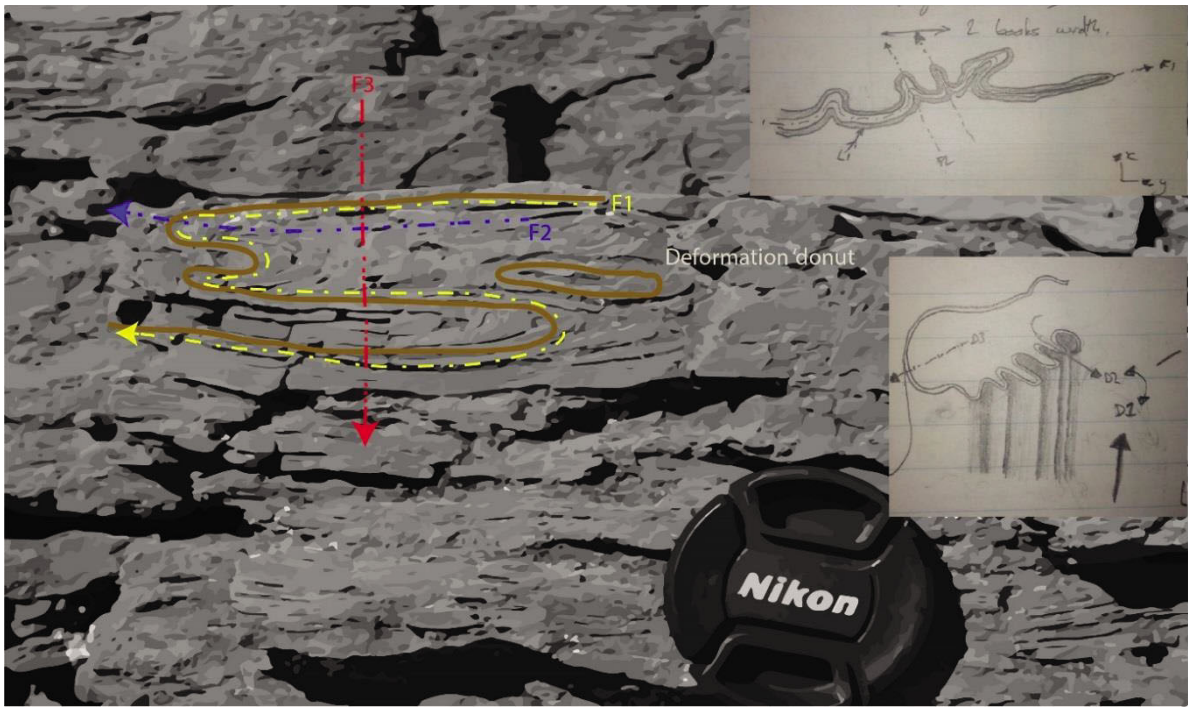

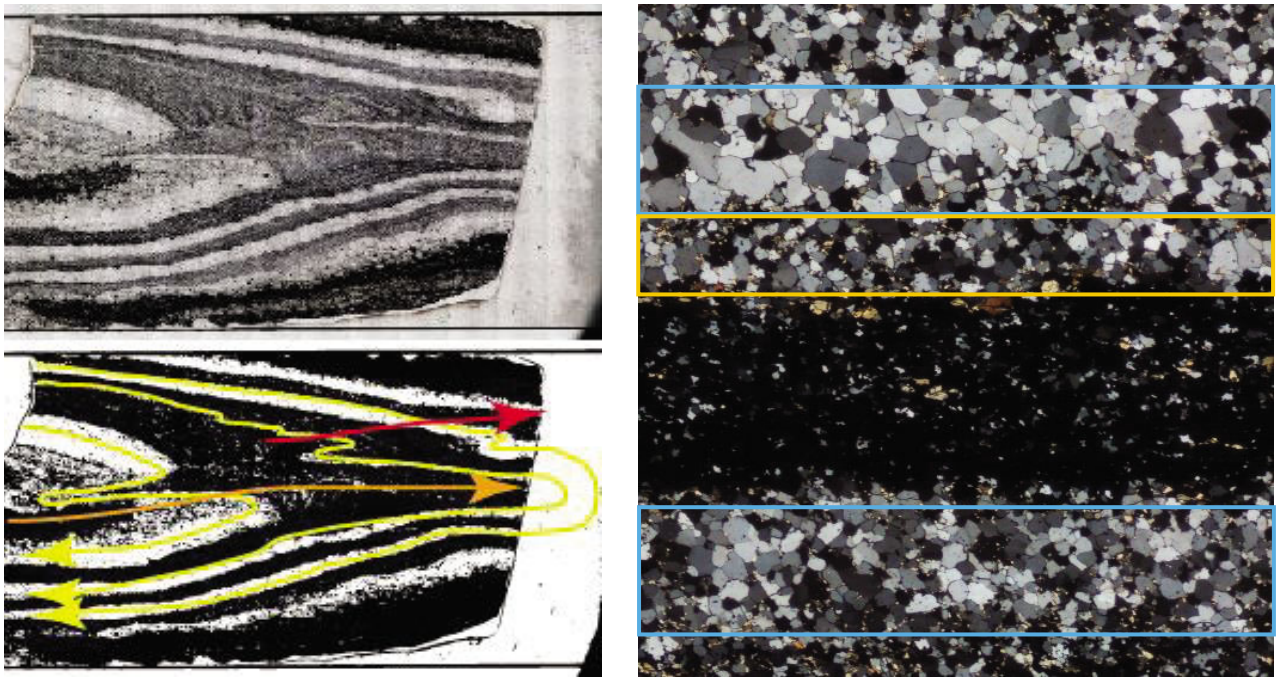

Figure 12c – Left – Showing a slide taken from a BIF father away from the dome. F1 is shown in yellow, F2 in orange and F2+ in red. F1, F2 and F3 exhibit similar planar directions. Right – 2 generations of recrystallisation. Phase 1 in orange outline and phase 2 in blue. These are outlined in detail in table 1.

4.2.1.1 General Petrography: Please refer to table 1 for detailed summary.

Spaced, fold affected, quartz and hematite foliations. Outcrop is preferentially planar to regional scale trending. Microscale and macroscale folding is occurring throughout the outcrop and thin sections (fig12c). Grain boundary recrystallization is seen within the foliations as well as a high amount of undulose extinction within the larger grains (fig12c). This undulose extinction is only seen within the larger grains (phase2) and is indicating a period of high stress and strain at a lower temperature. For this to occur, two deformation events would most likely suffice, with recrystallisation occurring and then undulose extinction occurring during a later (probably retrograde) event.

4.2.2 Serpentinite Schist field appearance and field relationships.

Throughout the whole section schist was present. It was a dominant green in the regional folds with a very serpentinite look, but took on a browner rougher schistose appearance (mainly due to weathering) in the straighter margins between the regional folds. It had a pervasive sheety fabric and a secondary minor fabric which was darker in colour. The main minerals present were elongate green minerals, and minor dark pyroxene minerals. There was also minor small dark brown hornblende. The strike direction of the schistose minerals was averaged north south along the whole section. The fabric showed 2 folding events; The F1 folds exhibited isoclinal closures striking 015 and then being refolded by a co axial planar to the BIF F2 striking around 040. Crenulation lineations were apparent co planar to F1.

Figure 12d – Crenulated serpentinite schist with a pervasive F1 fabric truncated 40 degrees by a F2 crenulated fabric. .

Figure 12e – Prior image of serpentinite schist. 4x zoom, 10x zoom and 25x zoom respectively.

4.2.2.1 General Petrography: Please refer to table 1 for detailed summary.

Elongate, euhedral fan like phenocrysts with an elongate preferential direction co planar to outcrop strike. Minerals include, epidote, serpentinite and muscovite. Epidote is a dull green to clear and has low birefringence colours (a common by product metamorphic mineral).

Muscovite has a high birefringence, is elongate, irregular and rounded. It commonly is stained from nearby hematite grains. Serpentinite is elongate platy and green in TS.

4.2.3 Interbedded Meta Basalts field appearance and field relationships.

These outcrops along the section were always associated with interbedded BIF and schist and ranged from pure black smooth homogeneous basalts to rough lineated gabbros. The southern section was dominated by homogeneous fine grained lineated meta-basalts on the boundary to gneiss, but gradually graded to an intermediate, clastic, coarse grained, equigranular within a fine grained sugary mafic matrix toward the core. The quartz grains ranged from 0.5 - 2mm in size, inter bedding with a fine grained, foliated, homogenous outcropping amphibole (S1 - 314/89/S). These boundaries within the interbedded unit were very clearly defined by bedding surfaces. Amphibole minerals elongate to create an L1 lineation (80--->266). This Lineation was apparent throughout the section and rotated around folds.

Fig12f – Left - Meta basalt columns, faintly lineated with a vertical dipping lineation.

Fig12g – Above - Close up photo of a lineated Meta basalt column. Outcrop scale foliations were not visible. Vertical lineations were present.

4.2.3.1 General Petrography: Please refer to table 1 for detailed summary.

Very fine grained from 0.01-0.03mm minerals. Minerals range from 80% low birefringence amphibole with cleavages at 120 and 60 degrees, to 18% low birefringence, low interference colours, orthorhombic, orthopyroxene. This rock contains around 2% silicates which are generally larger grains that surrounding amphibole and OPX.

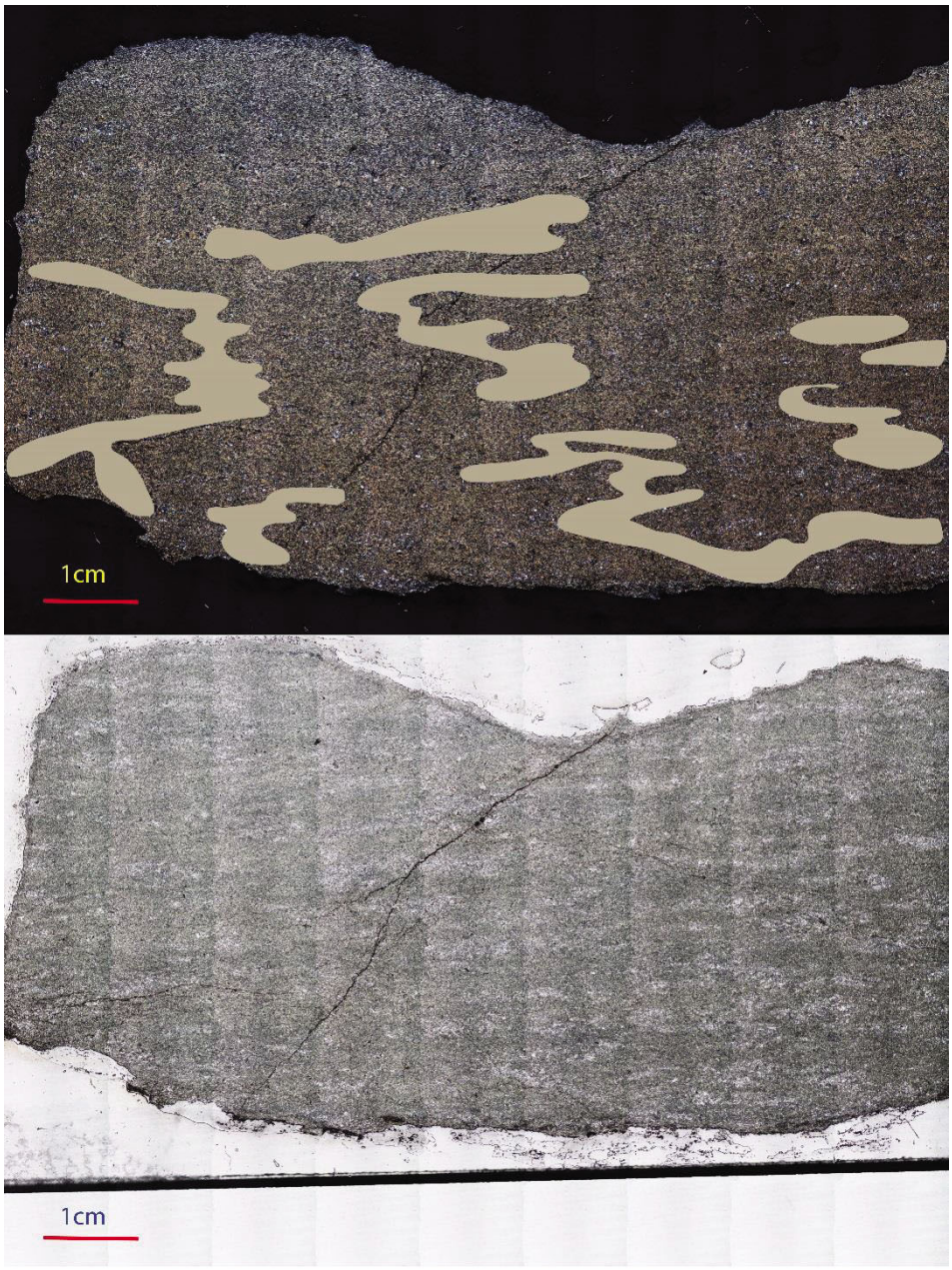

Faint bands visible throughout the thin section and this rock may be the protolith to the altered serpentinite schist seen in previous outcrops.

Figure 12h – XPL and PPL respectively of the meta-basalt unit. Small banding is seen in TS but not in outcrop. 4x zoom.

4.2.4 Layered meta-peridotite field appearance and field relationships:

This highly erosion resistant unit is in direct contact with BIF and schist units. Is it a greenish black in outcrop and weathers green with small lenticular actinolite augens. These elongate augens have a white feldspar like ring surrounding the internal structure and texture. The outcrop exhibits a main S1 pervasive foliated fabric (334/72/E) which is sub parallel to the small crenulations seen in hand specimen. Crenulations are seen co planar to mineral elongation but dip in the opposite direction at 350/76/W and have a pole azimuth of 22 → 354. The outcrop contains small folding that mimic the micro scale crenulations we see in previous serpentinite schists. The outcrop is hard to break with a hammer and glistens in the sunlight. Minerals in outcrop sample resend black elongate amphibole, white feldspar and slaty actinolite.

Figure 13a – Meta peridotite with the red arrow defining the main S1 fabric. White minerals seen are feldspar and black minerals are amphibole. These are creating a dominant L1 fabric.

4.2.4.1 General Petrography: Please refer to table 1 for detailed summary.

Fine grained 0.01-0.1mm, 80%, elongate, nucleation rich altered amphibole. Abundant in poke marks and rotated to be co planar with outcrop strike Myrmekite abundance within the amphibole bands is also apparent. 5% subhedral, Plagioclase, is only seen within siliceous ribbons, has multiple twins and exhibits grain boundary migration recrystallization. Actinolite augens have a fan like appearance. 15% silicate make up the rest of the slide mainly in ribbons. Quartz has 2 different minerals. One being affected major amounts of seritisation due to metasomatism. And the second showing grain boundary recrystallization. The newer grains also exhibit windowing and pinning on new grain boundaries.

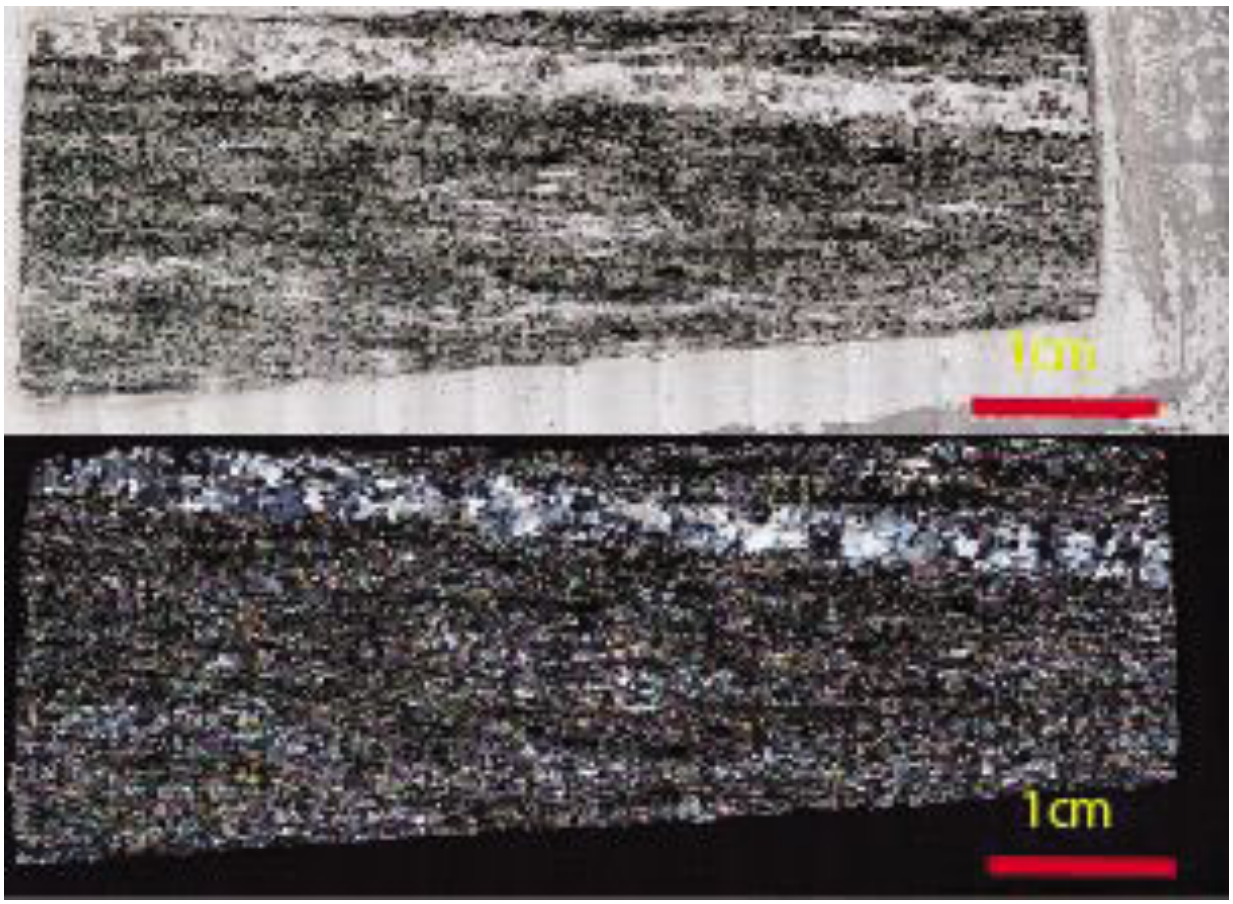

Figure 13b – Peta peridotite PPL and XPL images. Siliceous ribbons are seen within the slide with amphibole making up the rest of the slide.

4.2.5 Foliation field relationships

Foliations in each unit varied in degrees throughout the section but generally all foliations were co planar to regional outcrop strike.

4.3 S1 First Foliation –

Quartz banding within BIF units (fig12c) is interpreted to be the S1. It generally strikes around 320/75/E, dipping with a high angle eastward. It has thing banding (5 – 10mm), with these bands decreasing with proximity to the granites. Serpentinite schist, meta-peridotites and meta-basalts all exhibits this S1, generally in outcrop strike.

4.4 S2 Second Foliation -

The second foliation is seen in thin section with elongation and preferential growth of recrystallised quarts grains. These grains elongate co planar to F2 folding events. Small rotations of grains are also seen toward this F2 fold axis of 018/80/E. Quartz grains are continuous elongates around fold hinges and thus is interpreted to be a younger event. This S2 is evident in the serpentinite schist with figure 13a outlining crenulation axial planes co planar to BIF outcrop S2 planes.

4.5 S3 Third foliation –

The third foliation is interpreted to regional scale folding and is only seen in large scale. Figure 12b outlines the folding seen in high strain zones with S3 coplanar to F3 axial plane at 060/80/E.

Age relationships are outlined in the geological history section.

4.6 Optical Microscopy of 4 greenstone units:

Rock name	Slide #	Table 1 - Notes
BIF Outer margin	123	Fine grained, euhedral, 0.2 – 1mm, decussate quartz and hemeatite mix. A high amount of irregular boundaries typically associated with grain boundary migration. 2 generations of spaced quartz foliations are seen. The first with 98% quartz and 2% opaques with larger grains, undulose extinction and no preferential direction. Windowing and pinning is plainly visible in this well developed quartz. Quartz grains are seriate in size moving toward the center of the bands. The second with 60% quartz and 40% opaques shows evidence of deformed polycrystalline quartz. Grains are very small, potentially formed during a second event at a lower temperature (sub grains rotation recrystallization). Grains are rotated co planar to bands. Opaques have a 'blown apart' texture, with small angular edges and very minimal large grains. Although small amounts of amphibole are associated with the larger grains. Undulose extinct quartz grains are rotated and elongated at low angles indicating potential retrograde metamorphism following recrystallisation.
BIF close to the core	124	Similar to the above BIF, this BIF has been affected by higher temperature due to its proximity to the pluton. 2 quartz spaced foliations are seen again. The first is 0.05mm – 0.1mm 75% quartz randomly mixed with >0.5mm 25% opaques. The polycrystalline anhedral quartz exhibits random orientation with no preferential growth direction. Small nucleation's are dominant throughout this quartz band indicating grain boundary migration. The second is a smaller polymineralic grained band with 0.03mm – 0.05mm 50% quartz, 10% hornblende and 40% opaques. The opaques in this slide are mixed with brown honeblende possibly indicating post or inter kinematic growth between two events.

Metaperidotite with actinolite augens	111	Fine grained 0.01-0.1mm, 80%, elongate, nucleation rich altered amphibole. Abundant in poke marks and rotated to be co planar with outcrop stike Myrmekite abundance within the amphibole bands is also apparent. 5% subhedral, Plagioclase, is only seen within siliceous ribbons, has multiple twins and exhibits grain boundary migration recrystallization. Actinolite augens have a fan like appearance. 15% silicate make up the rest of the slide mainly in ribbons. Quartz has 2 different minerals. One being affected major amounts of seritisation due to metasomatism. And the second showing grain boundary recrystallization. The newer grains also exhibit windowing and pinning on new grain boundaries.
Serpentinite Schist	108	Elongate, euhedral fan like phenocrysts with an elongate preferential direction co planar to outcrop strike. Minerals include, epidote, serpentinite and muscovite. Epidote is a dull green to clear and has low birefringence colors (a common by product metamorphic mineral). Muscovite has a high birefringence, is elongate, irregular and rounded. It commonly is stained from nearby hematite grains. Serpentinite is elongate platey and green in TS.
Meta Basalt sticks	112	Extremely fine grained, 80% anhedral, amphibole, cleaved at 120 and 60 degrees. Minerals are green in PPL and have low to middle, first order birefringence in XPL. Some grains have classic simple twinning with moderate relief. Other minerals include 18% orthopyroxene. The OPX has low first order yellow to brown birefringence colours, is subhedral orthorhombic in shape and has low interference colours affecting the grains. It has high relief common for the proximity to Fe minerals with minimal staining. 2%, euhedral, twinned silicates. These are grey in XPL and clear in PPL with extinction at right angles. The rock is massive and has no discernable alteration throughout the slide.

Table 1: Detailed petrography of the greenstone units at the boundary of the granites.

4.7 Dykes:

There were multiple dykes throughout the area ranging from tonalite to dolerite with a range of textures.

- Dolerite Dyke field appearance and field relationships: The dolerite dyke was consistent within the first 10kms from the margin. It cross cut strata (E/W) perpendicular to main dome trend (N/S). It exhibited a homogeneous outcrop with micro scale feldspar clasts randomly orientated at the contact. The dyke had an extremely fine grained green dark black matrix that was sugary and smooth in texture. The rock had no clear orientation, from the general strike of the outcrop which was parallel to the foliation of the schist. Small elongate variole clast's form when moving from the boundary to the middle of the dyke. These clasts consist of non-metallic platy black spinifex mineral inclusions surrounded by 0.5mm ring of feldspar. The matrix changes from a feldspar clast matrix to a homogenous matrix when moving toward the boundary.
- Tonalite dyke – This dyke was seen in all areas as the absolute last contact between the greenstone boundary and the first gneiss. Extremely fine grained recrystallised matrix with 80% silicates and 20% lineated vertically, elongated, biotite minerals. L1 was 65→095. This dyke composition ranged between monzonite and monzogranite.

5. Granodiorite Gneiss:

Field appearance and field relationships:

Multiple areas of gneiss occurred throughout the outcrops but all tectonites exhibited a granodiorite composition. Areas of higher strain were observed in close proximity to lower strain areas yet the rocks had very similar composition. A varying set of granodiorites are described in detail in this section. The described outcrop was 5kms in from the margin of the greenstones (figure 15) and ranged from interbedded altered amphibolite to Fe affected granite nodules. The outcrop was large (200m x 150m), flat and well exposed. It had minimal vegetation and minimal soils. The outcrop displayed onion weathering on large granodiorite boulders.

Fig14 – Section 1 with magmatic patterns on more mafic matrix rocks. Small lenses of more siliceous minerals formed augens in the outcrop. This outcrop has a higher temperature texture with multiple tonalite veins crosscutting each other.

1. Migmatitic area with high strain, tonalitic melt streaks that cross cut each other within a foliated S/L Tectonite. Elongated feldspar was observed in an S1 (N/S) foliation direction. This contained a cross cutting shear (030/25/E) and what seemed to be an injection within the same outcrop introducing bands of melanic and leucocratic melt. This area was dominated by cross cutting mafic and tonalitic dykes with shearing seen in outcrop at millimetre scale. The shearing was offset sinistrally in a SE direction. (Fig14)
2. Moving eastward. The second area starts to exhibit large euhedral cubic feldspars with no orientation and randomly scattered. They make up the majority of the rock within a fine to medium grained foliated S tectonite matrix. The matrix consists of biotite that wrap around the feldspar clasts in some cases and butt up to others nearby, the remainder of the matrix is quartz. The feldspars are phaneritic and very pure with no inclusions, but do show signs of magmatic growth or zoning. (Fig15a)

Fig15a- Section 2 with dominant euhedral feldspars

3. Phaneritic euhedral feldspars disappear and a strong foliated S Tectonite dominates. This area is highly affected by four generations of dyking. A Fine grained banded migmatitic dyke, a medium grained tonalitic dyke, a coarse grained phaneritic quartz dyke and a feldspar dominant leucogranite dyke. The area is highly foliated by elongate fractured biotite minerals within a fine to medium grained silicic grey matrix. Small feldspar clast's are included within this area, and are elongated co planar to the foliation. Lineation is very faint through biotite elongation with simple shear dominating the area as kinematic indicators show direction of shear. Sigmoidal feldspars are dominant with tails showing dextral top to the west movement when looking north. S-C fabric is seen within the biotite minerals showing up dip movement.

5.1 General Petrography: Please refer to table 1 for detailed summary.

Two distinct areas of recrystallisation is seen within this sample, along with feldspar grain rotation, and formation of quartz ribbons in areas of low stress. These ribbons form co planar to grain rotation in the pressure shadows (Fig 15b). Relict feldspars record D1 magmatic growth, and include small microcline and biotite inclusions. Rotation of these inclusions within the clast point to intertectonic growth. This confirming a D2 tectonic event where quartz growth is co planar to outcrop strike. Myrmakite growth into relict feldspar indicate hydration probably associated after crystallisation within the magma chamber. This slide is a good indicator of two stages of deformation.

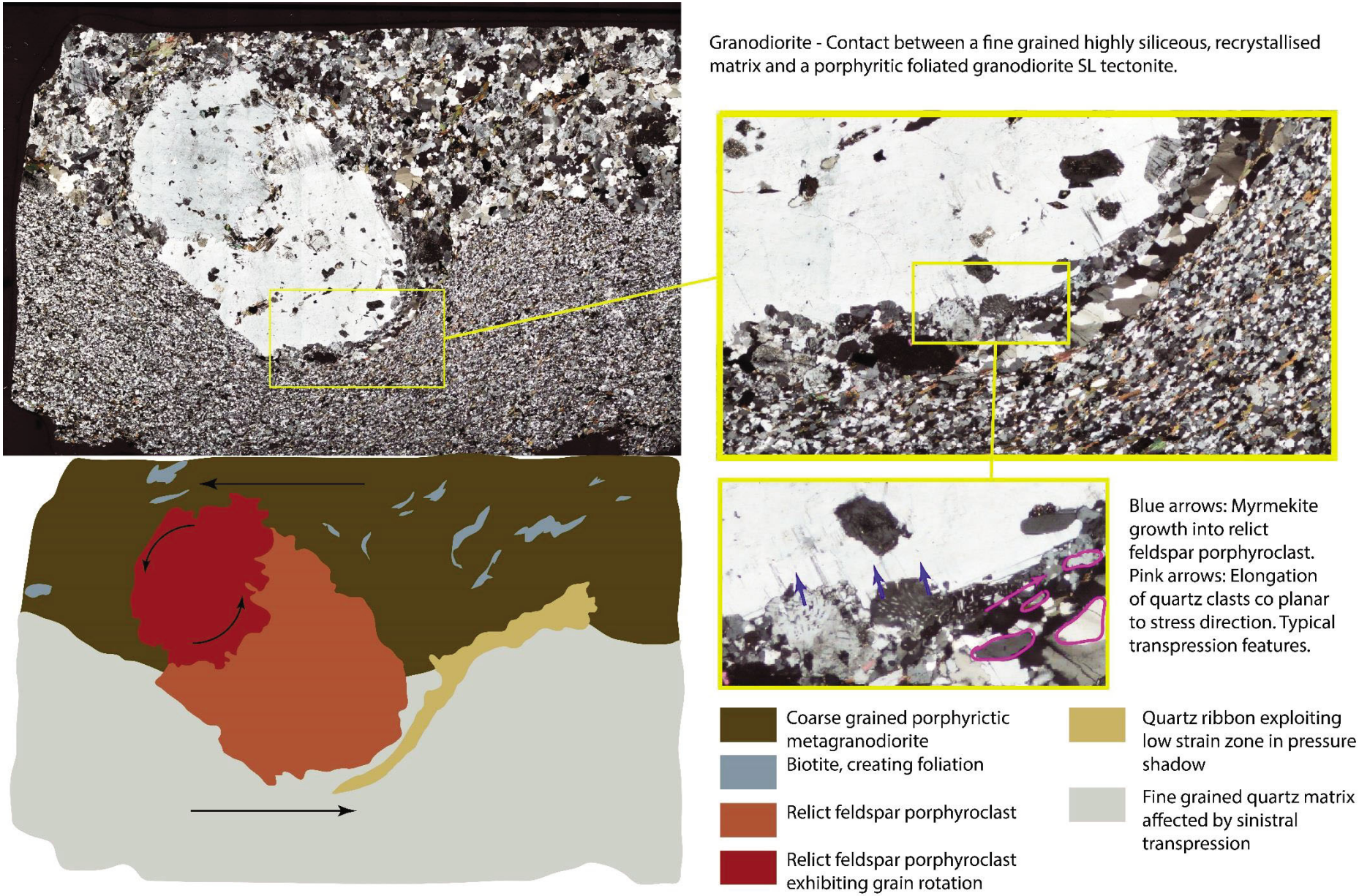

Figure 15b – Sinistral movement of feldspar porphyroclasts. Grain boundary rotation is seen within relict porphyroclasts. S Tectonite.

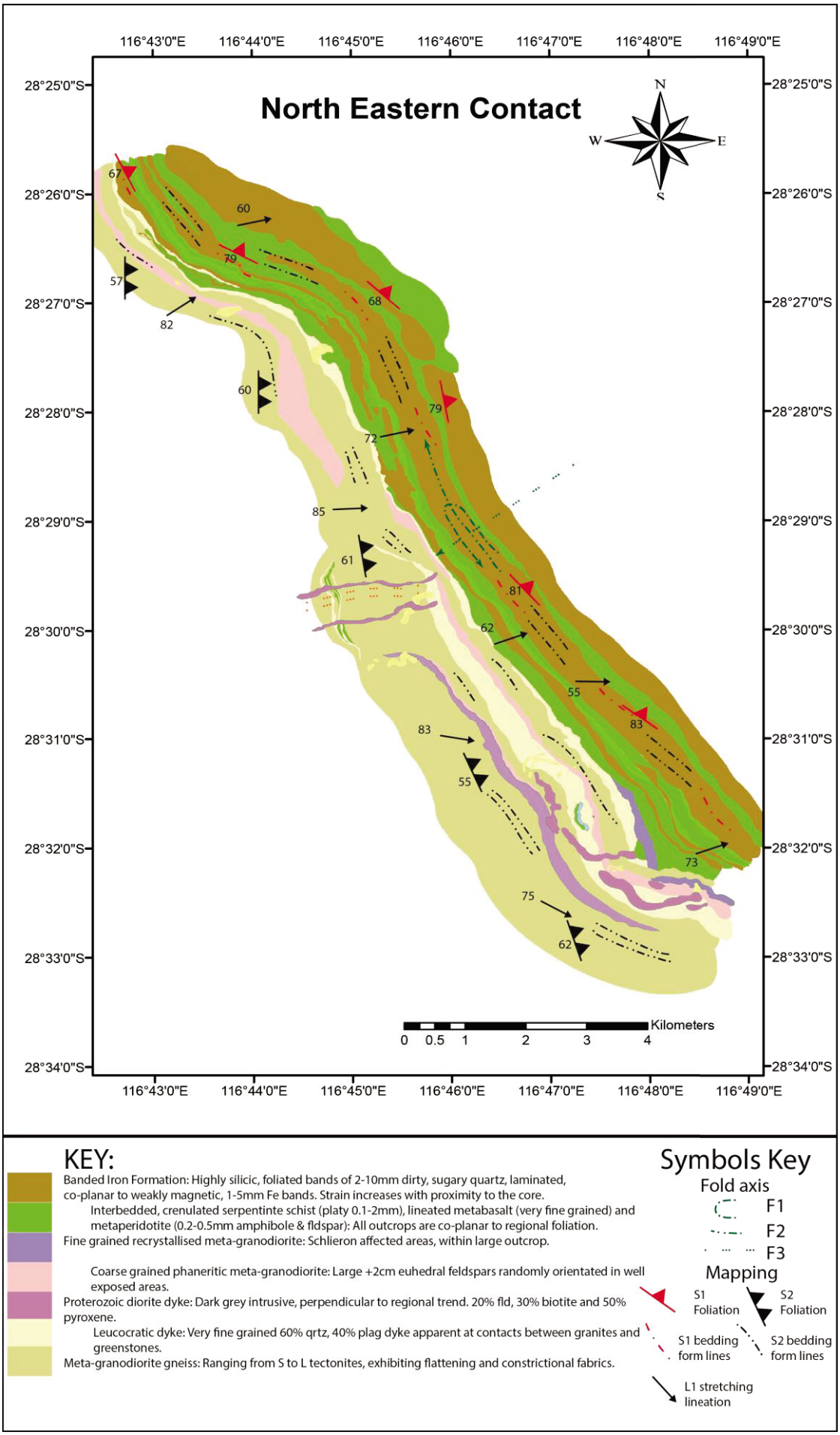

*Figure 16a: Mapped section with structure. General outcrop trend was NW/SE. Greenstone package is outline in brown and green while granites are in beige. *See key.*

6. Cross Section of the mapped area:

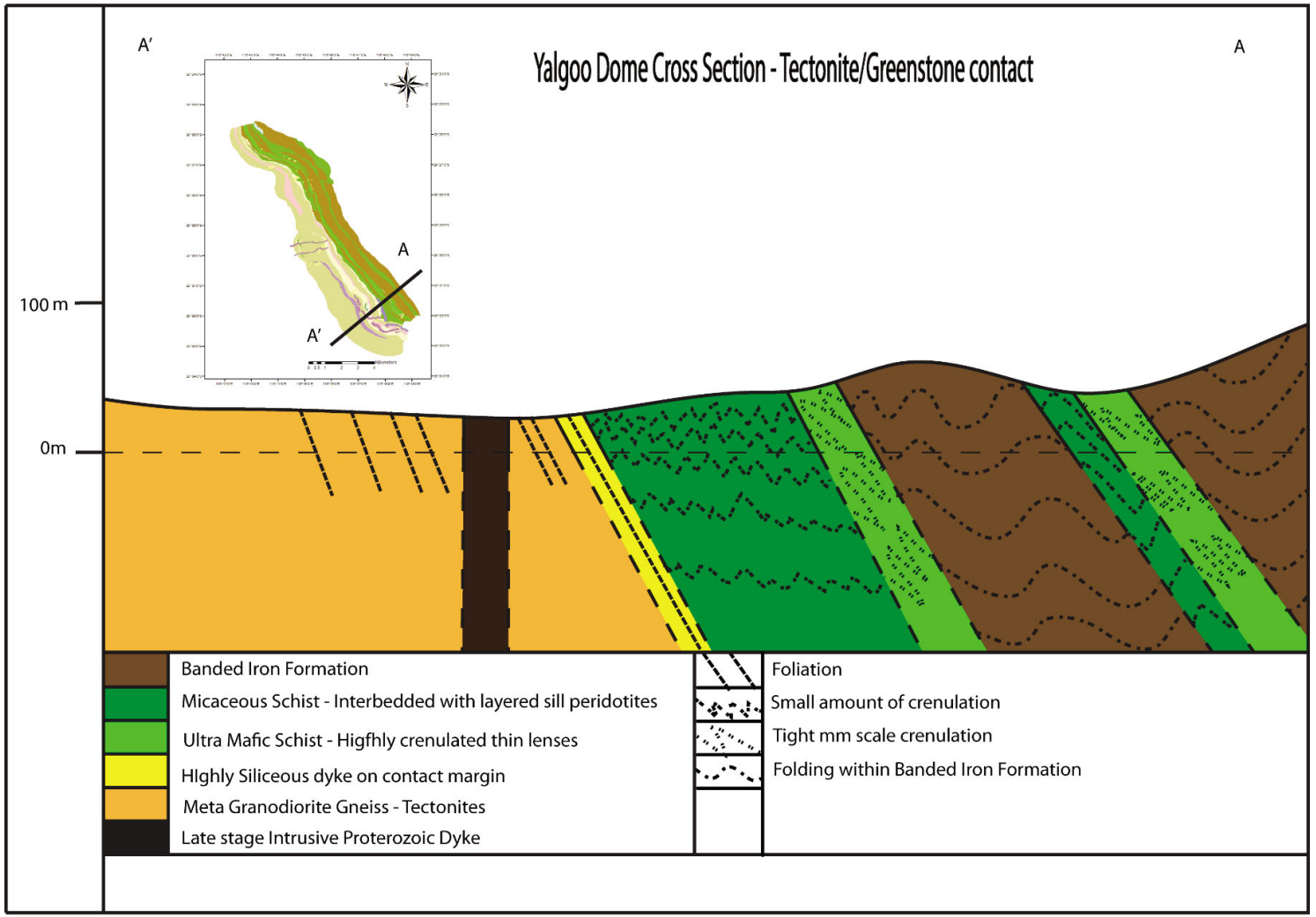

Figure 16b:

A Cross section was created through a detailed mapped area. This area was chosen as is had the most outcrop and visible structure. The section identifies key areas of interest within the BIF, greenstone and gneiss units. BIF units contained evidence of sheath folding with a preferred fold plane, co-planar to outcrop strike. Ultra mafic units contained highly crenulated areas at mm scale. Micaceous schist's contained crenulations along the foliation and were very faint the closer I was to the centre of the dome.

7. Tectonite description

7.1 Lithological units mapped:

Six tectonites were mapped, determining their field relationships. These were L, LLS, LS, SL, SSL and S, there were additionally 2 sub categories within a SSL Tectonite section outlined in detail above and seen in (fig14 & 15a) these were; a highly affected phaneritic K-feldspar section with blasts greater than 10mm (figure15a), and an area with higher temperature textures (additional veins, elongate feldspar and schlieren). The southern mapped section was a dominant monzogranite/monzonite gneiss with a dominant lineation (L Tectonite). Moving north, outcrops changed into a foliation dominant granodiorite gneiss(S Tectonite). A general description of the two tectonite end members is below:

Field appearance and field relationships:

L Tectonite: Biotite creating mineral stretching lineation 42→ 074, within a very fine grained sugary texture matrix, made up of equal percentage of quartz and feldspar (80%). No Large clasts are seen in outcrop. Very homogeneous rock outcrop with no foliation present.

Fig17a – Top and side view of the L tectonite Granodiorite.

- *S Tectonite*: Dominantly granodiorite with biotite creating a foliation and lineation. Pure S Tectonite were observed in the north section of figure 19a. This was the only locality of a pure un-lineated sample. These were largely affected by phaneritic cubic euhedral K feldspar with simple twinning 15-30mm and were scattered randomly. They had no preferred orientation but were banding in localised areas. Biotite created the pervasive fabric (fig 17b) within these S Tectonite areas and folded around the existing clasts. The mineral assemblage was 30% biotite, 50% K-feldspar, 20% quartz. The biotite were elongated from 2mm – 10mm and were averaging 8mm forming a foliation and exhibited s-c fabric (fig17a). There were groupings of black shiny cubic pyroxene minerals creating lenticular elliptical clast's concentrating in small accumulations. The quartz was very rough throughout the section, and looked to be re crystallising around the feldspars. There was oblique conjugate brittle deformation throughout the tectonites looking to be stronger around Proterozoic dykes, striking north south.

Fig17b – Pure S Tectonite Granodiorite. Clasts can be seen to be affected by either magmatic growth or internal zoning. Clasts rotation is also seen.

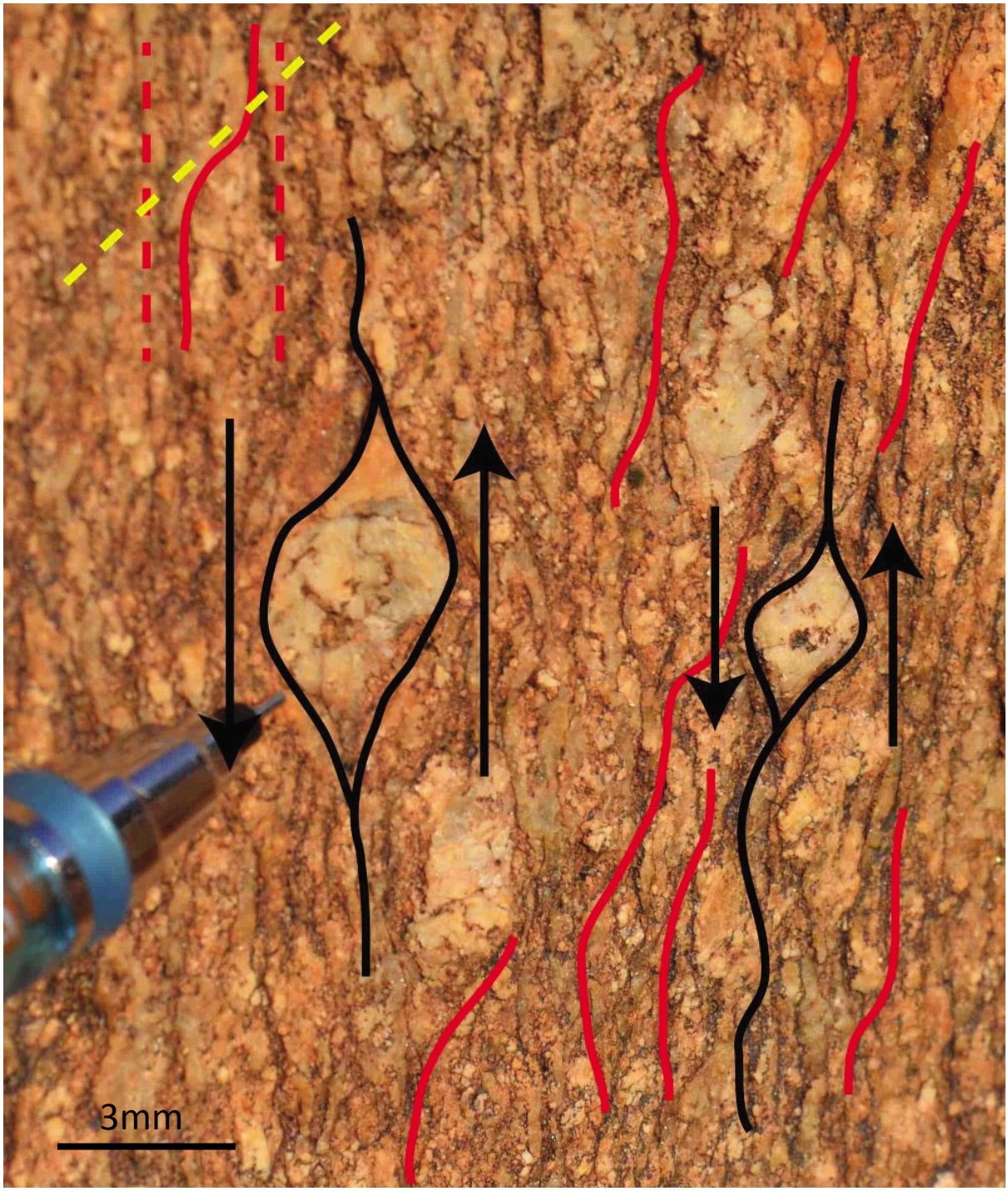

Fig17d – Pure S Tectonite Granodiorite. Sinistral rotation of sigma clasts viewed on outcrop perpendicular to foliation and parallel to lineation. S-C fabric is also seen outlined by dominant biotite.

Sigma clasts with sinistral motion were visible in outcrop along the XZ plane (fig17d),

although the abundance of the indicators was very limited.

7.1.1 General Tectonite Petrography: Please refer to section 11 for a detailed summary

L Tectonite: 70% highly altered relict and recrystallised quartz, mixed with 30% zoned and altered feldspar dominate this lineated tectonite. Quartz grains are overall bigger and annealed. Undulose extinction is apparent throughout with rotation of grains toward lineation. Feldspar are K dominant with single twinning and high degrees of sericite alteration.

S Tectonite: 60% euhedral quartz, affected by undulose extinction and grain boundary recrystallisation. 40% feldspar with a mix between plagioclase and microcline. Twinning is abundant in these fractured and rotated blasts. Small amount of zoning is present. Biotite creates the foliation. Evidence of boudinage is seen within TS, with associated recrystallisation within necks. Migmatite and sericite alteration is also abundant within S Tectonites.

Figure 17e – L Tectonite vs S tectonite thins section images. Lineations extend throughout the l tectonite via biotite stretching. The biotite in the S tectonite can be seen to be cut off while creating the foliation.

8. Distribution of Tectonites

Distribution of tectonites was parabolic in relation to regional folding. L Tectonites were abundant near to internal folding and areas of high deformation (close proximity to folded and refolded BIFs). Where S Tectonites were seen at areas of low deformation. The combination of this analysis identifies that tectonite formation is strain dependent, where constriction forms L tectonites and flattening forms S tectonites (fig 10a, 10b).

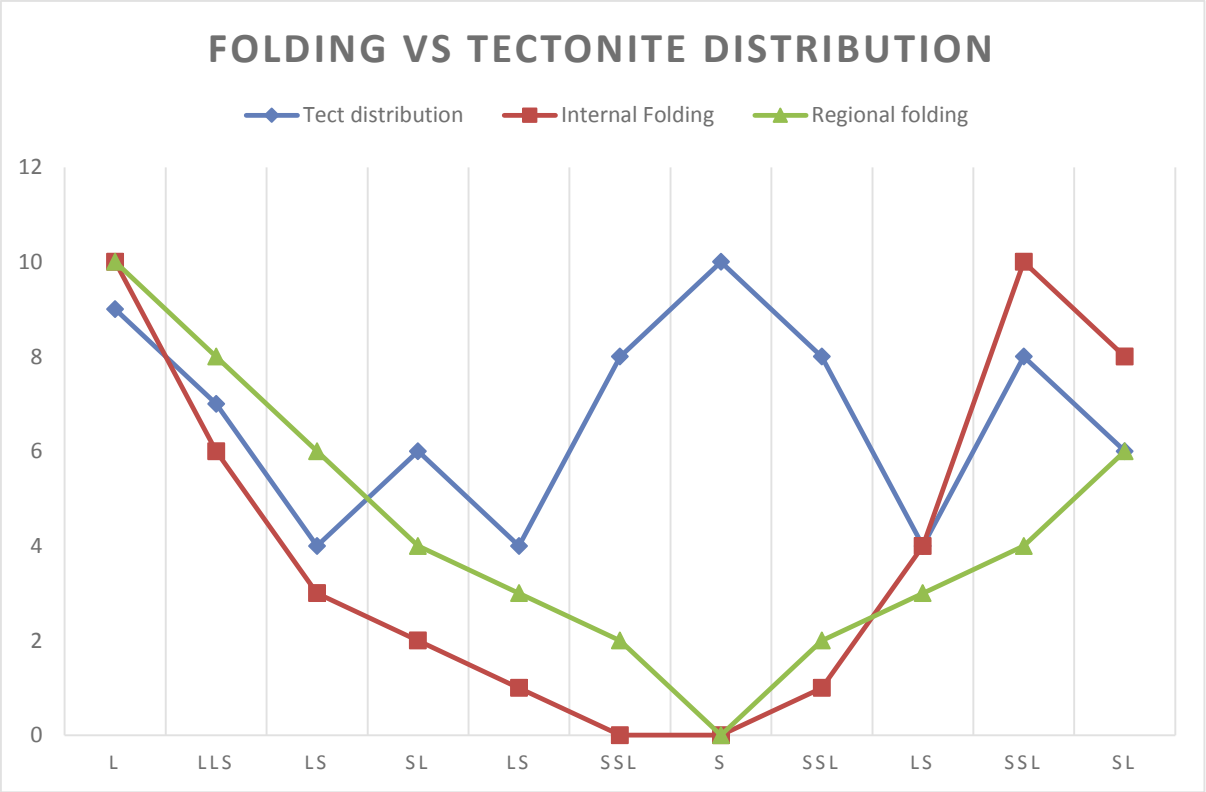

Figure 18 – Regional and internal folding vs tectonite distribution table. X values identify tectonite type. Y values indicate degrees of value with 10 being the highest possible value. "The S Tectonite is 100% identifiable within an area affected by 0% of folding".

The comparison introduces the idea of a combination of tectono-metamorphic processes and doming. This can be seen above with the foliations dominant at low folding areas. Lineations are dominant through vertical pluton emplacement and constriction, with S tectonites forming through tectonic process or a higher stress combination of the two.

The following map shows the distribution of tectonites throughout the mapped section. A detailed description of the key is outlined in the tectonite petrography section.

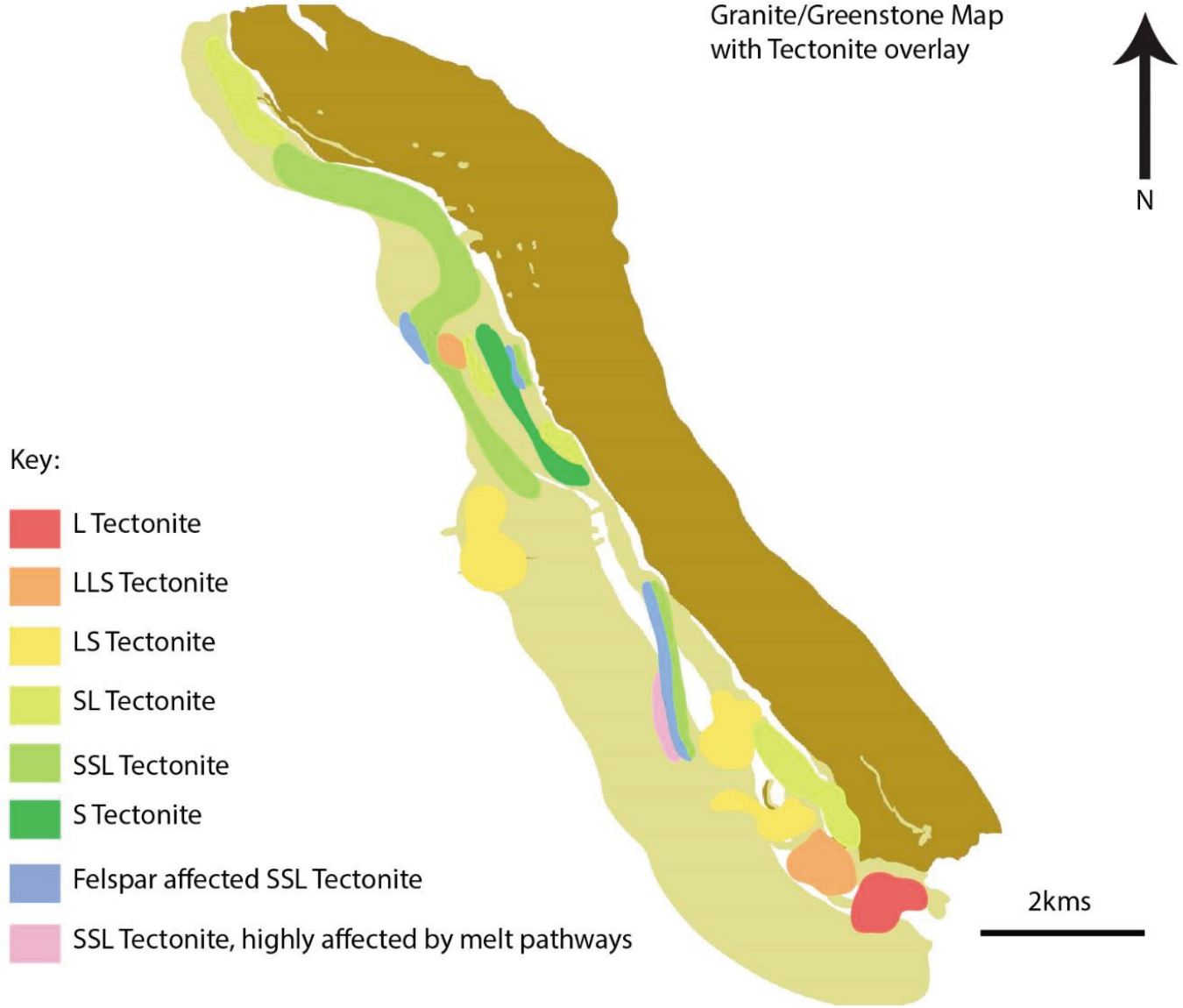

Figure 19a – Tectonite distribution map, overlaying the granite/greenstone map. Varying degrees of tectonite is seen above outlined in the key.

9. Stereonet Analysis

Plotting of structural data was done using stereoplot, dividing each outcrop into corresponding colours, according to type. The data plotted outlined general foliation trend and general lineation trend. The data was recorded along the northwest transect concentrating on the main S1 pervasive fabric, with any unique features noted. When all the data was plotted individually, it outlined the following folds:

F1 Greenstones 353/85/E	N/W trending, moderately plunging (55°) to the east, upright (85°), tight (19°), circular, symmetric, mm to meter scale outcrop fold.
F2 Greenstones 026/62/E	N/W trending, moderately plunging (42°) to the east, steeply inclined (62°), close (31°), circular, asymmetric Z, meter scale outcrop fold.
F3 Regional fold 060/86/E	W trending, steeply plunging (62°) to the north, upright (86°), close (35°), circular, symmetric, km scale regional fold.

Table 2: Fold analysis

Planar fabrics in figure 20 outline the regional fold that the dome is affected by. Rotation of planar dipping directions rotate southward upon northward movement in the transect (fig 19b) due to regional folding. Linear fabrics are clustered with an average direction for all fabrics to be dipping 60 toward the east. The grouped data of the lineations outlines that it is the last event or is being shielded from greater tectonic processes affecting the rest of the dome. This dyke graphically confirms (light blue dots in fig 20) rotation from a westward dip to a southward dip. This change is easily observed in figure 20a shown by rotation of arrows. Due planar fabrics forming as the last event from regional tectonic processes occurring after or contemporaneously with pluton emplacement, it can be said that the constrictional formations of L tectonites have been shielded by the tectonic processes, and not rotating.

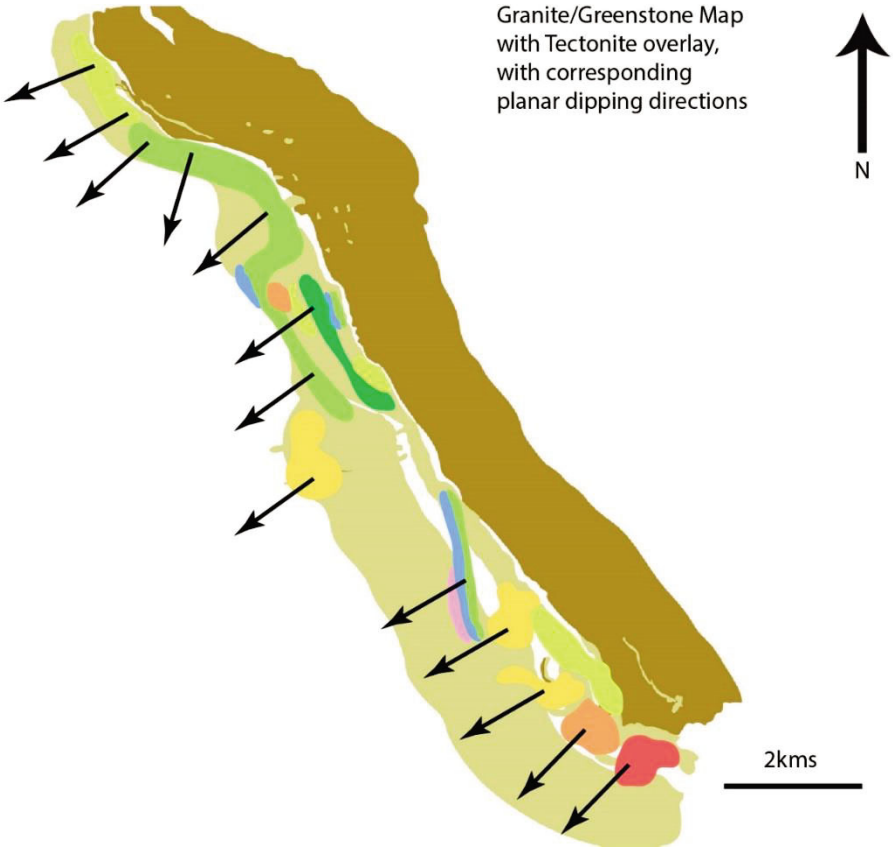

Figure 19b – Granite greenstone overlay indicating dipping directions of planar fabric.

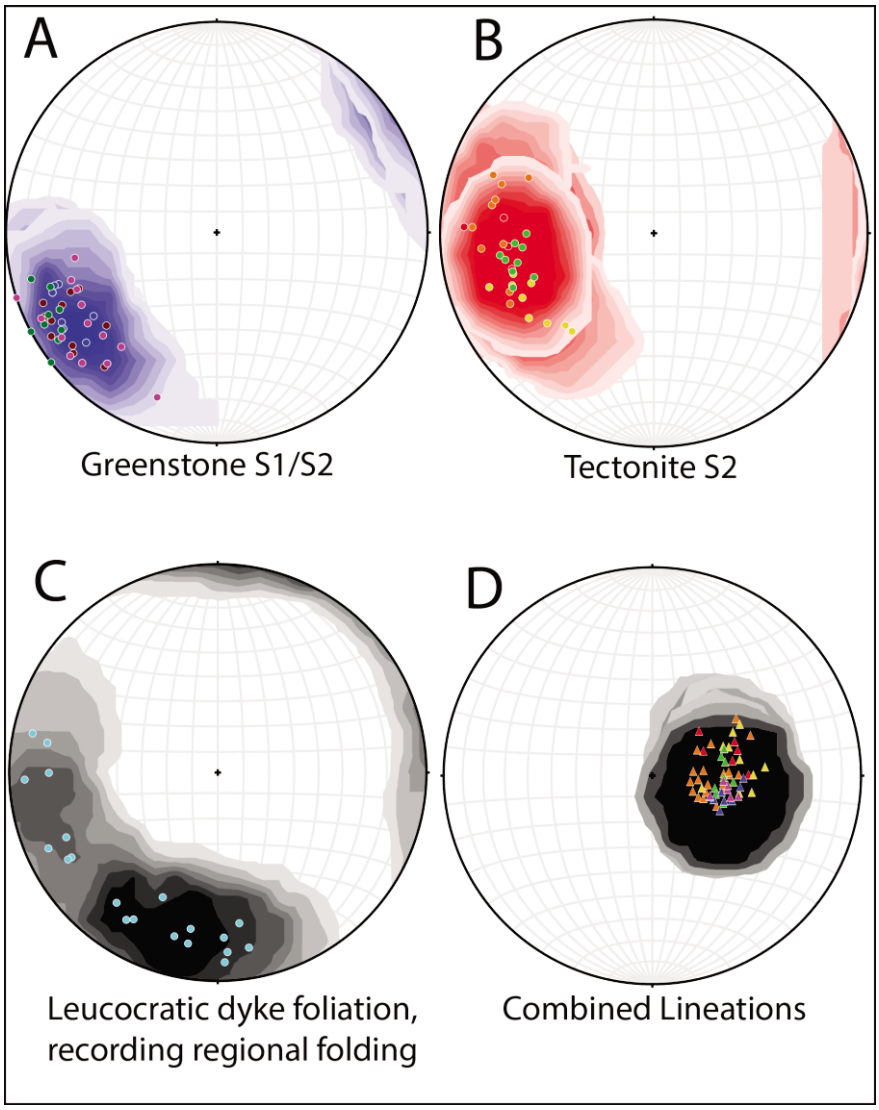

Figure 20 – Stereo-net data for Greenstones (top left), Tectonites (top right), regional tonalite dyke (bot left) and lineations (bot right).
Greenstones show initial folding event or sagduction/sheath folding process. Tectonites outline another tectonic influence and the tonalite dyke records all events of the regional scale folding event. Lineations all plot within a small area indicating very similar stretching lineations, intersection lineations and crenulation lineations.

10. Flinn diagram analysis

Classic prolate and oblate analysis via a Flinn diagram was done to confirm strain ellipsoid stretching directions of L and S Tectonites. Stretching along the XY plane will give a cigar shape ellipsoid, while flattening along the XZ plane will outline a pancake ellipsoid. The data outlined that L tectonites collected from the field plotted within the prolate extensional field and the S tectonites plotted within the oblate flattening field. This confirmed field observations of linear (cigar shaped L tectonites) and planar (pancake shaped S tectonites) tectonites throughout the section.

Data was plotted from the statistical values collected in table x and normalized to fit within a value of 5.

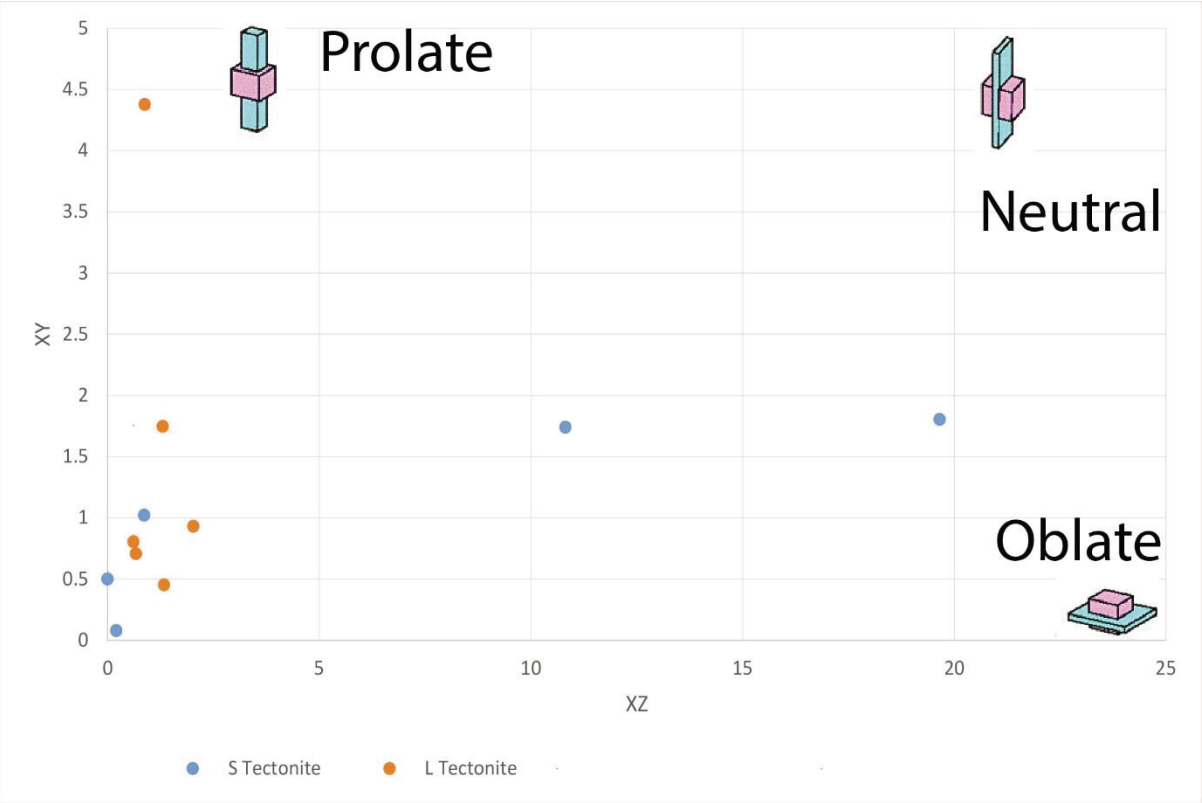

Figure 21 – Statistical values of S tectonite VS L tectonites. Values plotted confirmed field relationships of linear dominant fabrics in the south and planar dominant fabrics in the north.

11. Tectonite General Petrography

11.1 Introduction

This chapter outlines samples analysed to gain a better understanding of the mineral assemblage, tectonic indicators, magmatic textures and any metasomatic process that have occurred within the North East section of the Yalgoo Dome. This section will also outline deformation sequences and any over printing that has occurred within the samples. This will help us identify sequences of events, mineral relationships, any recrystallization and metamorphism identification.

11.2 Analytical Method

Fifteen samples were mounted on glass slides and polished to a thickness of 30µm. These are from specific areas correlating to potential variations in deformation events (Pure S, S>L, L>S and L). These areas are located at the extreme south and every quarter to the extreme north of the mapped section (fig 19b). The samples were analysed under petrographic microscope, looking at PPL and XPL. The sampled sections and results are tabulated below.

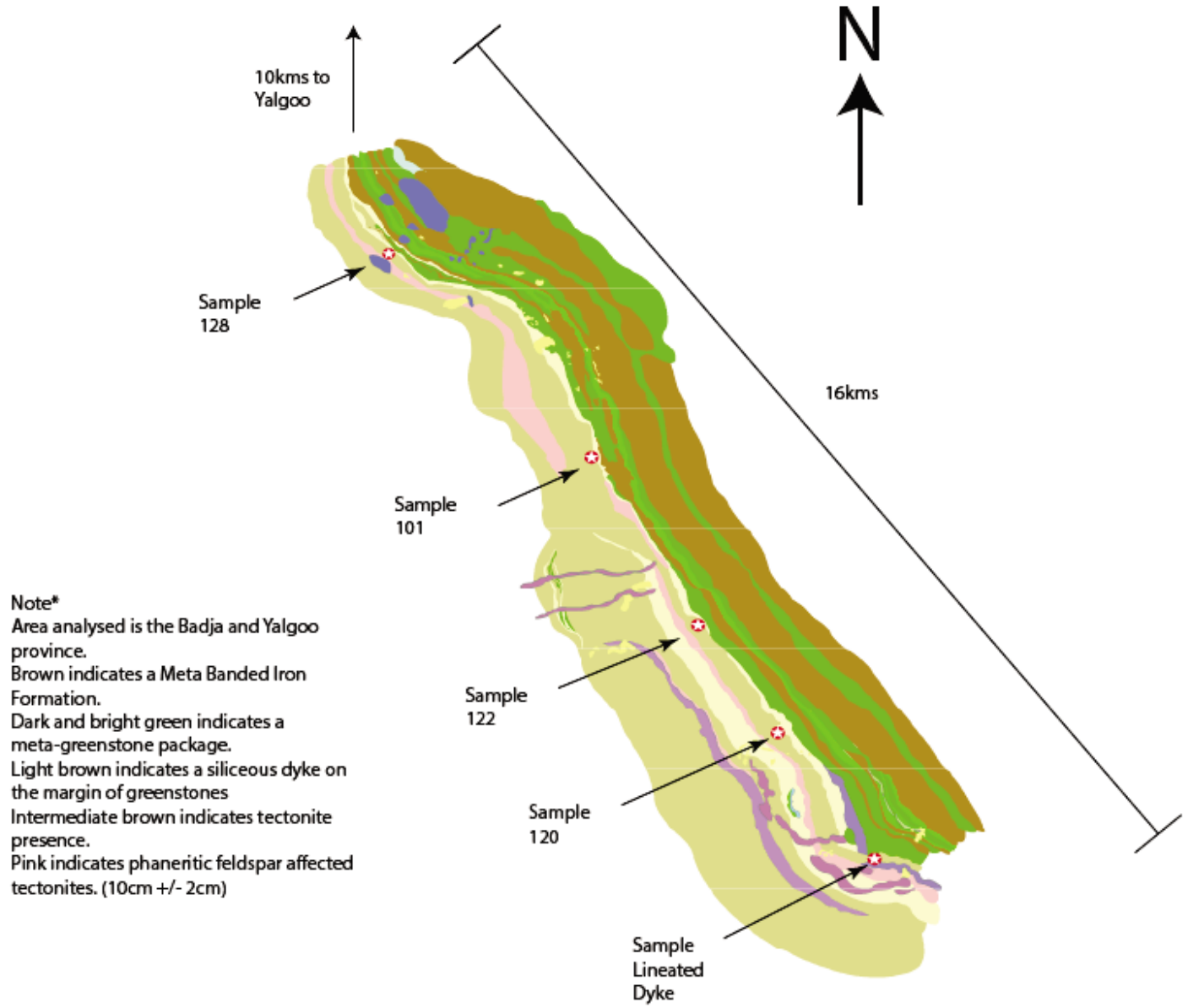

Figure 22 – Analysed areas within the dome for deformation, mineralogy and formation identifying the evolution of the dome.

Minerals	Mode & Sample #	Mineral Size mm	Table 3 - Notes – S Tectonite – ZY cut
	101		All Samples were analysed under 2x and 5x zoom in PPL and XPL
Quartz	55%	Min: 0.5 Max: 15 Mean: 6	Undulose extinction visible in 90% of minerals, mainly within the larger grains. The smaller grains are unaffected due to younger recrystallization. The quartz is preferentially growing into smaller minerals with triple junctions forming at 30° angles. Multiple poikiloblastic xenoliths are visible within the larger grains.
Microcline (undeformed)	10%	Min: 3 Max: 50 Mean: 10	Grey and black twinning, with the microcline spreading into younger quartz grains. Mymakite texture at boundaries of K feldspar and quartz.
Microcline (deformed)	15%	Min: 2 Max: 60 Mean: 6	Cross hatch, highly altered mineral with a slight graphic texture, looks to be older than the undeformed microcline as boundaries overprint. Multiple poikiloblastic xenoliths with a very weathered appearance, some crystals have subhedral margin but are mainly anhedral.
K Feldspar	5%	Min: 0.5 Max: 2 Mean: 1	Single twinning when found unaltered. Anhedral margins and mainly always in contact with microcline.
Biotite	6%	Min: 1.5 Max: 7 Mean: 5	Brown to light brown pleochroism at 90°, elongate, planar with cleavages parallel to foliation. Biotite forming the main S1 fabric within the rock.
Green Horneblende	3%	Min: 0.5 Max: 15 Mean: 6	Green to dark green, there are also some minor amounts of brown horneblende. Green is associated with quartz while brown is associated with microcline.
Apatite or albite?	1%	Mean: 0.2	Associated next to microcline crystals. Clear, low relief, high birefringence in the 1st order. Clear with brown staining in other areas. May be staining from the iron oxides.
Myrmakite	5%		Wormy vesicular patterns, always associated next to or recrystalising the microcline.
Opaques, Titanite, CPX, Chlorite	Minor amounts		Multiple opaques of Hematite (Fe3+). Highly fractured and randomly scattered. Possible source from the close by BIF's.

Minerals	Mode & Sample #	Mineral Size mm	Table 4 - Notes – SSL Tectonite – ZY cut
	128		All Samples were analysed under 2x and 5x zoom in PPL and XPL
Quartz	70%	Min: 0.1 Max: 2 Mean: 0.3	Euhedral large grains, undulose extinction visible in 50% of minerals, mainly within the larger grains. Randomly oriented minerals, Larger grains are heavily fractured and annealing. Multiple poikiloblastic xenoliths are also visible within the larger grains.
Microcline (undeformed)	15%	Min: 0.2 Max: 1 Mean: 0.4	Grey and black twinning, with the microcline is spreading into younger quartz grains. Smaller amounts of myrmakite texture at boundaries of K feldspar and quartz. Highly fractured and random. Foliation within blasts is co-planar with S1 foliation.
Biotite	7%	Min: 0.5 Max: 1 Mean: 0.6	Brown to light brown pleochroism at 90°, elongate, looks to be crystalizing along fractures. Biotite is forming the main S1 fabric within the rock. The sheets look altered and deformed, they have a fractured look about them.
Brown Horneblende	3%	Min: 0.2 Max: 1 Mean: 0.3	Minimal amounts, pleochroic from brown to dark brown and glassy. Seems to be associated near Apatite.
Apatite	2%		Associated next to microcline crystals. Clear, low relief, high birefringence in the 1st order. Clear with brown staining in other areas. May be staining from the iron oxides.
Myrmakite	3%		Wormy vesicular patterns, recrystallisation occurring at anheadral microcline boundaries.
Opaques, Titanite, CPX, Chlorite	Minor amounts		Multiple opaques of Hematite (Fe3+). Fractured clasts have a preferred orientation co-planar to S1.

Minerals	Mode & Sample #	Mineral Size mm	Table 5 - Notes – SL Tectonite – ZY cut
	122		All Samples were analysed under 2x and 5x zoom in PPL and XPL
Quartz	40%	Min: 0.2 Max: 2 Mean: 0.5	Grains are rotating toward foliation direction. Slide appears to have relic sigma clasts that have been recrystallized and deformed. Some are circular euhedral (younger) and others are completely altered, anhedral, fractured clasts (older)
Microcline (undeformed)	20%	Min: 0.2 Max: 3 Mean: 0.7	Large altered crystals, some look to be rotated with evidence of a foliation within. Poikiloblastic quartz xenoliths remain within the grains.
Biotite	20%	Min: 0.4 Max: 1 Mean: 0.6	Brown to light brown pleochroism at 90°, elongate, planar with cleavages parallel to foliation. Preferentially forming around relic sigma clasts or quartz. Some of the biotite look to be altering to epidote potentially meaning a retrograde environment.
Myrmakite	10%	Mean: 0.6	Invading microcline from a quartz origin along anheadral boundaries. 95% of microcline grains are being affected in this area showing wormy vesicular patterns.
Apatite	5%	Mean: 0.2	Associated next to microcline crystals. Clear, high relief, high birefringence in the 1st order. Colourless.
Muscovite	2%	Mean: 0.1	Minor amounts, colourless, accosiated near biotite, co planar with foliation, not deformed.
Opaques, Titanite, CPX, Chlorite	3%		Multiple opaques of Hematite (Fe3+). Highly fractured and randomly scattered. Much more within the sample than other samples.

Minerals	Mode & Sample #	Mineral Size mm	Table 6 - Notes – LS Tectonite – ZY cut
	120		All Samples were analysed under 2x and 5x zoom in PPL and XPL
Quartz	65%	Min: 0.2 Max: 10 Mean: 5	Low relief, dirty quartz, zoned larger grains from a dirty poikiloblastic middle to euhedral boundaries. Grain rotation has occurred as the pieces of quartz have broken apart. Heat may not have been enough for crystals to deform plastically. Undulose extinction through large crystals, and is not present in small crystals. Annealing, recovery and static recrystallization present. Static recrystalisation is probably due to an H2O component.
Microcline (undeformed)	20%	Min: 0.5 Max: 15 Mean:	Minimal amounts, crystals have been fractured and scattered. Original clasts may now be exploded. Very messy look, cooler rocks, not as close to the margin of the dome and is showing signs. Large crystals with messy edges, quartz is recrystalising into the Microcline. Definite foliation running through the microcline, which is, rotated 40 degrees to S1 in the rock. Grains are highly poikiloblastic (very pockey) these may possibly be old plagioclase grains.
Microcline (deformed)	N/A		
K Feldspar	N/A		
Biotite	8%	Min: Max: Mean:	Brown to dark brown pleochroism. Elongate and streaky. Biotite is on the verge of altering into chlorite. This may be altering into chlorite through retrograde metamorphism. Seems to be 2 distinct types of grains, 1; newer grain with a platey smooth texture, 2; an older grain with a streaky appearance and visibly deformed.
Green Horneblende	6%	Min: Max: Mean:	Foliated, pale green to mottled green pleochroism. Flakey and sheety. Biotite and epidote replacing the hornblende in some areas.
Apatite	1%	Mean:	High birefringence colours. Very small amounts, usually located next to quartz. Apatite is colourless but sometimes takes on a cloudy appearance. Apatite is also seen within the centre of the cloudy altered quartz. Some small amounts within this slide have iron staining.
Myrmakite	N/A		
Opaques, Titanite, CPX, Chlorite	Minor amounts		Titanite is seen within the zoned poikiloblastic quartz. Elongate, randomly oriented and monoclinic. Displays a high birefringence.

Minerals	Mode & Sample #	Mineral Size mm	Table 6 - Notes – L Tectonite – ZY cut
	L Dyke		All Samples were analysed under 2x and 5x zoom in PPL and XPL
Quartz	55%	Min: 0.5 Max: 15 Mean: 6	Undulose extinction visible in 90% of minerals, mainly within the larger grains. The smaller grains are unaffected due to younger recrystallization. The quartz is preferentially growing into smaller
Microcline (undeformed)	10%	Min: 3 Max: 50 Mean: 10	Grey and black twinning, with the microcline is spreading into younger quartz grains. Mymakite texture at boundaries of K feldspar and quartz.
Microcline (deformed)	15%	Min: 2 Max: 60 Mean: 6	Cross hatch, highly altered mineral with a slight graphic texture, looks to be older than the undeformed microcline as boundaries overprint. Multiple poikiloblastic xenoliths with a very weathered appearance, some crystals have subhedral margin but are mainly anhedral.
K Feldspar	5%	Min: 0.5 Max: 2 Mean: 1	Single twinning when found unaltered. Anhedral margins and mainly always in contact with microcline.
Biotite	6%	Min: 1.5 Max: 7 Mean: 5	Brown to light brown pleochroism at 90°, elongate, planar with cleavages parallel to foliation. Biotite forming the main S1 fabric within the rock.
Green Horneblende	3%	Min: 0.5 Max: 15 Mean: 6	Green to dark green, there are also some minor amounts of brown horneblende. Green is associated with quartz while brown is associated with microcline.
Apatite	1%	Mean: 0.2	Associated next to microcline crystals. Clear, low relief, high birefringence in the 1st order. Clear with brown staining in other areas. May be staining from the iron oxides.
Opaques,	Minor amounts		Multiple opaques of Hematite (Fe3+). Highly fractured and randomly scattered. Possible source from the close by BIF's.

12. Metamorphism

12.1 General Metamorphism

Contact and regional metamorphism was observed in outcrop moving toward the center of the dome. A general texture change due to heat and pressure was seen in outcrop through a variety of observations, these are noted below:

- Banded Iron Formation: Thinning of hematite bands from cm to mm scale moving closer to the margin. High grade folding changes when moving to the core. Multiple generations and rootless folding is seen at the outer margins, conversely when moving toward the dome, tighter more siliceous folding is seen. Mineral mix with the last generation of BIF seen to display minimal folding and straight bands are seen.
- Greenstone: Similar to the meta-BIF unit, the greenstones are stretched northwest along the whole transect. This is probably due to a combination of pure and simple shear. The meta-peridotite unit evolves from a rough grained unit with visible euhedral amphibole porphyroblasts (farthest from the margin) to a unit with fine grained, lineated, elongate, cleaved columns.
- Quartz rich tonalite: Upon reaching contact from the greenstone and the granite, runs a highly siliceous dyke varying from 1m to 10m in some areas. This was visible at all areas upon contact between greenstone and granites. Forming during intrusion of the pluton this dyke is likely formed from mobilisation of silicates from the surrounding hydrous greenstones.

With contact from the pluton directly impacting the surrounding greenstones, grain boundary recrystallisation was apparent with proximity to the margin and the core (fig 12c).

12.2 Subset of Metamorphism: Hydrothermal alteration component

12.2.1 Sericite and Myrmekite

Sericitization is one of the more common types of hydrothermal alteration found in felsic rocks (Que and Allen, 1996). Although sericitization can occur in multiple areas within feldspar grains, these samples showed definitive sericitization within the core showing outward growth, leaving the margins of the feldspar vacant. Sillitoe (1979) outlines multiple case studies within Au, Cu mineralisation areas such as the Yalgoo dome where seritisation is quite common.

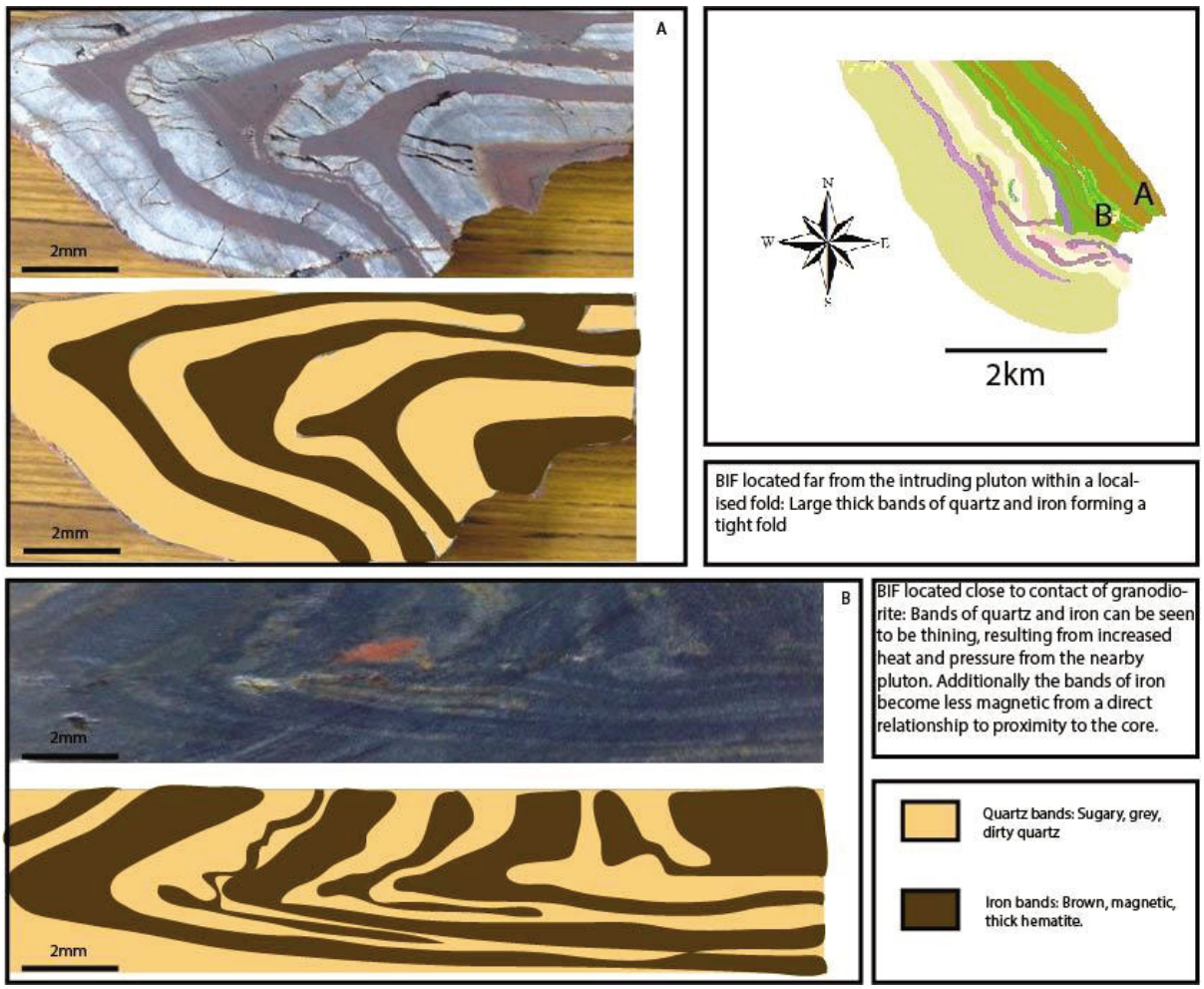

Figure 22a – Contact metamorphism of BIF. Top image is 2kms from contact of pluton and the bottom image is 500m from contact of the pluton.

13. Deformational history

13.1 Summary from field observations:

Data and fabrics obtained from the field results, thin sections and stereo net analysis all display signs of multiple generations of events. Some textures display permanent deformation through grain rotation and undulose extinction yet some plastic display intracrystalline deformation only visible in thin section. With deformation inducing strain and raising lattice energy in grains, recovery acts upon impeded grains. This recovery and dynamic recrystallization process is seen clearly in (fig 15b) where polymineralic quartz, feldspar and mica align to produce elongated grains and schistosity.

Multiple events occurring throughout the Yalgoo Batholith has created this well preserved greenstone and granites sequence.

2 distinct options for the tectonic evolution and deformational history are presented;

1. Syntectonic emplacement: After initial formation of the greenstone packages, volcanism and pluton emplacement dominated. The initial D1 event of degasification of a tonalitic pluton resulted in uplift into overlying greenstones. The pluton consequently creates associated sheath folding within BIF units and a dominant lineated fabric seen on the X plane of the Greenstones (fig12a, 13a). This emplacement aided toward the creation of sigma clasts (fig 17a) seen on the X axis of SL tectonites showing sinistral movement. During this emplacement, contemporaneous N/W regional shearing occurred creating a sinistral N/W shearing component. This continued during cooling of the pluton and associated surrounding contact and regional metamorphism. A second influx of tonalite creating a D2 event then creating migmatites.

2. Multiple stage deformation (fig22): Tectonic processes dominate a faulting greenstone terrain where thrusting and fault drag potentially occurs. D2: Greenstone packages are overturned through a process of fault propagated folding. D3: The granite pluton rises through the crust, amalgamating large sections of greenstones from the surrounding country terrain, consequently hydrating the melt and increasing the melt temperature. During emplacement, the surrounding greenstone packages sink through sagduction processes, creating deformed planar fabrics and solid state recrystallisation of the initial greenstone packages. Importantly, this intrusion creates a trending, dome specific, eastward dipping strata (fig22c). During the described emplacement, contact metamorphism affects surrounding minerals creating polymorphs (actinolite) and associated fabrics (fig12c, 22b). Pluton associated deformation ceases but retrograde metamorphism continues through low angle sub grain rotation. D4: Regional scale N/W transpression occurs in a sinistral motion causing tectonites to form within areas of different stress and strain (fig10a). L tectonites form in the south and the north, but continuous episodes of this transpressional phase overprints previous lineated fabrics due to strain at specific locations, consequently over printing, forming SL tectonites. Brittle simple shearing affects local areas of outcrop forming offset dykes and sheared areas within outcrop.

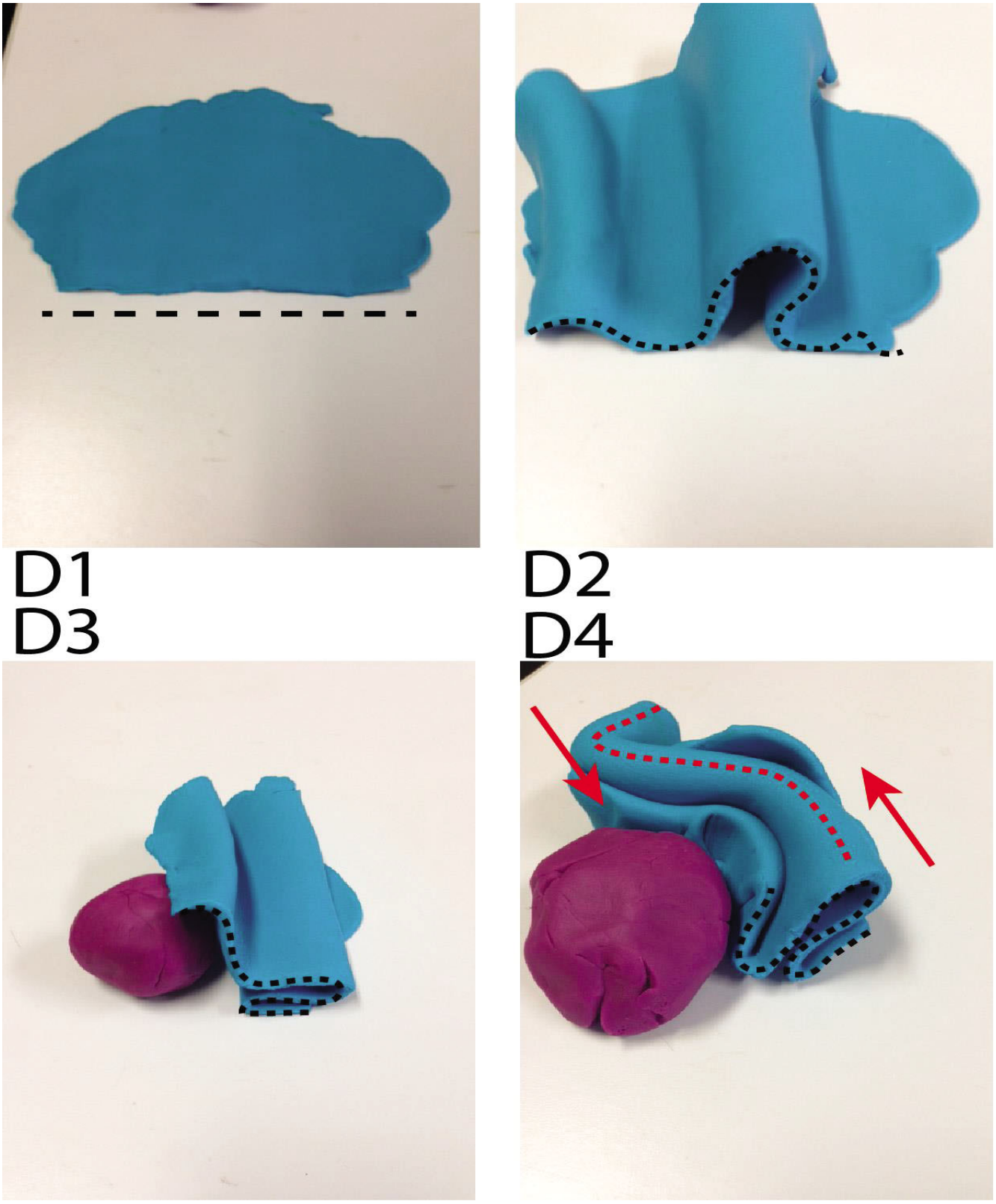

Figure 22b – Multiple stage deformation shown through moldable play dough. D1, D2, D3 and D4 are all affected by different stress, temperature and strain on the associated outcrops. Blue dough indicates greenstones and purple indicates an intrusion.

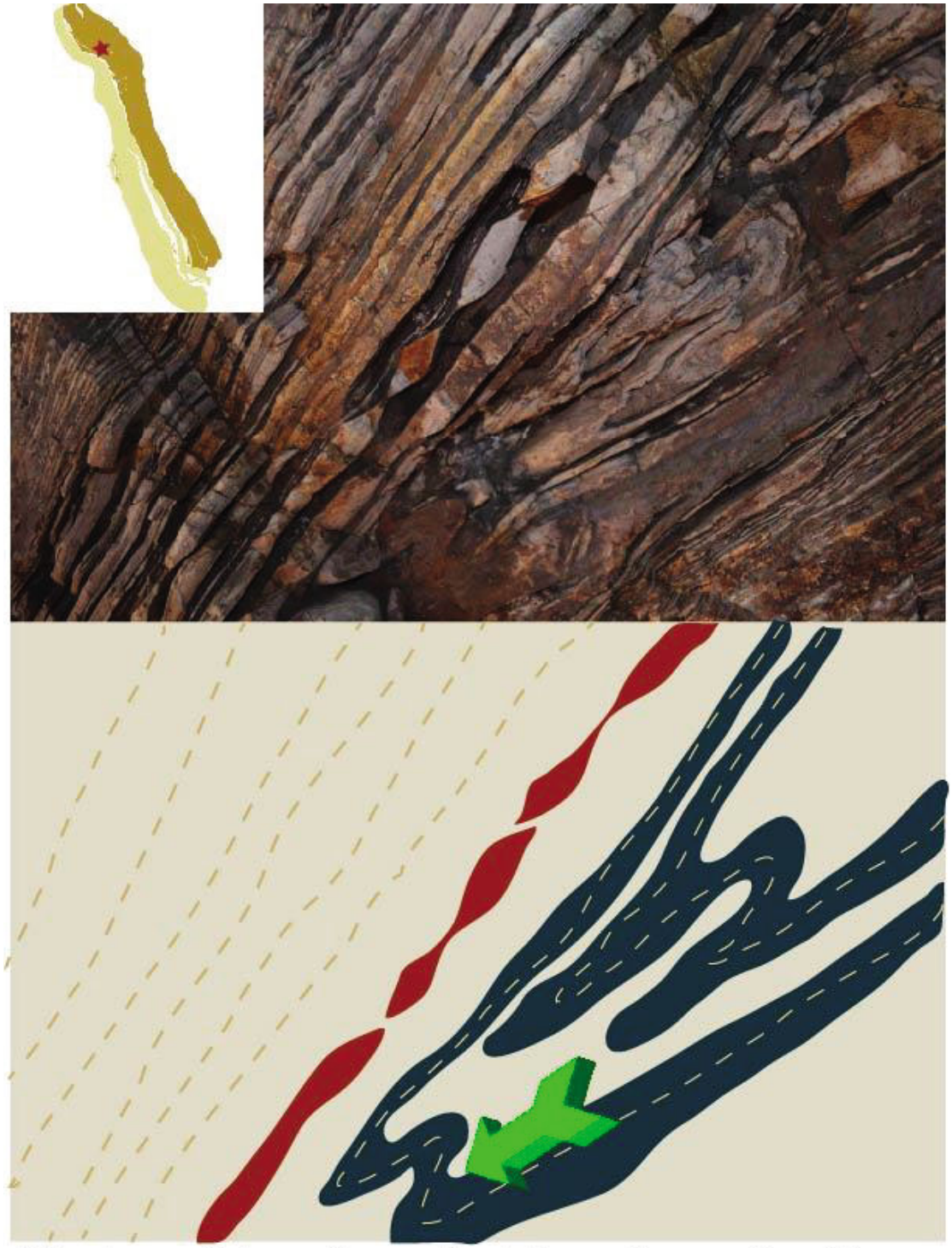

Figure 22c – Deformed BIF outcrop, illustrating boudinage and isoclinal folding in stratigraphic sequence. Dotted lines indicate planar fabrics, red indicates boudinage and blue outlines folding within the BIF sequence.

14. General Geological History based on field relationships: Yalgoo greenstones and granites.

14.1 Introduction:

The following table is constructed to outline the associated events as per interpretation from field studies. It is intended to give the reader a summary and general description from details described in the previous sections. A text outline combined with a geological table will be used to illustrate the history.

14.2 Geological History:

A volcanic arc, deep water depositional environment hosts original chemical muds, forming Algoma style banded iron formations. Deposition continues forming layers of BIF. Contemporaneous basaltic flows and obduction through over thrusting of oceanic mafic and ultramafic rocks, interbed these layers creating initial greenstone sequences. Tectonic processes impacting the arc from the west push eastward, folding the package initially. Deep mantle processes initiate a felsic magma chamber, and associated rising of the pluton begins. Crystallisation starts to occur as the pluton cools, and produces large euhedral, cubic feldspars (15a, 17a) and large quartz clasts. As the pluton rises, contact is made to the greenstone package, consequent solid state re-crystallisation and contact metamorphism commences. Intrusive and extrusive mafic units metamorphose to form interbedded serpentinite schists and meta-peridotite layers. Upon initial contact folding changes (fig22b) from a tectonic dominated thrusting to sagduction related folding recording vertical lineations. Consequently recording three folds in the BIF outcrops. An F1 isoclinal fold that is folded sub parallel to a F2 tight fold followed by a F3 regional gentle fold which is hardly seen in outcrop, but easily visible in aero photo.

Contact metamorphism continues with the BIF recording contact aureoles (higher temperatures and strains (fig22a)), with proximity to the contact of the granite dome intrusion. Cooling and mineralogical recovery continues.

Tectonic processes reactivate sinistrally in a NW motion with rotating transpressive movement. This forms folds within the outcrops and tectonite textures are created. L tectonites dominant in hinge zones affected by a combination of pure and simple shear, gradually changing into a succession of L to S tectonites moving northward. S tectonites dominate in the simple shear environment to the north. Planar features are formed in the extension dominant area in the north dominated by simple shear. Regional folding occurs later folding the F3 fold described above and diorite dykes exploit axial planes of the folding event throughout the dome.

Detailed Geological History Table					
Yalgoo Dome					
Symbol	Facies	Erosion	Intrusion, Metamorphism: symbol	Description	Earth Movement
					Uplift and major erosion to present day
				Diorite dyke	
			D5, F3		Regional EW trending, steeply plunging, upright, close, circular, symmetric folding.
				Offset brittle deformation. Offset leucocratic dykes	NW-SE sinistral faulting
	S & L Tectonites		D4, F2	Combination of extension and compression	NW-SE trending, mod E plunging, steeply inclined, close, circular, asym Z, transpressional folding
				Low grade met'm (meta peridotite formation)	Sagduction of greenstone package
				Hydration of melt, from ingestion of surrounding greenstones.	
	L Tectonites		D3	Circular, Felsic diapir, contact met'm	
	Non-conformity			Uplift and erosion	
			D2, F1	Low grade met'm (local slaty foliation and schistose development)	Regional, E Thrusting, fault prop folding and drag folding.
	Chemical muds				
	Deep marine, Basalt eruptions				
	Dunite, Hazbergite,		D1		obduction oceanic crust

Fig 22d – Geological history, outlining processes involved from initial formation.

15. Outstanding analytical work

To be provided by GSWA. As part of the research thesis, samples were to be collected and prepared for geochemistry and geochronology. Items have been submitted for analysis but there are no results at time of submission.

15.1 Geochemistry

15.1.1 Methodology and acquisition.

Samples were taken from specific areas in the north and south of the mapped area to delineate any anomalous chemistry within the S and L Tectonites. The rocks were acquired using a sledge hammer from dry, fresh outcrops at optimal locations. They were then recorded and bagged in the field until I returned to the Department of Minerals and Petroleum at Carlisle. The samples were then crushed to fists sized specimens with any weathering, dirt, moss or additions removed. This process of contaminant removal was done by saw. The samples were then scrubbed, washed and dried on an oven to ensure no contaminants were present.

Geo chemistry was sent off for analysis as part of ongoing research and a thesis component for GSWA. Results have not been collected or analysed.

15.2 Geochronology

15.2.1 Methodology and acquisition.

Samples were taken from buckets at Macquarie University on the 25th of August and crushed via a hydraulic crusher, into small size fragments around the size of a thumb. The fragments were then take and processed with a Selfrag to split the sample into individual grains and minerals. The processing within the Selfrag was done at 200 point surges until the samples were completely disintegrated. The product was then sorted into via <600

micron mesh and <300 micron mesh with the remaining fine grained product panned. This was then separated into heavy mineral panned, and light mineral panned products. All products in their corresponding micron sizes were then dried in a dehumidifying oven at 90 degrees Celsius. Once these dried they were transferred to non-stick paper and a hand magnet was used to remove any large magnetic minerals. The concentrate was then put through a Frantz Machine to separate magnetic minerals by increasing the magnetic field. This was done 3 times each at 10, 22 and 60 volts. Once the samples were processed via the Frantz machine the samples were run through mineral separation using a density solution. The samples were analyzed via mineral density solution separation at a density of 3g/cm3, this allowed the zircons to drop down through a funnel while quartz, feldspar and apatite floated within the liquid. The samples were then flushed with de ionized fluid to remove any of the density solution, and looked at under microscope to attain percentages of zircons for a 1gram concentrate. Sorting was then done under microscope and samples were packed and sent to the Geological Survey of Western Australia, Department of Minerals and Petroleum for mounting and analysis.

The extracted zircons had a definable size difference in the concentrate that was extracted. There were 2 sizes; smaller elongate grains that were a lighter pink colour, hexagonal, and were interpreted as Zircons, but could also have been titanite. The second zircon was a larger grain, dark brown in colour with a euhedral crystal structure, the faces exhibited concoidal fracture patterns on some surfaces.

Geo chronology was sent off for analysis as part of ongoing research and a thesis component for GSWA.

The table on the following page outlines the samples.

Sample number	Zircon % per 1 gram	Zircon description
214101 Magnetic Zircons	40%	Dark brown to dark reddish brown, large, elongate prismatic, tabular, euhedral, angular, concoidal fractures.
214101 Non-Magnetic Zircons	10%	Light Pink to colorless, small, euhedral, elongate prismatic, tabular, angular zircons.
214138 Non-Magnetic Zircons	30%	Dark brown, large, elongate prismatic, euhedral, angular, concoidal fractures.
214139 Non-Magnetic Zircons	25%	Dark brown large and light pink small, elongate, euhedral, angular, concoidal fractures.
214140 Non-Magnetic Zircons	15%	Light pink small, elongate prismatic, euhedral, angular, hexagonal, concoidal fractures.

Table7: Description of zircons posted to the GSWA for processing, mounting and dating.

16. Part 2: Research Project: 'Doming' or regional structural interference pattern – Insights from tectonite type.

16.1 Introduction

Tectonites exhibit a range of internal and external structures dependant on the specific singular or multiple strain mechanisms and deformation kinematics at the time of formation. Early work by Flinn (1965) outlines the variation in homogeneous strain directly impacting tectonite formation. Due to linear and planar formations, the study of internal textures can be valuable in determining previous metamorphic conditions. Rocks with pure linear fabrics, (L tectonites), often indicate nearly perfect constrictional deformation, conversely S tectonites, appropriately indicate near perfect flattening strain. Sullivan (2013) combines detailed study on constrictional formations (L Tectonites), outlining local variations from external boundary conditions can localize components of constriction. This includes releasing and restraining bends in shear zones, linear channels in shear zone boundaries, intersections between shear zones, and foliation triple junctions between ballooning diapirs. Combining the conditions outlined above, L tectonites are often localized internally in fold hinge zones, similar to the Yalgoo dome (fig 19a). The most common factor in the formation of L tectonites is an external kinematic framework that involves simultaneous transport of perpendicular shortening in two directions. Therefore, large domains of L>S and L tectonites are a common feature of orogen-parallel elongation. These With constrictional and flattening strain throughout the dome, initial formed L tectonites combine with a later transpression event stretching and rotating producing range of L to S tectonites, forming in different margins.

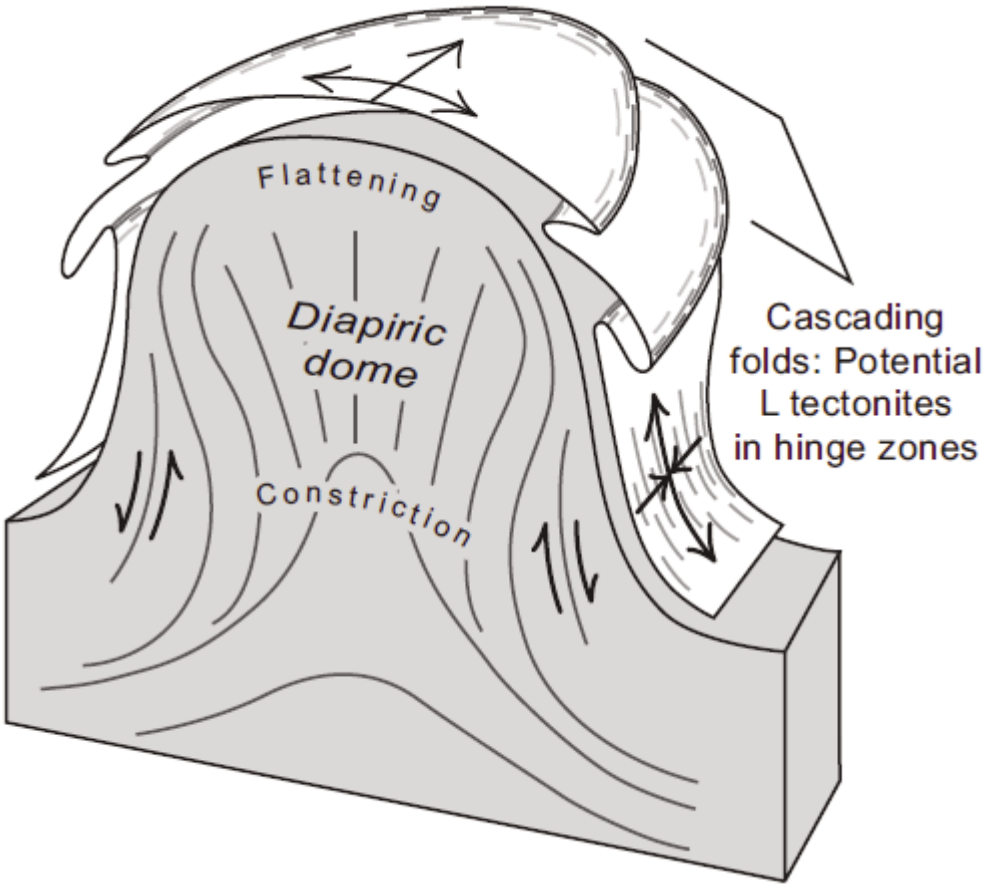

Figure 23a – A rising diapiric dome adapted from Sullivan (2013), forming L tectonites on the margins of the dome possibly combining with sagduction. Dominant flattening occurs at the top of the dome.

Sullivan combines multiple case studies of L tectonite formation, and outlines lengthening shear being the most common external kinematic framework under which L tectonites form. In every case, second- and third-order mechanisms play important roles in the partitioning and localization of constriction and flattening, consequently forming L and S tectonites. Importantly, constrains of external boundary conditions are very important in forming L tectonites in areas of density-driven vertical doming or tectonics (fig23a). However, in many other geological settings, internal variations in structural setting and rheology appear to be the most common forcing mechanisms specifically driving localized L tectonite formation (fig23b). L tectonites tend to form in compositionally homogeneous rocks similar to the

granodiorite gneiss found throughout Yalgoo, while heterogeneous rocks (Greenstone and BIF's) accommodate constriction through folding. With this research, it is said that, L and L>S tectonites are commonly found in fold hinge zones, which is seen within Yalgoo outcrop. Finally, any episode of additional local or regional metamorphism, can obscure original textural relationships, although orientation of the grains and original crystal lattice could provide proof to its original formation.

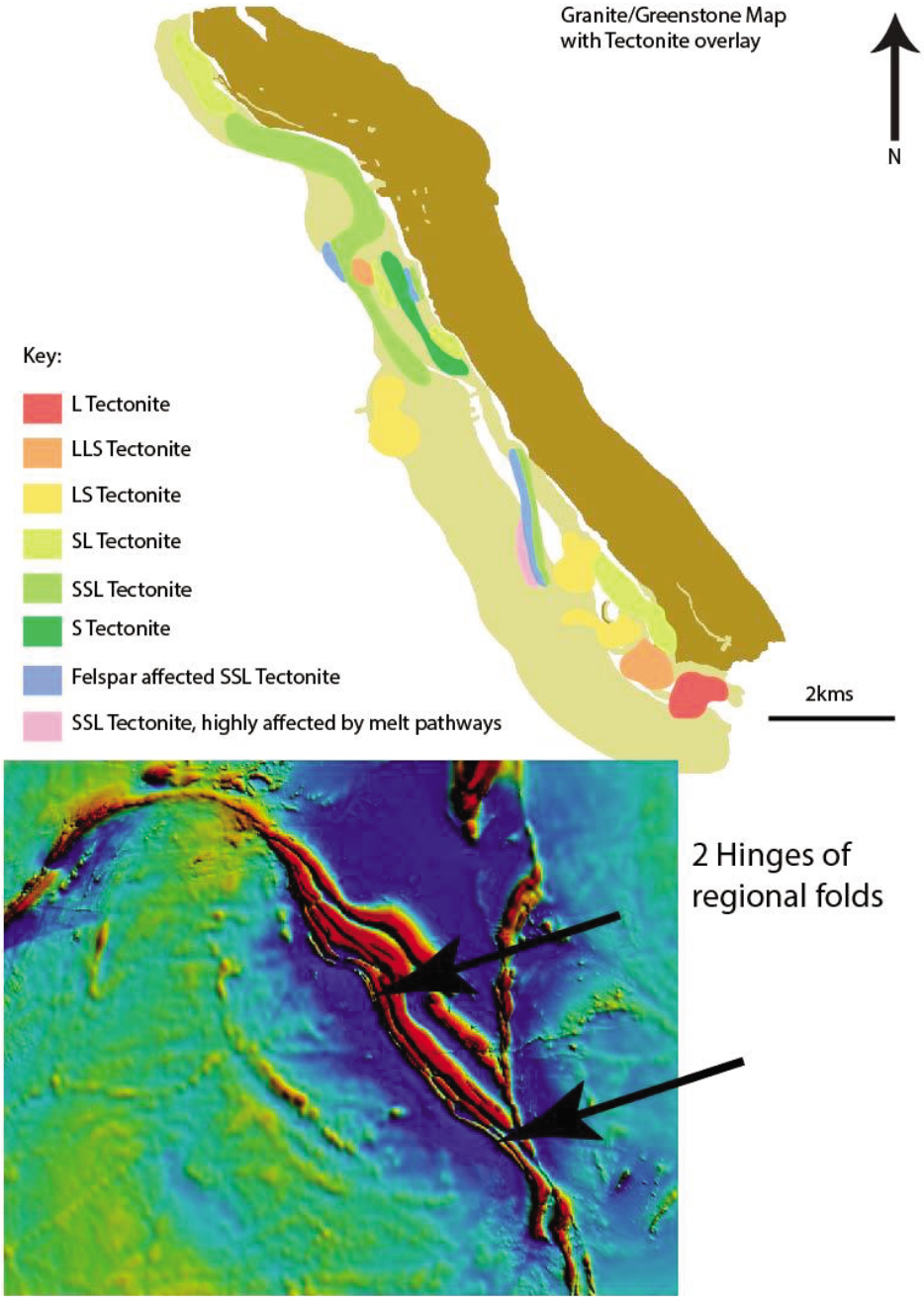

Figure 23b – Image outlining that, linear dominant fabrics are associated with the hinge zones of regional folds. L tectonites were found in the south and the middle section of the mapped area.

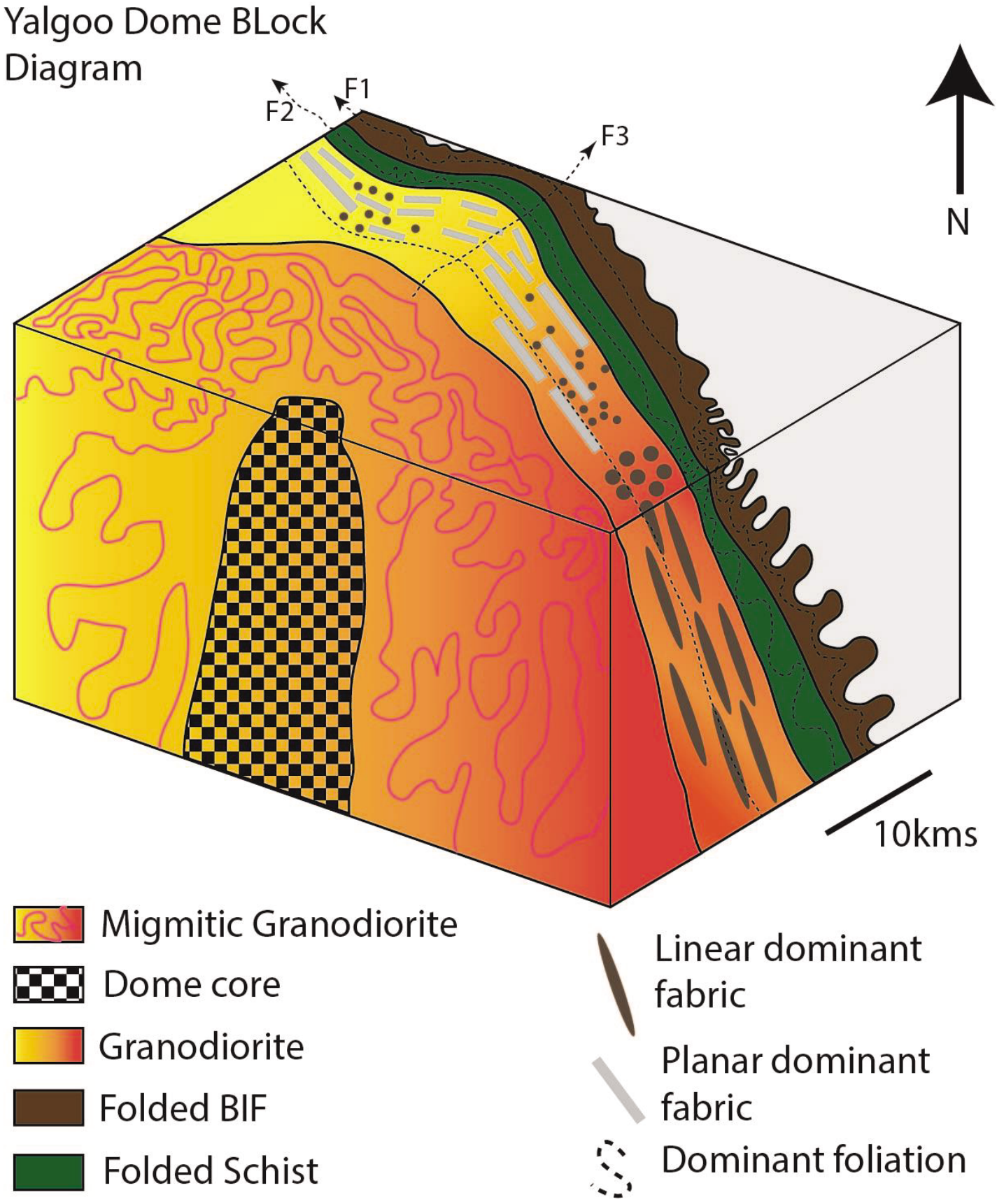

Figure 23c – A block diagram cartoon illustrating the internal structure of the Yalgoo dome. Note Lineations are associated with hinge zone of fold outlined in figure 23b.

16.2 Aims

This chapter aims to characterise crystallographic orientation and microstructure using statistical data collected to outline shape, and area percentage of 7 different values within differing stages of tectonite development. Additionally 3 samples, an L tectonite (Yal), a SL tectonite (128) and an S tectonite (101) aim to be analysed via SEM analysis to constrain metamorphic temperature grade and slip directions ascertaining if the sample are affected by coaxial or non-coaxial deformation . All samples will be compared to ascertain crystallographic orientations, with an aim to better constrain the deformation and evolution of this unit. The S & L tectonite will be mapped on the XY and ZY plane to view deformation within quartz ribbons (XY) and grain deformation along the horizontal plane (ZY). Finally, temperature change through metamorphic grade will be analysed through pole figure comparison aiming to achieve any change in grade from L to S Tectonite.

16.3 Analytical methods

16.3.1 Statistics

3D statistical data was analysed for each slide (different cuts) by coloring in different sections of PRIOR images, assigning them different colours for seven categories. These colours were then input into ImageJ and statistical values were noted in Excel. Values were then normalised to 100%. Outcrop sampling was done with the Y axis co planar to regional strike.

16.3.2 Scanning Electron Microprobe

Representative sites for EBSD mapping were chosen in three samples in order to obtain data across areas of differing quartz microstructure and deformation: The samples were analysed for areas to be mapped. It was important to attain areas of clean homogeneous quartz, varying in size and shape, additionally on the boundary of plagioclase. Relict and recrystallised clasts were also looked for but these returned messy readings.
Electron Backscatter Diffraction (EBSD) analysis was undertaken on a Zeiss Scanning Electron Microscope (SEM) with a HKL NordleysNano high sensitivity EBSD detector, using the HKL CHANNEL5 analysis software from Oxford Instruments. Data was collected from mechanically polished thin sections with a final mechanochemical polish using colloidal silica. Thin sections were subsequently coated with ~3 nm of carbon. The SEM was run at a high vacuum with an accelerating voltage of between 20 - 24 kV, a beam current of 8.0 nA, and with an aperture of 30 µm. The sample was tilted to an angle of 70°, with tilt correction applied in the Zeiss SEM software. EBSPs were processed with 2 frame averaging, 4x4 binning, ~55 theoretical reflectors and 8-11 bands.

Several maps were produced from the obtained mapping sequence, displaying different properties of the sample. Band contrast maps display data quality, with lighter colours showing areas of good quality patterns and lines representing grain boundaries in these maps.

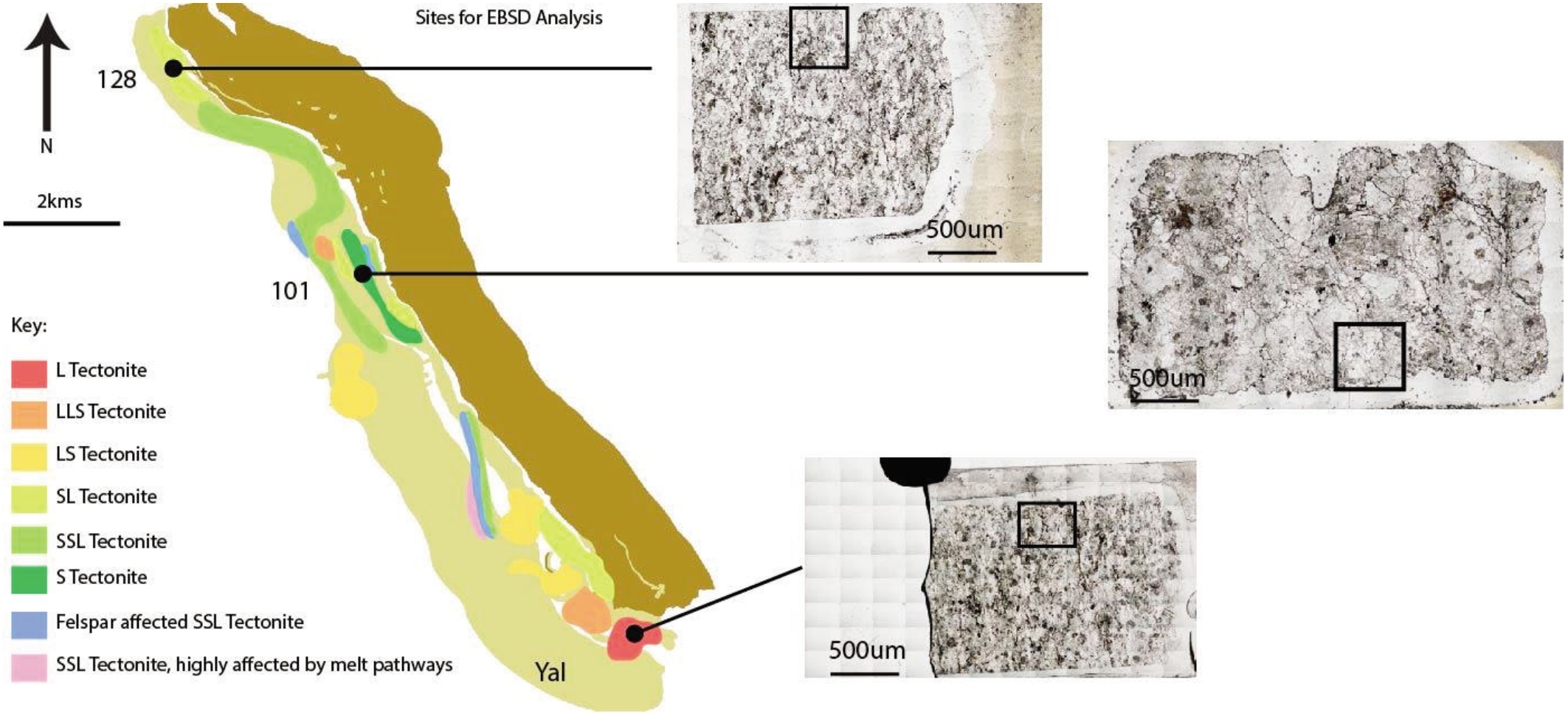

Figure 24 – Outlying locations where samples were taken for SEM analysis. Areas of clean quartz within this section were chosen for mapping sites.

Euler angles are introduced with different coloured lines on the grain boundary indicating different degrees of grain boundary angle. These are: angles greater than 10° in black, in between 10° and 5° in red and angles less than 2° in yellow. Phase maps are produced and coloured by the identification of the minerals by the software, based on crystallographic properties. Orientation maps are also produced, with colour of grains on the map corresponding to crystallographic orientation within the sample.

Post-acquisition data processing was undertaken using CHANNEL5 software suite. This included removal of non-indexed points via the removal of wild spikes and then extrapolation of points from neighbouring data points (up to 4 neighbouring data points). Crystallographic orientation information is presented via the use of pole figures (equal area, upper hemisphere projections), with each figure representing the orientation of a quartz crystal axis in the sample coordinate system where x is horizontal, y is vertical and z is perpendicular to the sample surface. This information is also shown as contoured plots with grayscale colour schemes in plotting Pole Figures. This outlines CPO patterns of quartz on c & a-axes.

Figure 25 – Cuts for each block used in the following section

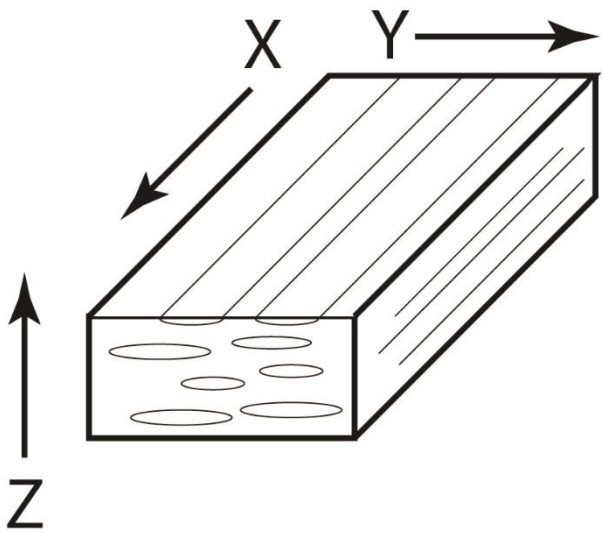

16.4 Statistics Results

A 3D image was ascertained from the individual grains. Relict quartz and recrystallised quartz showed different elongation along different planes when analysed as a whole 3D shape. 3D analysis of the 2 end members (L and S tectonite) is explained below.

Table 8 – Categories for analysed statistical values. Values are in percentages of thin section area. This section cuts are noted in the heading of each slide label.

	Raw value Statistics - not normalised - values in %								
	Slides								
Percentages	Yal1 - ZY	Yal2 - XZ	Yal3 - XY	120-ZY	122-ZY	101-1-ZY	101-2-XZ	101-3-XY	128-ZY
Relict Quartz	3.3	0.4	1.9	3.5	6.8	4.1	5.7	4.2	3.3
Relict Feldspar	0.2	1.3	2.5	7.4	8.1	16.7	10.9	7.9	1.2
Recrystallised Quartz	4.5	0.3	2.5	3.1	10	9	8.7	1.7	1.6
Recrystallised Feldspar	0	0.1	0.38	1.1	2.3	1.1	0.7	2	0.7
Recrystallised fine grained Qrtz and Fld	52	79	51	38	19.3	24	30.6	28	54.1
Quartz Ribbons	1.9	0	3.8	21	25	24.6	10.3	21.8	12.1
Myrmekite	0	0	0	0.5	0	0.9	1.3	0.9	0.4
Sum	61.9	81.1	62.08	74.6	71.5	80.4	68.2	66.5	73.4
Normalised	100	100	100	100	100	100	100	100	100
	Normalised values to 100%								
Percentages	Yal1 - ZY	Yal2 - XZ	Yal3 - XY	120-ZY	122-ZY	101-1-ZY	101-2-XZ	101-3-XY	128-ZY
Relict Quartz	5.33	0.49	3.06	4.69	9.51	5.10	8.36	6.32	4.50
Relict Feldspar	0.32	1.60	4.03	9.92	11.33	20.77	15.98	11.88	1.63
Recrystallised Quartz	7.27	0.37	4.03	4.16	13.99	11.19	12.76	2.56	2.18
Recrystallised Feldspar	0.00	0.12	0.61	1.47	3.22	1.37	1.03	3.01	0.95
Recrystallised fine grained Qrtz and Fld	84.01	97.41	82.15	50.94	26.99	29.85	44.87	42.11	73.71
Quartz Ribbons	3.07	0.00	6.12	28.15	34.97	30.60	15.10	32.78	16.49
Myrmekite	0.00	0.00	0.00	0.67	0.00	1.12	1.91	1.35	0.54
Total	100.00	100.00	100.00	100.00	100.00	100.00	100.00	100.00	100.00

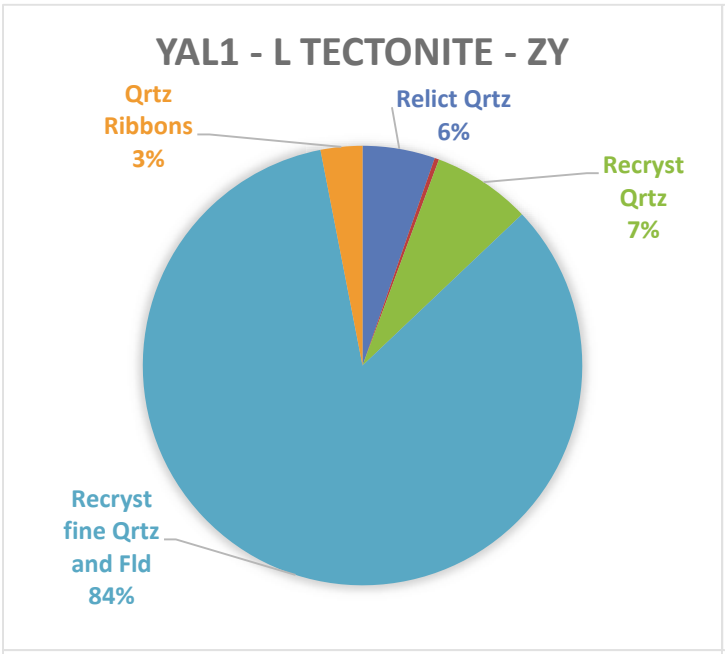

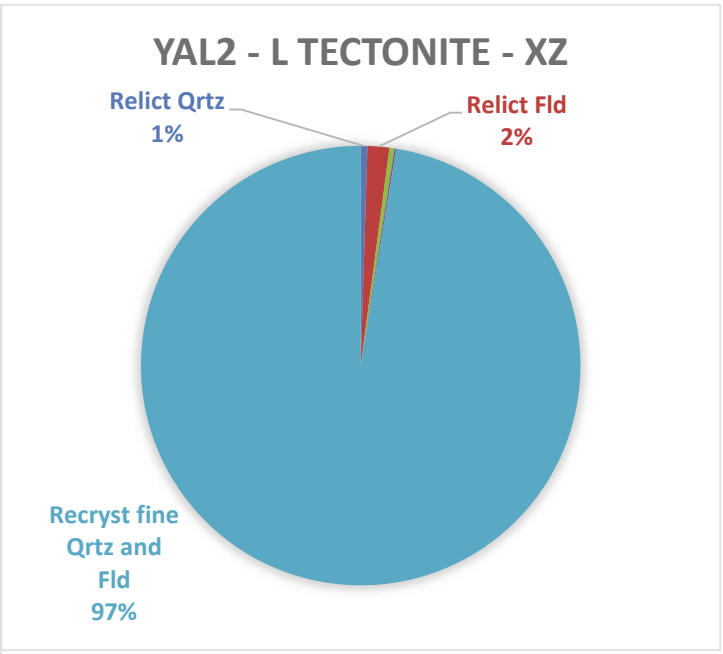

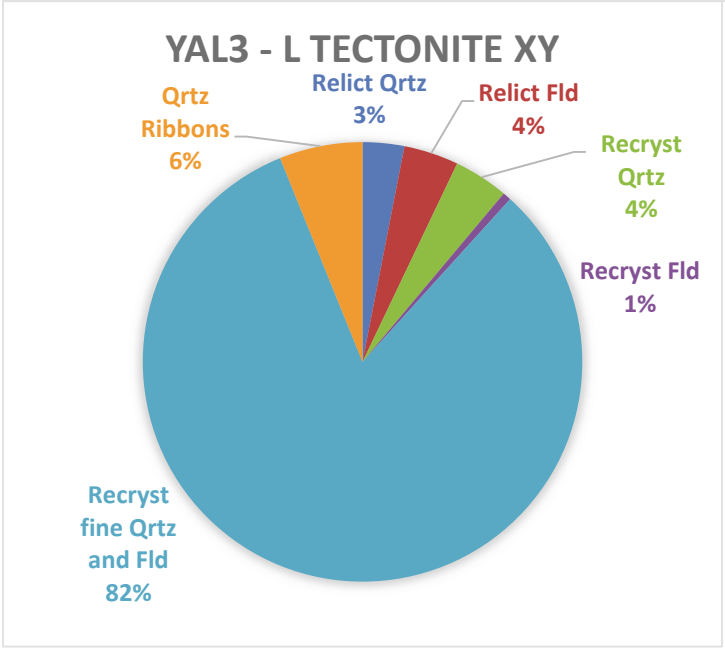

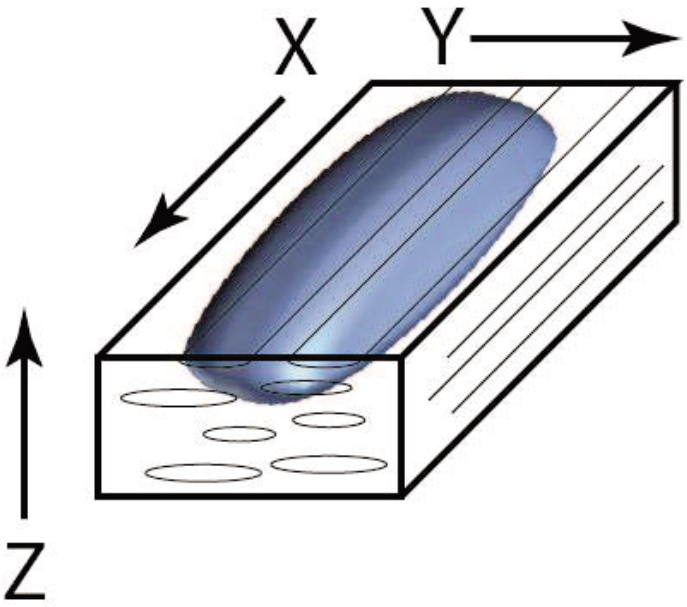

Fig26 – Cigar shaped lineations

L Tectonite – Sample Yal – this section was dominated by recrystallised fine grained, quartz and feldspar, similar to outcrop description. This was very obvious along the XZ plane with maximum grains present, indicating maximum strain perpendicular to this plane cut along the X and Y axis. A small amount of recrystallised quartz (only 7%) is seen along the ZY plane indicating a small amount of parallel extension to surrounding outcrop. Relict quartz ribbons were visible in thin section. Although faint, these ribbons were fine grained, rotated recrystallised quartz grains.

Large relict quartz and feldspar grains were absent throughout this area. There was no myrmekite or sericite alteration viable in this section. Some small relict grains (5%) was visible on the ZY plane. The clasts displayed asymmetry with low energy shadow zones visible at each end.

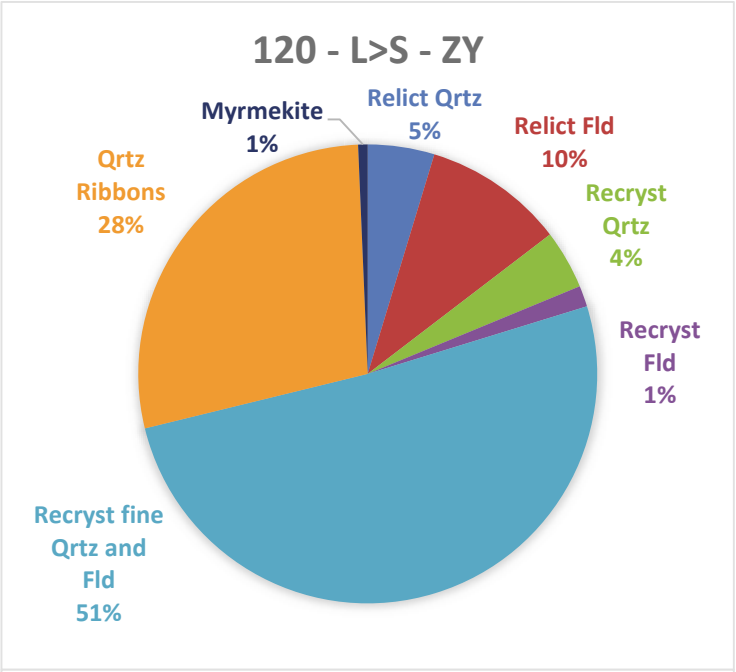

L>S Tectonite – Zoned relict feldspars with large amounts of inclusions stand out in this section. The boundaries of these clasts are reducing due to recrystallisation of surround fine grains quartz and feldspar mix. Quartz ribbons bend around existing relict quart and feldspar clasts and pinch out on the ends. Small amounts of myrmakite are seen in junctions between quartz and feldspars making a triple junction. Over printing of recrystallised quartz is seen in small sections within the quartz and feldspar mix.

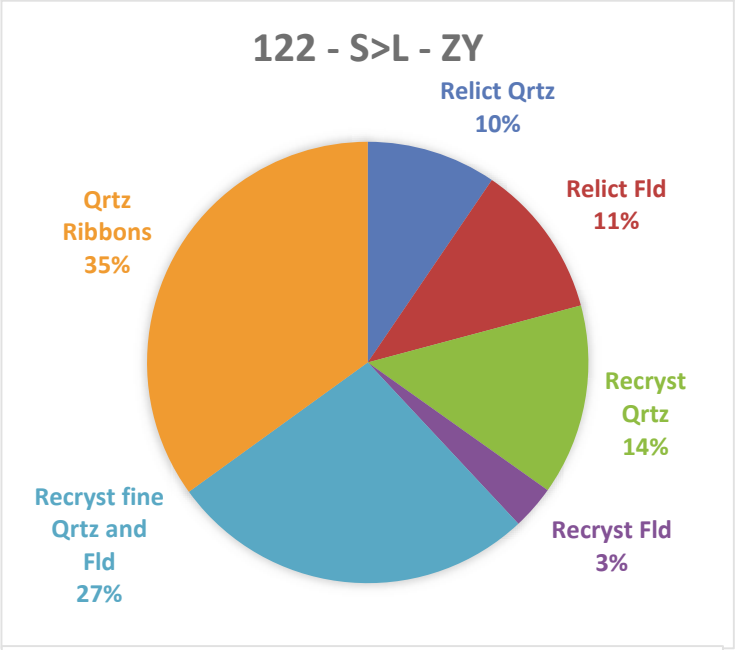

S>L – Relict feldspar dominates some sections of this plane and are large in size. Affected by cross hatched twinning and large amounts of zoning. Relict quartz exhibit small amounts of undulose extinction toward the centre of the clast. Elongation of grains is preferential to strain direction of X and Y, and is apparent in recrystallised quartz. Quartz ribbons look to be expanding into surrounding materials with small inclusions seen within some ribbons. There is no visible myrmekite within this sample.

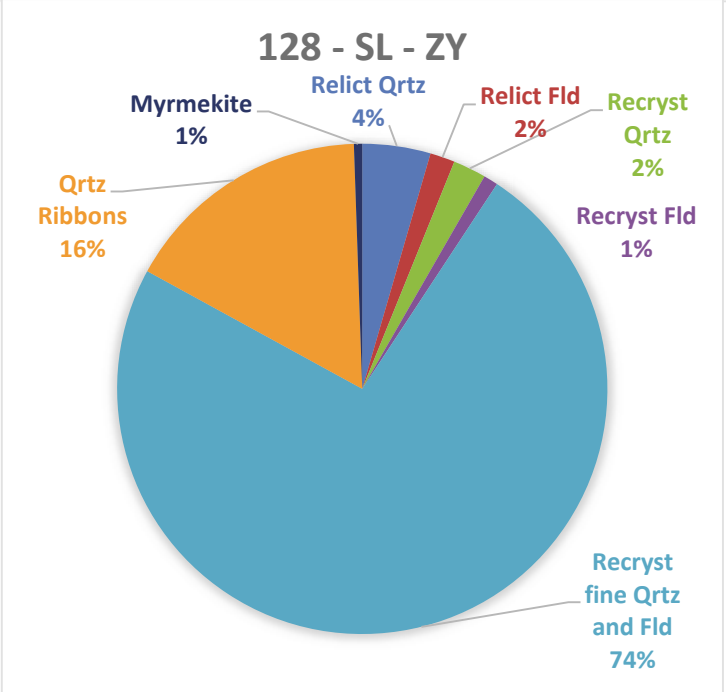

SL – High amounts of recrystallised fine grained quartz and feldspar are dominant in this section. With recrystallisation moving into surrounding relict quartz and feldspar. Boundaries display pinning and windowing with small amounts of grain rotation. Undulose extinction is minimal in recrystallised fine grained mix. Quartz ribboning is still seen although minimal, with large amounts of undulose extinction. Extinction angles are offset 60° to planar directions of the ribbons. Relict feldspar are thin slivers where cross hatching is dominant.

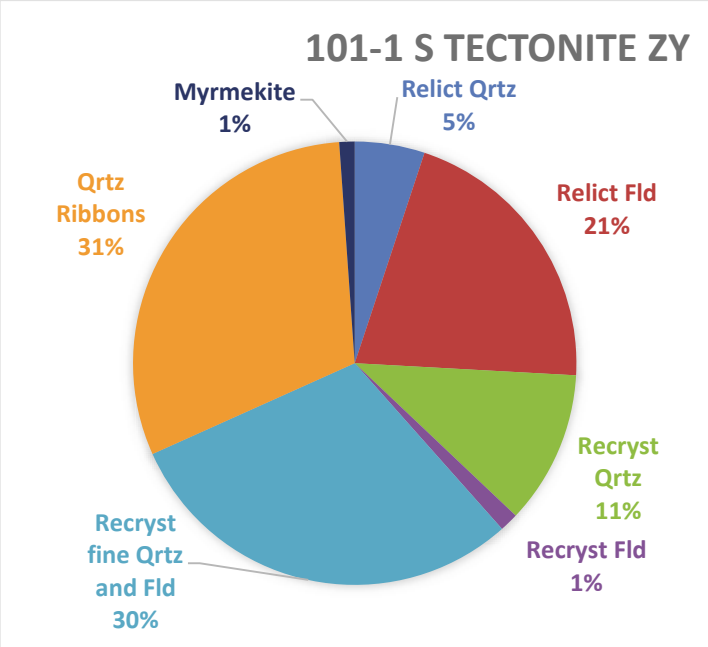

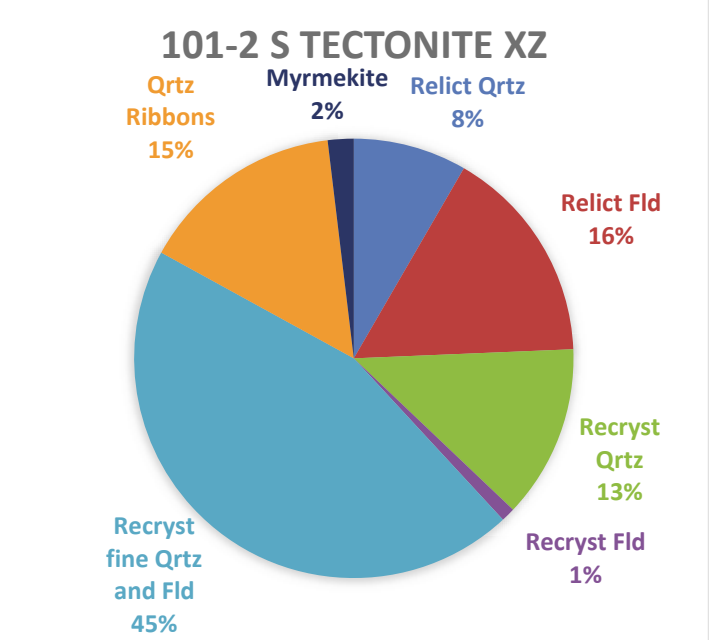

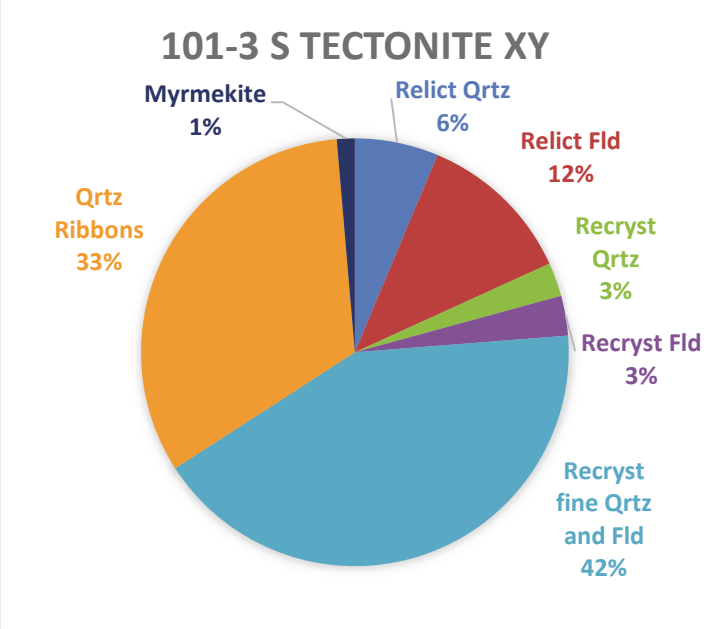

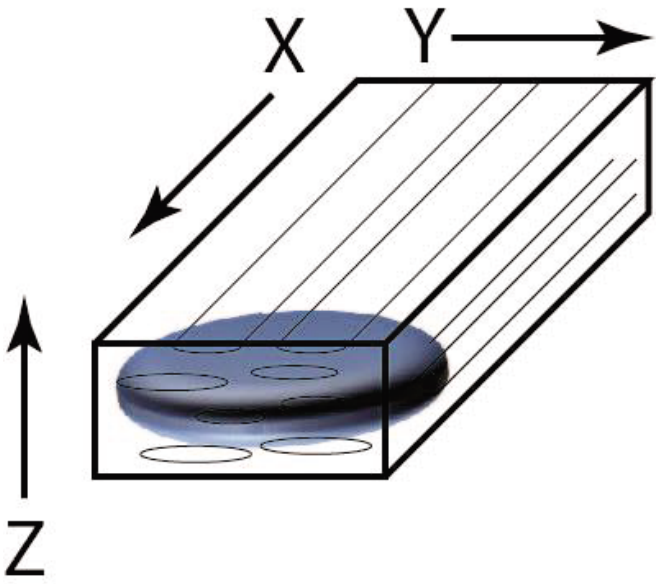

Fig27 – Cigar shaped lineations

S Tectonite – Sample 101 – this section displayed high amounts of quartz ribbons along each plane. Stretching was observed along the XY plane with constriction primarily along the XZ plane. Fine grade recrystallised quartz and feldspar was visible surrounding quartz ribbons with ribbons looking to be expanding into the finer grains. Fine grain quartz and feldspar had a different growth compared to the quartz ribbons. The mix still elongated along the XY plane but was also elongated along the XZ plane with constriction in only 1 direction (ZY plane). Relict quartz was observed along XZ and displayed small amounts of sinistral rotation but were mainly interpreted as asymmetrical sigma clasts.

Recrystallised quartz apparent in relict quart ribbons and seemed to be growing into neighbouring fine grade quartz and feldspar mix. At these triple boundaries with relict feldspars, myrmekite is clearly visible.

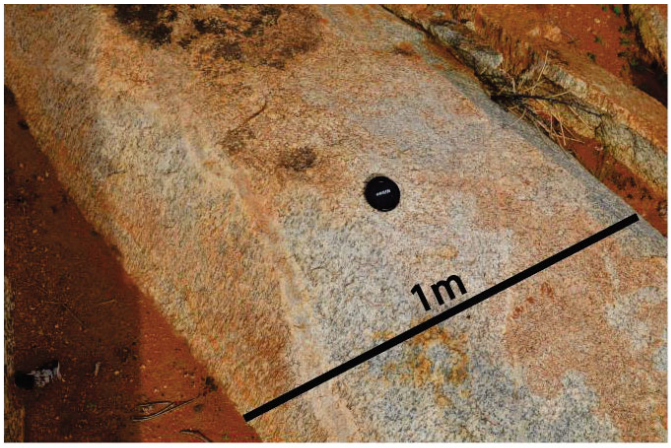

XY Plane view

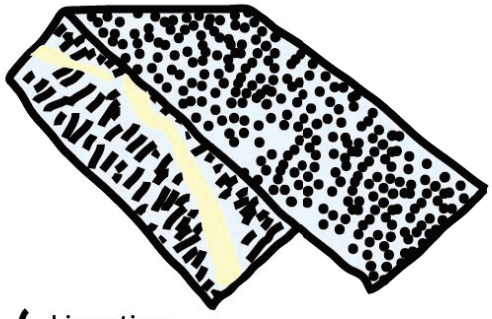

Lineation

42 ---> 074

Crosscutting Tonalite band.

Fine grained, grey, sugary siliceous matrix

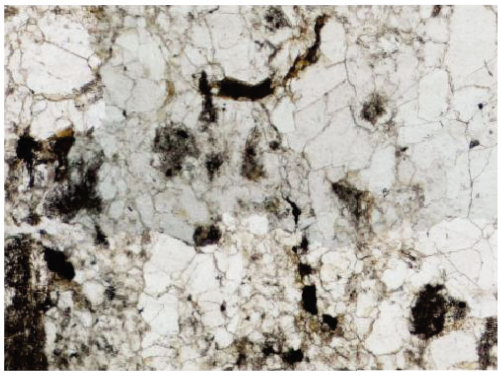

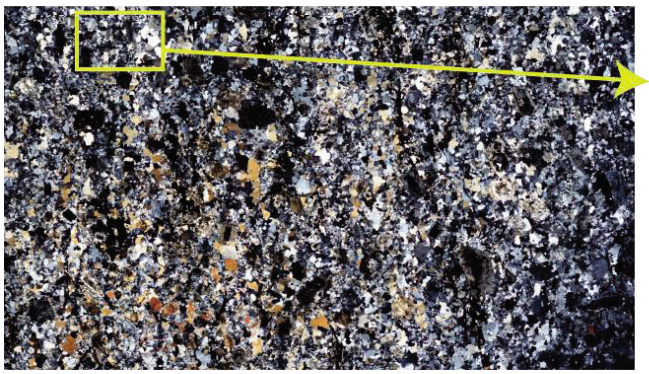

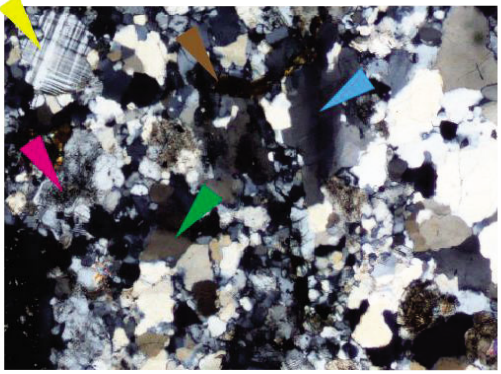

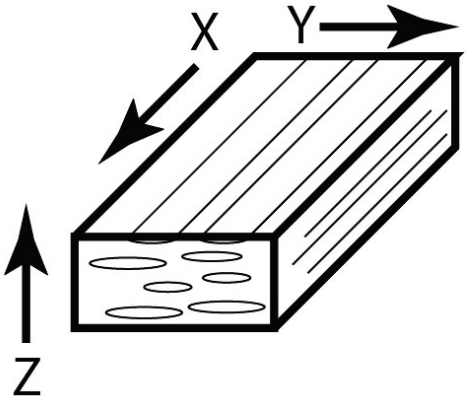

Relict quartz ribboning

Recrystallised quartz, exhibiting extinction

Biotite

Sericite alteration

Recrytallised feldspar

Figure 28 – YAL (L tectonite) thins section cut. Elongation of quartz grains is seen combined with relict quartz ribbons.

16.5 Crystallographic orientation relationships. A summary of EBSD data

Three definable temperature gradients were distinguishable in pole figures when all slides were rotated to the correct plane. Metamorphic grade is decreasing with foliation presence. 101 – 1 – ZY (S Tectonite sample, fig29): Medium temperature, 128 – 1 – ZY (SL Tectonite sample, fig 30): Low to medium temperature, Yal – 3 – ZY (L Tectonite sample, fig 31): Low temperature (comparative view figure 33b).

Dauphine twinning is visible in all samples with spikes around 60 degrees outlined in the misorientations profile maps.

Minimal sub grain rotation (under 10°) is seen in the S tectonites (fig 29). A small increase is seen within the SL Tectonite in respect to neighbour correlated grains. The L tectonite records the highest amount of sub grain rotation with correlated neighbouring grains. These values are measured within the fine grained recrystallised quartz areas of the thin section. The trend of sub grain rotation is also decreasing with foliation presence.

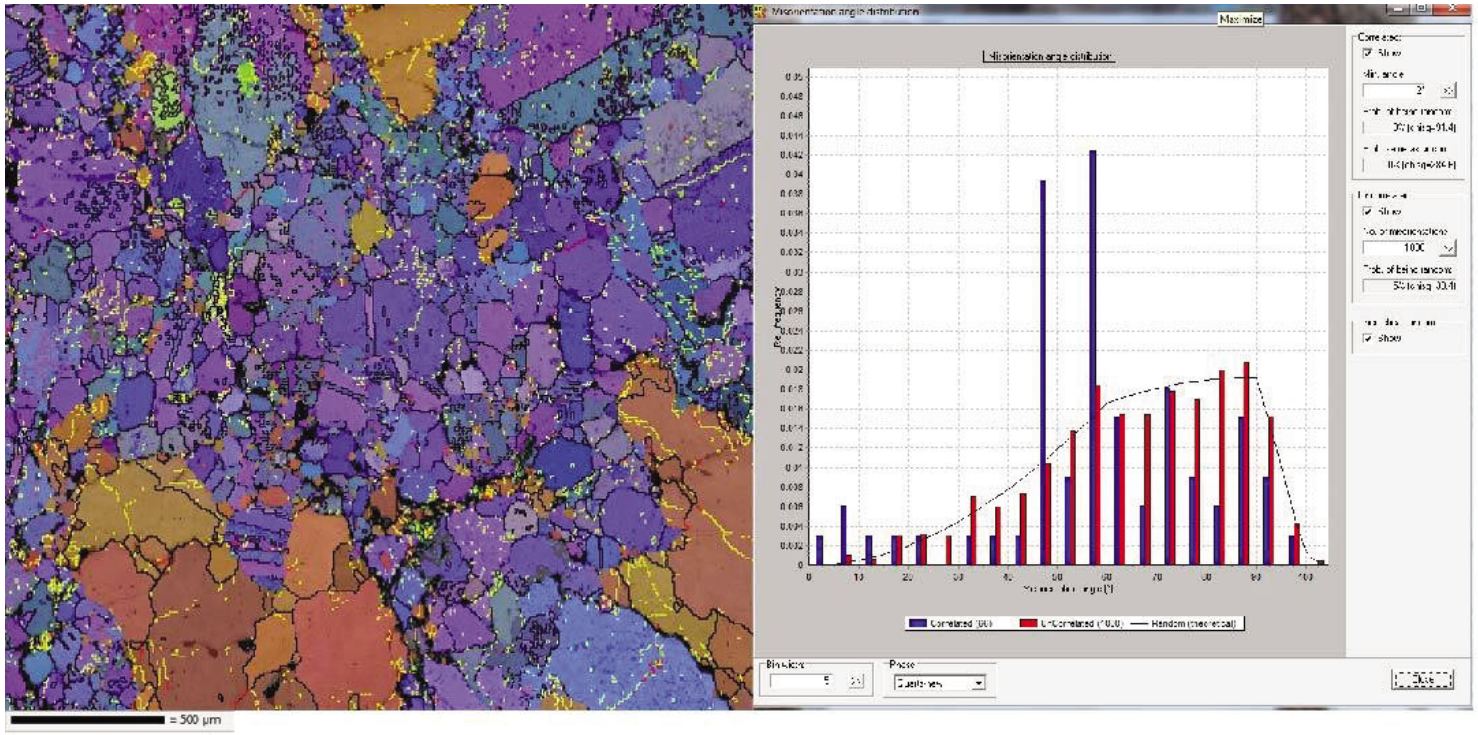

A left- Euler angles and quartz phases overlaying a band-contrast map.
B right- Misorientation angle distribution chart, blue indicates correlated grains, and red indicates uncorrelated grains.

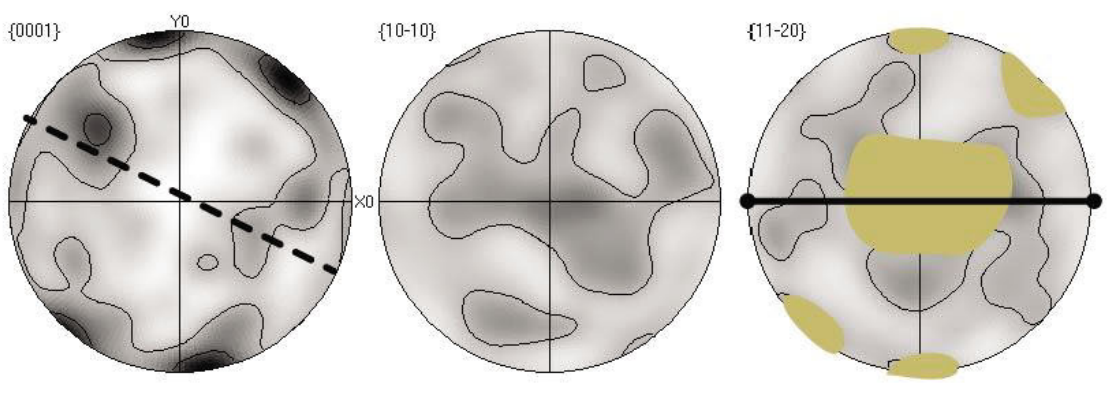

C bottom- Pole figures of quartz CPO. Slides (XY cut) were rotated in the virtual chamber to represent the correct axis.

Figure 29 – Sample 101 ZY. Band contrast with euler angles map angles greater than 10° in black, in between 10° and 5° in red and angles less than 2° in yellow. Pink indicates quartz with an increase in colour indicating increased deformation. Pole figures outline a medium temperature metamorphic grade within this set of rocks.

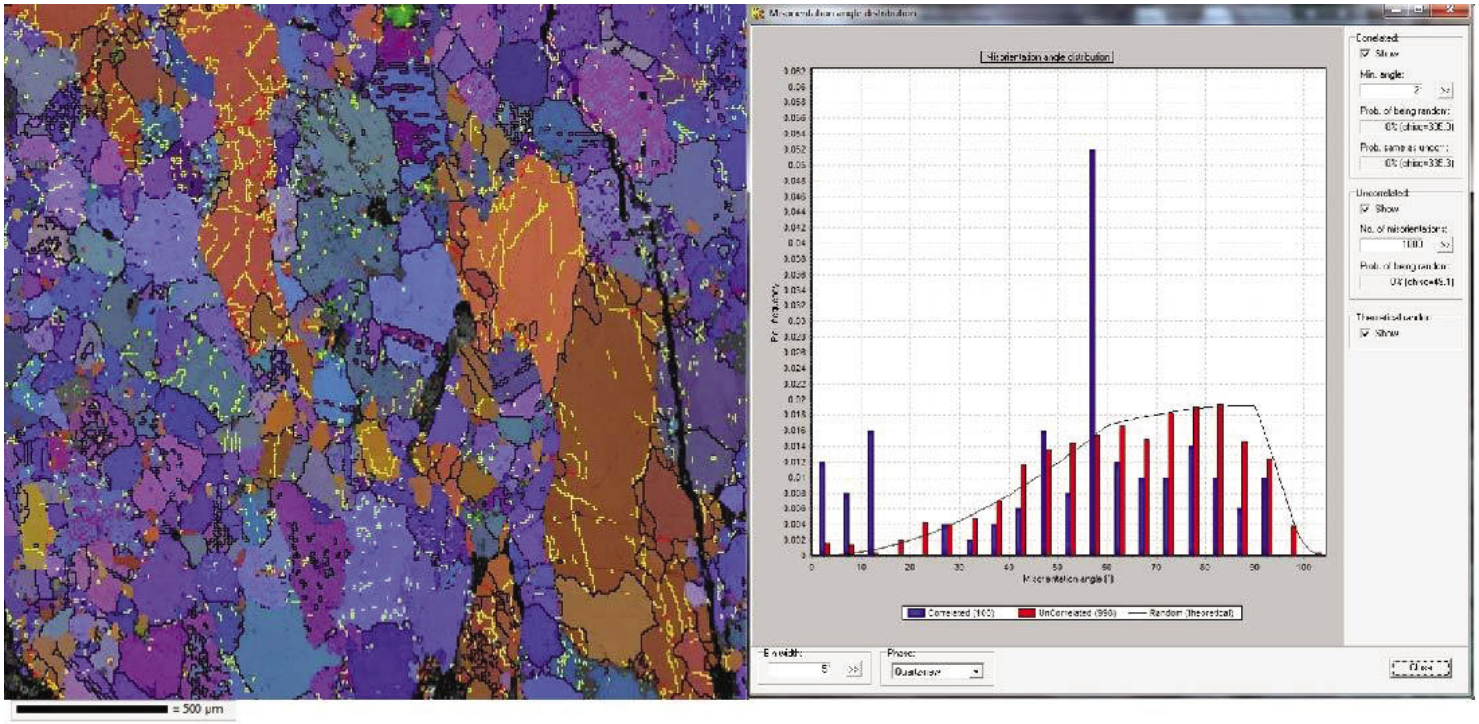

A left- Euler angles and quartz phases overlaying a band-contrast map.
B right- Misorientation angle distribution chart, blue indicates correlated grains, and red indicates uncorrelated grains.

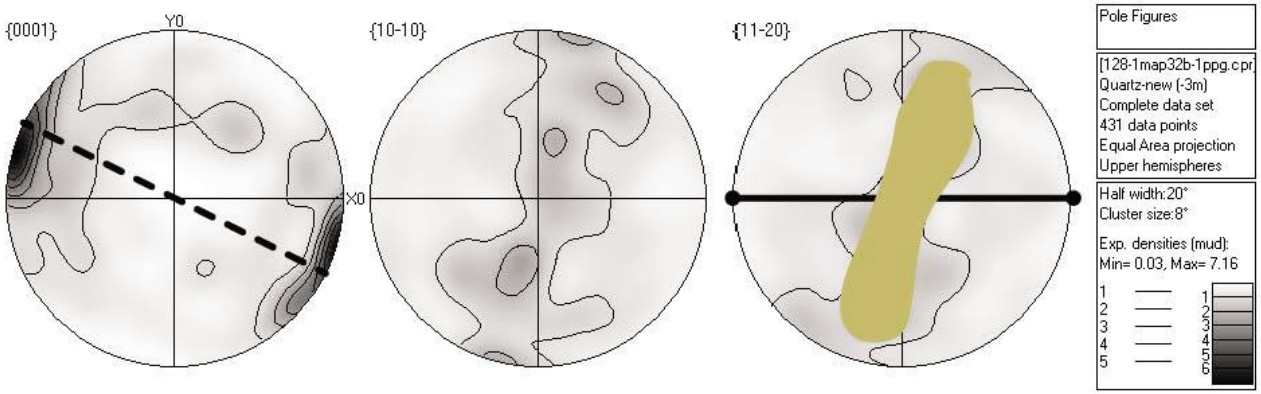

C bottom- Pole figures of quartz CPO. Slides (XY cut) were rotated in the virtual chamber to represent the correct axis.

Figure 30 – Sample 128-1 ZY. Band contrast with euler angles map angles greater than 10° in black, in between 10° and 5° in red and angles less than 2° in yellow. Pink indicates quartz with an increase in colour indicating increased deformation. Pole figures outline a low to medium temperature metamorphic grade within this set of rocks.

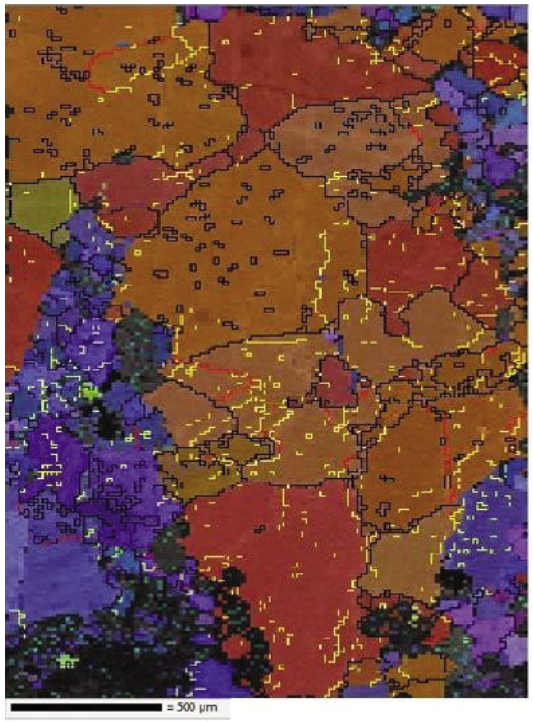

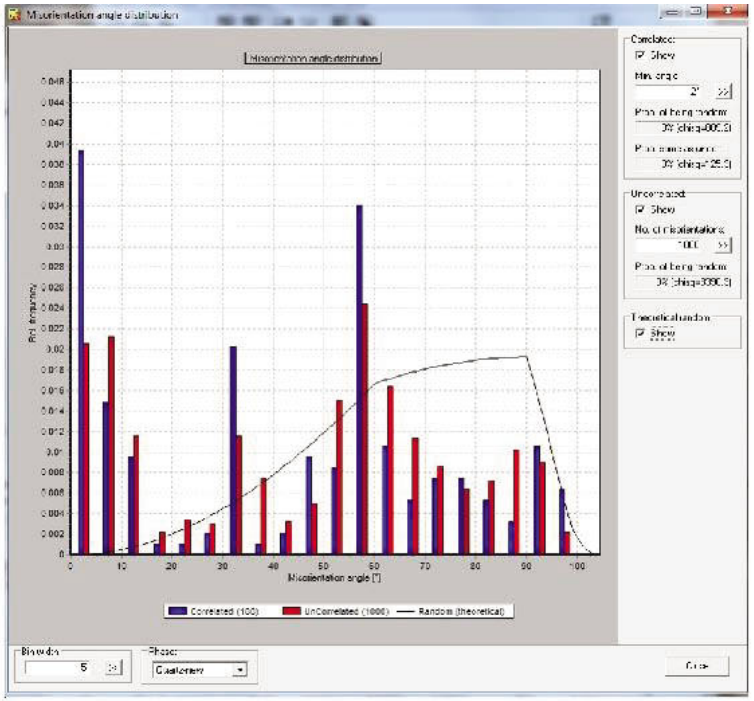

A left- Euler angles and quartz phases overlaying a band-contrast map.
B right- Misorientation angle distribution chart, blue indicates correlated grains, and red indicates uncorrelated grains.

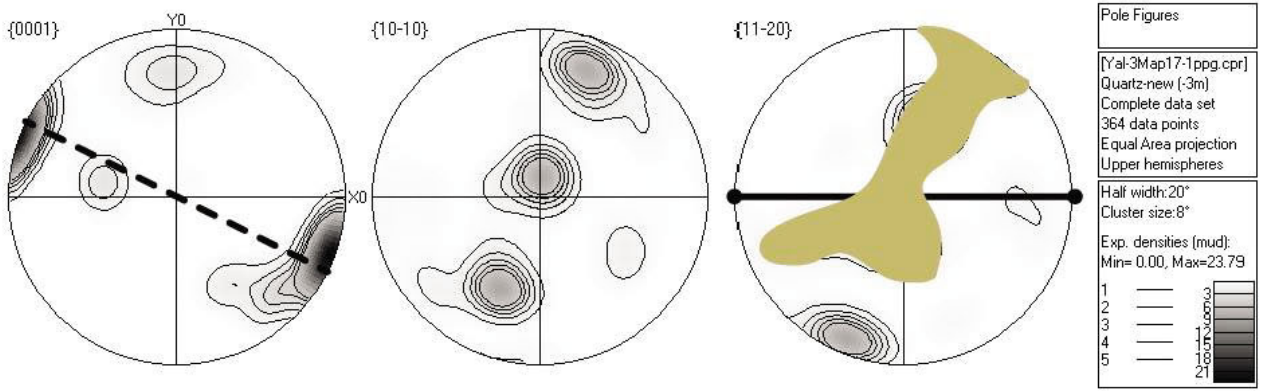

C bottom- Pole figures of quartz CPO. Slides (XY cut) were rotated in the virtual chamber to represent the correct axis.

Figure 31 – Sample Yal3 ZY. Band contrast with euler angles map angles greater than 10° in black, in between 10° and 5° in red and angles less than 2° in yellow. Pink indicates quartz with an increase in colour indicating increased deformation. Pole figures outline a low temperature metamorphic grade within this set of rocks.

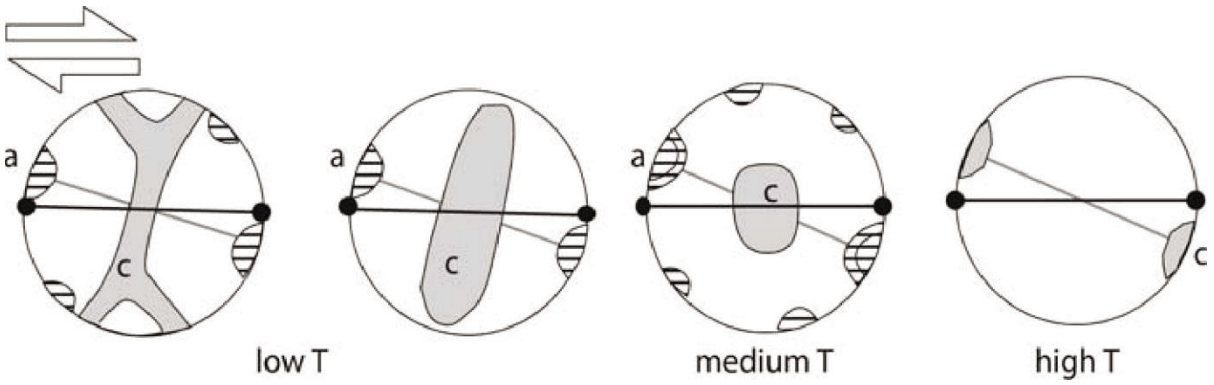

Figure 32 Above - Passchier and Trouw (2005) Microtectonics explanation of LPO patterns of quartz c-axis (solid colours) and a-axis (striped colours). This deformation series is directly related to quartz deformation in Yalgoo. Figure 33 Below – S, SL and L tectonites respectively from top to bottom outlining differing temperature grade metamorphism, directly relating to Passchier and Trouw's models above.

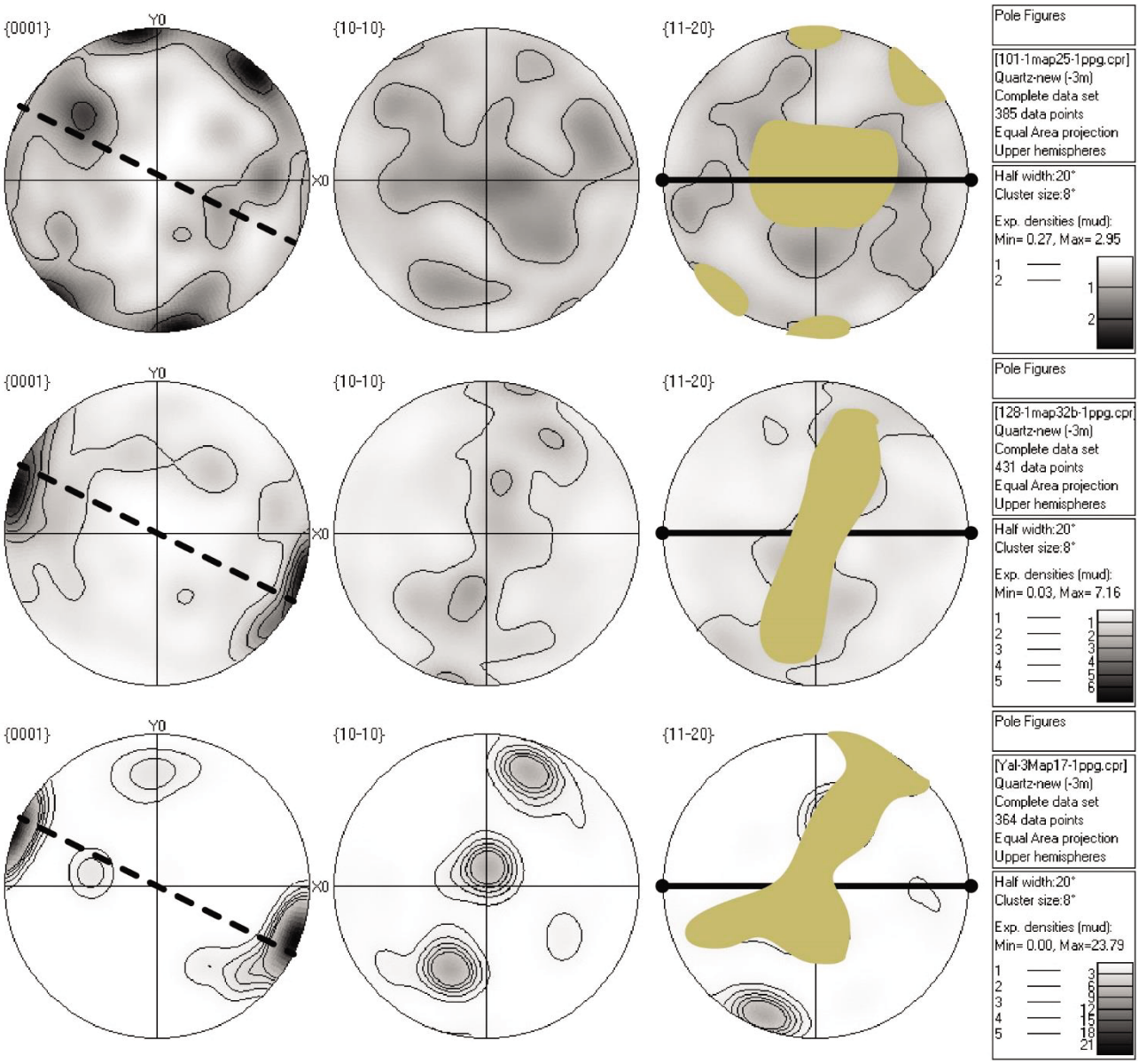

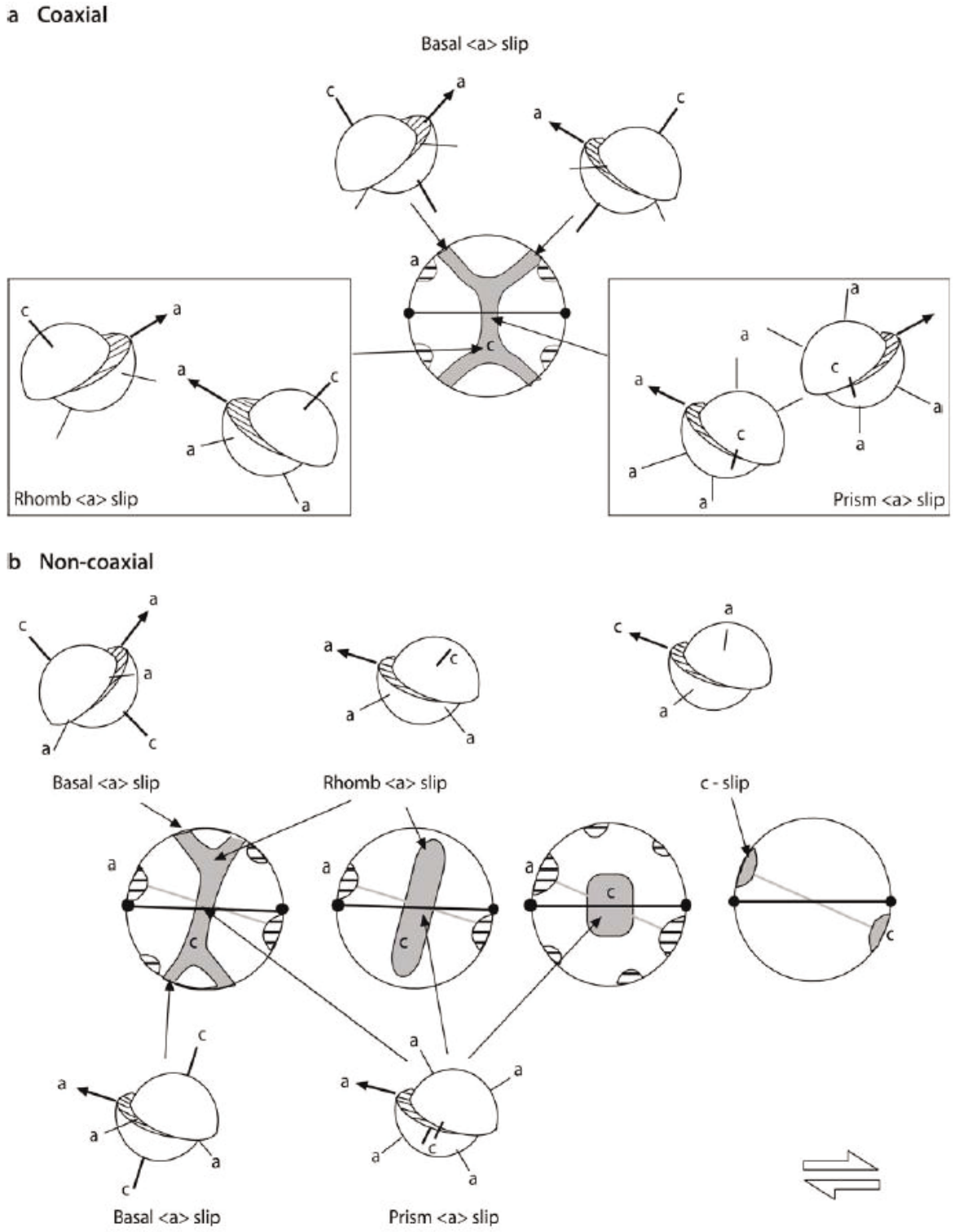

Figure 34 - Passchier and Trouw (2005) Microtectonics outlining non coaxial and coaxial slip systems in regards to Basal, Rhomb and Prism slip planes.

16.6 Interpretation of SEM results

S Tectonites (fig29), were formed in a medium temperature metamorphic grade. This sample shows low amounts of sub grains rotation and is dominated by high angle grain boundaries, indicating solid state processes acting upon the sample. This sample records one non coaxial progressive deformation event at medium temperature generally interpreted around 650 degrees but not hot enough form point maxima aggregation along the a-axis. Prism <a> slip is evident within this sample confirming 1 event of medium temperature.

SL Tectonites (fig30), were formed in a low to medium temperature metamorphic grade. This sample importantly records two deformation events, non-coaxial basal and prism slip along the a-axis. Minimal sub grain rotation is also recorded but indicates that it is occurring.

L Tectonites (fig31), were formed in a low temperature metamorphic grade. This sample also shows the most low angle sub grain rotation and is probably due to an area of lesser strain allowing dislocations to creep into surrounding sub grains causing lattice rotation. This is common during deformation and recovery. A strong cluster on the C-axis importantly indicates basal <a> slip, low temperature, non-coaxial deformation.

The overall trend of the samples is conclusive with documented trends of recovery and recrystallisation within rocks, these being temperature dependant as outlined in, Wilson (1975), Bouchez (1977), Lister and Dornsiepen (1982). Recrystallisation acts slower at low temperatures, as is seen within L tectonites having higher amounts of sub grain rotation. With the S tectonites being subject to higher temperatures the quartz is generally ductile and loses strength. Over printing structures suggest that linear fabrics may have formed first within this dome, subsequently being overprinted by planar fabrics. Importantly fabrics are also deformation dependant.

17. Discussion

Through detailed examination in section 2, 16.1 and previous work complete by Foley (1997) and Caudery (2013), it is interpreted that a rising diapir initiated greenstone package folding and sagduction whilst creating initial linear fabrics. Formation of the fabrics consisted of a combination of downward moving subsiding greenstones and the upward moving pluton (section 16.1). Potential continual injections of magma into the ballooning pluton followed, creating a migmitised core. Contemporaneous North West sinistral shearing initiated formation of the planar fabrics recorded in this thesis. These fabrics are visible trending northward, evolving from linear to planar fabrics, (changing from L to S Tectonites) signifying non co-axial, progressive deformation. Specific locations outline specific fabrics, which therefore indicates a problem within a one stage progressive deformation theory. If planar fabrics are thought to take on the last shearing deformation event then why are lineation's present in one specific location within the gneiss. This section will start by discussing field and laboratory evidence, to analyze tectonic processes after initial emplacement. Followed by a discussion of the formation of the Yalgoo dome, focusing on the North-East Tectonites.

17.1 Part 1: One or Two tectonite specific deformation events.

A discussion with regards to tectonic events forming planar and linear fabrics will be provided in the following section for two options.

17.1.1 One event

One single transpressive event creating tectonite fabrics during initial emplacement: Similar to traditional monoclinic shear zone models, this option outlines stretching lineations co linear to vertical emplacement and foliations co planar to shearing direction, which is

conformable to descriptions from the mapped area, outlined in the field relationships section. Lineations group together when plotted onto a stereonet, outlining high angles dipping to the east. Foliations are dominant in areas away from folds (fig24) within the middle mapping section. This planar fabric is probably due to extensional strain, contemporaneously affecting the shearing granite, dominating the middle of the dome. Problematically, only one location for pure L Tectonites throughout the whole mapped section, outlining if only one progressive transpressional event is occurring during initial emplacement then why are pure L tectonites only seen within one fold hinge in the southern section?

17.1.2 Two events

One doming event with one tectonic event, producing varying overprinting relationships: This theory outlines initial formation of L tectonites within fold hinges, similarly described by Sullivan (2013) in section 16.1. This single event concludes, with a period of recovery and sub-grain rotation largely affecting L tectonites within fold hinges, as hinge zones are predominantly areas of high stress. A simple North West shearing event is either reactivated or a new process affects the newly formed faint L tectonites. Strain increases and older fabrics are overprinted from the new deformation mechanisms.

17.2 Field evidence

L tectonites are specifically seen within the southernmost section of the mapped area (fig24), within fold hinge zones. A distribution of the other tectonites trend northward along strike of the dome, with planar dominated fabrics exclusively in the north, and associated with straighter unfolded sections. Field evidence suggests specific areas of higher strain, shown by outcrops of finer grade granodiorite combined with melanic schlieren. Higher temperature indicators are also visible in the form of large euhedral feldspars (fig15a) and

dominate specific areas within outcrop (section 5). These areas of higher temperature and strain are planar dominant, recording limited lineations and no evidence of clast rotation. Importantly planar dominant areas contain quartz ribbons within thinsection, indicating extensional forces. These S tectonite quartz ribbons contain large quartz grains (fig29) with sharp boundaries, contracting dramatically with the L tectonites showing relict quartz ribbons, fine grained recrystallized margins (fig31) and a major fine grained recrystallised quartz and feldspar matrix. The recrystallised zones within thin sections are interpreted to outline two periods of recrystallisation, initially forming L tectonites over a large extent with a second period of shearing, concentrating strain and forming S tectonites. Folding vs tectonite distribution (fig18) also confirms linear fabrics associated with fold zones which conforms to the one and two event option.

17.3 Laboratory Evidence

Statistically, S tectonites have a higher percentage of larger grains, interpreted to be formed through higher temperatures and less strain. Pole figures confirm this increase in temperature during metamorphic formation outlined in section 16 (fig33), siding with a two stage theory. Additionally SL tectonites record Medium to Low temperatures and L tectonites record Low temperatures. Interestingly data from SEM and EBSD work outlined, multiple events recorded for non-coaxial slip systems. S tectonite recording 1 event, SL recording 1 or possibly 2 events, and L tectonite recording 2 events. This data also shows that the L tectonite is recording two events, but is somehow shielded from the second event (potential transpressional simple shear deformation) creating widespread planar fabrics.

17.4 Formation Discussion

In summary, a two stage model is proposed. An initial vertical, doming event, producing constrictional strain toward the margins forming initial, faint linear fabrics. Minimal planar fabrics may have been in the early stages of formation (micas aligning and quartz grain elongation) within the flattening section toward the top of the dome. A second tectonic event is activated, a NW transpressional movement creating linear fabrics to rotate and elongate micas to stretch and flatten into planar fabrics, parallel to the surrounding greenstone belt, forming the first SL fabrics throughout the dome. Extensional strain is focused in non-folded areas as the rheologically conformable SL tectonites accommodate the extension. S tectonites overprint the initial L tectonites and a tectonite grading is formed throughout the region.

Since the surrounding greenstones were folded in the initial emplacement through sheath folding, (with granites squeezing vertically through these sheaths) they have subsequently been contact metamorphosed and contain denser areas (Section 4.2.1 and 12.1), typically within folded zones. The second event via a simple shearing movement, shears past and preferentially exploits weaker planar fabrics within unfolded sections and does not affect lineated fabrics within folded areas of the sequence.

18. Conclusion

Magmatic evidence is seen within feldspar formation and solid state recrystallisation is seen within the gneiss outcrops. Caudery, Foley, Myers and Watkins all agree on a Yalgoo specific felsic diapir which is also conformable with the studies outlined in this thesis. Yalgoo shows clear sharp boundaries with intrusion related melt characteristics within S tectonite outcrop only recording one metamorphic temperature grade, and large amounts of fine grade recrystallised matrix with relict melt characteristics within L tectonites. Limited syn and post tectonic kinematic indicators were found hindering movement directions of the shearing.

A syn-tectonic/plutonic D1 stage may be applicable but unlikely as all fabrics would outline a planar record. The sheath folding can be seen to occur vertically with associated 'curtains' at the greenstone boundaries. Small dome and basin structures also form within the dome itself, highlighted by magnetic highs observable in geophysical maps. Pure L Tectonites are always associated nearby or next to these small doming structures and have a near vertical mineral (biotite) lineation, indicating upward movement and stretching along the vertical axis. How the lineation fabric is still recorded as a pure L tectonite, is proposed to be a result of shielding from the surrounding folded zones, but further work should be carried out to confirm this (3D modelling).

Pure S tectonites are not found near any dome structures and are purely foliated meta-granodiorite gneiss. This being the case, then tectonites can be said to primarily take the fabric influenced by the latest deformation event, pending heat controls and folded zones.

Combining all work outlined in this thesis, the Yalgoo tectonite evolution is developed by a multi stage formation where original deposited greenstone sequences are folded during E/W subduction, accretion and tectonic processes. A tonalitic pluton intrudes the greenstones and metamorphoses the surrounding greenstone packages and creates

complex sheath folds and interference patterns. A period of transpression then activates via regional tectonic influences, creating localised areas of highly foliated biotite rich S Tectonites. Recrystallisation and recovery takes over via sub grain boundary rotation. Further work through geochemical data can potentially outline if this is confirmed as a 2 stage pluton emplacement. Additional geochronology, comparing dates of the outer and inner margins can also confirm if the pluton margins have a different age to the core, also conforming a buoyant tail theory.

19. References

CAUDRY, J. (n.d.). Structural Evolution of the Yalgoo Dome, Yilgarn Craton, Western Australia.

BALLMER, M. D., ITO, G., WOLFE, C. J. & SOLOMON, S. C. 2013. Double layering of a thermochemical plume in the upper mantle beneath Hawaii. Earth and Planetary Science Letters, 376, 155-164.

BARLEY, M., KERRICH, R., REUDAVY, I. & XIE, Q. 2000. Late Archaean Ti-rich, Al-depleted komatiites and komatiitic volcaniclastic rocks from the Murchison Terrane in Western Australia. Australian Journal of Earth Sciences, 47, 873-883.

BERESFORD, S. W. & CAS, R. A. 2001. Komatiitic invasive lava flows, Kambalda, western Australia. The Canadian Mineralogist, 39, 525-535.

BLEWETT, R., CZARNOTA, K., GROENEWALD, P., MAAS, R., GOSCOMBE, B. & AUSTRALIA, G. 2009. Metamorphic evolution and integrated terrane analysis of the eastern Yilgarn Craton: rationale, methods, outcomes and interpretation, Geoscience Australia.

BOUCHEZ, J.-L. 1977. Plastic deformation of quartzites at low temperature in an area of natural strain gradient. Tectonophysics, 39, 25-50.

CAMPBELL, I. & HILL, R. 1988. A two-stage model for the formation of the granite-greenstone terrains of the Kalgoorlie-Norseman area, Western Australia. Earth and Planetary Science Letters, 90, 11-25.

CHAMPION, D. & SHERATON, J. 1997. Geochemistry and Nd isotope systematics of Archaean granites of the Eastern Goldfields, Yilgarn Craton, Australia: implications for crustal growth processes. Precambrian Research, 83, 109-132.

CZARNOTA, K., CHAMPION, D., GOSCOMBE, B., BLEWETT, R., CASSIDY, K., HENSON, P. & GROENEWALD, P. 2010. Geodynamics of the eastern Yilgarn Craton. Precambrian Research, 183, 175-202.

FLINN, D. 1965. On the symmetry principle and the deformation ellipsoid. Geological Magazine, 102, 36-45.

GEE, R., BAXTER, J., WILDE, S. & WILLIAMS, I. 1981. Crustal development in the Archaean Yilgarn Block, Western Australia. Spec. Publ. Geol. Soc. Aust, 7, 43-56.

IVANIC, T. J., VAN KRANENDONK, M. J., KIRKLAND, C. L., WYCHE, S., WINGATE, M. T. & BELOUSOVA, E. A. 2012. Zircon Lu–Hf isotopes and granite geochemistry of the Murchison Domain of the Yilgarn Craton: Evidence for reworking of Eoarchean crust during Meso-Neoarchean plume-driven magmatism. Lithos, 148, 112-127.

LISTER, G. & DORNSIEPEN, U. 1982. Fabric transitions in the Saxony granulite terrain. Journal of Structural Geology, 4, 81-92.

MAITRI (2011). Second favourite geology word: Crenulation. *Geology*, (http://vatul.net/blog/index.php/5896)

MYERS, J. S. 1990. Precambrian tectonic evolution of part of Gondwana, southwestern Australia. Geology, 18, 537-540.

MYERS, J. S. 1995. The generation and assembly of an Archaean supercontinent: evidence from the Yilgarn craton, Western Australia. Geological Society, London, Special Publications, 95, 143-154.

MYERS, J. S. & WATKINS, K. P. 1985. Origin of granite-greenstone patterns, Yilgarn Block, Western Australia. Geology, 13, 778-780.

PASSCHIER, C. W. & TROUW, R. A. J. 2005. Microtectonics, Springer.

QUE, M. & ALLEN, A. R. 1996. Sericitization of plagioclase in the Rosses granite complex, Co. Donegal, Ireland. Mineralogical Magazine, 60, 927-936.

REY, P. & PHILIPPOT, P. 2006. Archaean crustal geodynamics, finite strain fields, plumbing system, and ore deposits.

ROSENBERG, C. 2004. Shear zones and magma ascent: a model based on a review of the Tertiary magmatism in the Alps. Tectonics, 23.

SHARPE, R. & GEMMELL, J. B. 2001. Alteration characteristics of the Archean Golden Grove Formation at the Gossan Hill Deposit, Western Australia: induration as a focusing mechanism for mineralizing hydrothermal fluids. Economic Geology, 96, 1239-1262.

SILLITOE, R. H. 1979. Some thoughts on gold-rich porphyry copper deposits. Mineralium Deposita, 14, 161-174.

SULLIVAN, W. 2009. Kinematic significance of L tectonites in the footwall of a major terrane-bounding thrust fault, Klamath Mountains, California, USA. Journal of Structural Geology, 31, 1197-1211.

SULLIVAN, W. A. 2006. Structural Significance of L Tectonites in the Eastern-Central Laramie Mountains, Wyoming. The Journal of geology, 114, 513-531.

SULLIVAN, W. A. 2013. L tectonites. Journal of Structural Geology, 50, 161-175.

SUTTON, J. 1963. Long-term cycles in the evolution of the continents.

VAN KRANENDONK, M. 2008. New evidence on the evolution of the Cue–Meekatharra area of the Murchison Domain, Yilgarn Craton. Geological Survey of Western Australia, Perth, 39-49.

VAN KRANENDONK, M. & IVANIC, T. 2009. A new lithostratigraphic scheme for the northeastern Murchison Domain, Yilgarn Craton. Geological Survey of Western Australia, Perth, 35-53.

VAN KRANENDONK, M. J., IVANIC, T. J., WINGATE, M. T., KIRKLAND, C. L. & WYCHE, S. 2013. Long-lived, autochthonous development of the Archean Murchison Domain, and implications for Yilgarn Craton tectonics. Precambrian Research, 229, 49-92.

WANG, L., MCNAUGHTON, N. & GROVES, D. 1993. An overview of the relationship between granitoid intrusions and gold mineralisation in the Archaean Murchison Province, Western Australia. Mineralium Deposita, 28, 482-494.

WANG, Q., SCHI∅ TTE, L. & CAMPBELL, I. 1998. Geochronology of supracrustal rocks from the Golden Grove area, Murchison Province, Yilgarn Craton, Western Australia∗. Australian Journal of Earth Sciences, 45, 571-577.

WEINBERG, R., SIAL, A. & MARIANO, G. 2004. Close spatial relationship between plutons and shear zones. Geology, 32, 377-380.

WILSON, C. 1975. Preferred orientation in quartz ribbon mylonites. Geological Society of America Bulletin, 86, 968-974.

ZIBRA, I. 2012. Syndeformational granite crystallisation along the Mount Magnet Greenstone Belt, Yilgarn Craton: evidence of large-scale magma-driven strain localisation during Neoarchean time. Australian Journal of Earth Sciences, 59, 793-806.

20. **Appendix**

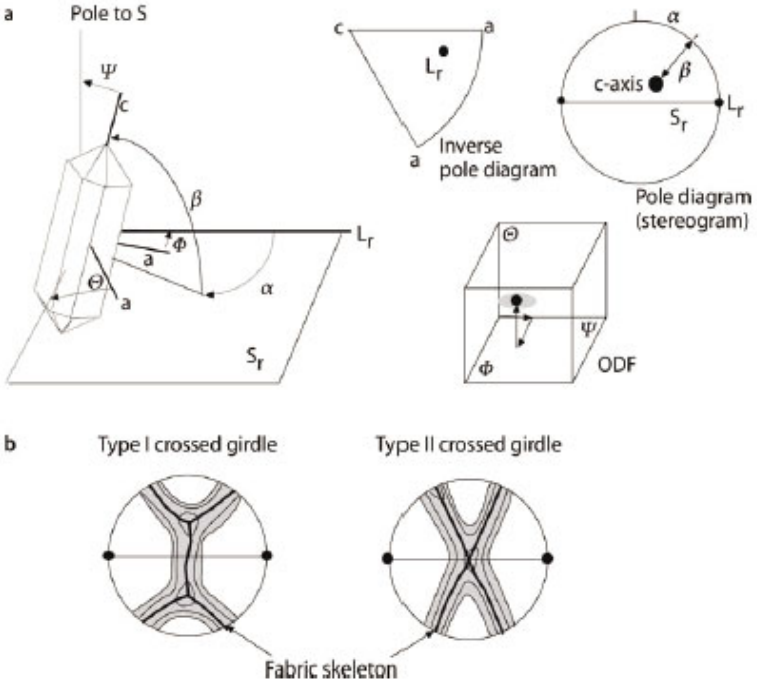

Fig. 4.40.
a Orientation of a quartz crystal in a reference frame defined by a foliation (S_r), lineation (L_r) and foliation pole. The full crystal orientation is given by Eulerian angles ϕ, ψ and θ. Orientation of the c-axis is given by angles α and β. Three diagrams that are commonly used to present LPO patterns are shown. In an ODF diagram the full orientation of the crystal is represented. In a pole diagram the orientation of individual axes of the crystal can be plotted; in this case, only the c-axis. In an inverse-pole diagram the orientation of L_r is plotted with respect to crystallographic axes. **b** Examples of pole diagrams with contours of pole density showing two types of crossed girdles (Lister 1977) of quartz c-axes. The shape of the girdles is highlighted by use of a fabric skeleton that traces the crests of the contour diagram

4.4.4
LPO Patterns of Quartz

4.4.4.1
Introduction

Figure 4.41 shows the influence of flow type and finite strain on the geometry of c-axis LPO patterns of quartz that accumulated by coaxial progressive deformation at low- to medium-grade metamorphic conditions (Tullis 1977; Lister and Hobbs 1980; Schmid and Casey 1986; Law 1990; Heilbronner and Tullis 2002; Takeshita et al. 1999; Okudaira et al. 1995). Small circle girdles are most common but in plane strain, small circle girdles are connected by a central girdle to produce Type I crossed girdles (Fig. 4.40b). Other c-axis LPO patterns that develop in coaxial progressive deformation are Type II crossed girdles, which seem to form in constriction (Fig. 4.40b; Bouchez 1978), and point maxima around the *Y*-axis of strain. Both patterns seem to form at higher temperature than the patterns shown in Fig. 4.41 (Schmid and Casey 1986; Law 1990). Increasing temperature also seems to cause an increase in the opening angle of the small circle girdles (Kruhl 1998).

In the case of non-coaxial progressive plane strain deformation, other c-axis patterns develop (Fig. 4.42) (Behrmann and Platt 1982; Bouchez et al. 1983; Platt and Behrmann 1986). Most common are slightly asymmetric Type I crossed girdles, and single girdles inclined to S_r and L_r (Burg and Laurent 1978; Lister and Hobbs 1980; Schmid and Casey 1986). At medium to high-grade conditions, single maxima around the *Y*-axis are common, while at high grade (>650 °C), point maxima in a direction close to the aggregate lineation L_r occur (Mainprice et al. 1986). c-axis patterns as shown in Figs. 4.41 and 42 represent only a small part of the full LPO of quartz and the orientation of other directions, such as <a>-axes, should also be known to allow interpretation of LPO development; in Figs. 4.41 and 4.42, patterns for <a>-axes are therefore shown beside c-axes. Nevertheless, c-axis patterns are most commonly represented in the literature since they can easily be measured on a U-stage; for other crystallographic directions more advanced equipment such as a goniometer (Sect. 10.3.5) is needed.

The patterns in Fig. 4.41 can be explained as an effect of the activity of slip planes in quartz; at conditions below 650 °C, slip in <a> directions on basal, prism and rhomb planes is dominant in quartz. As a result, <a>-axes tend to cluster close to planes and directions of maximum incremental shear strain (at 45° to ISA; Fig. 4.43a). In flattening, <a>-axes cluster in small circles around the shortening direction, similar to the situation in Fig. 4.39c. In constriction, a small circle girdle of <a>-axes around the extension direction forms and in plane strain there are two directions in the *XY*-plane. Slip on basal planes con-

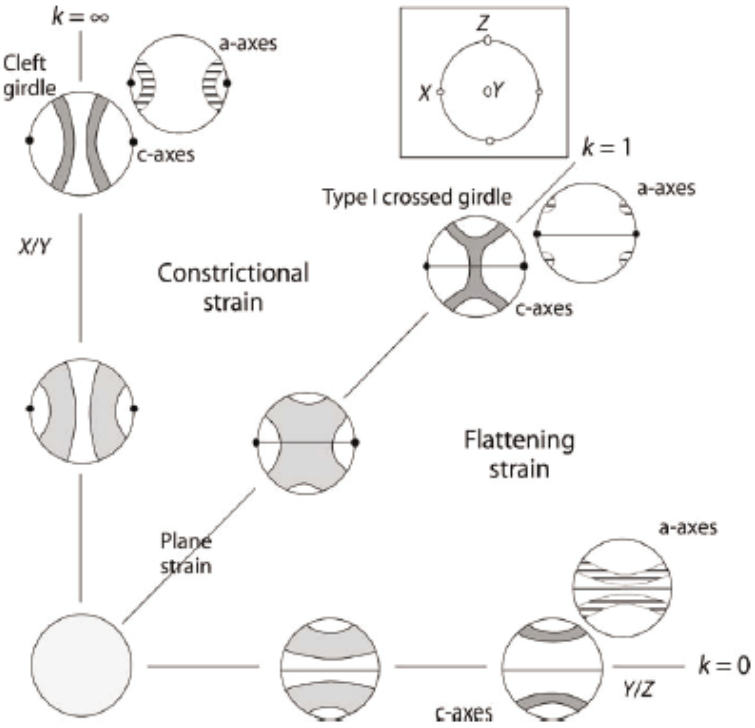

Fig. 4.41.
Flinn diagram showing the relation of geometry of LPO patterns of quartz c-axes (*grey contours*) and a-axes (*striped ornament*) with strain in the case of coaxial progressive deformation. An inset shows the orientation of principal strain axes in the pole diagrams. *Horizontal solid lines* in pole diagrams indicate reference foliation. *Dots* indicate reference lineation. (After Lister and Hobbs 1980)

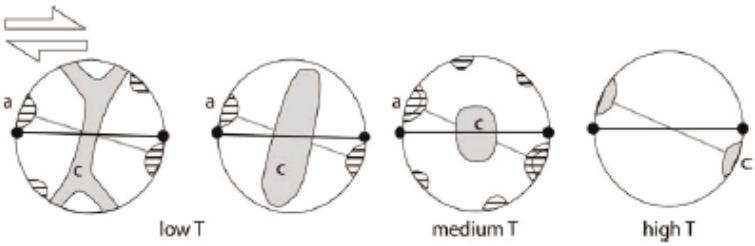

Fig. 4.42.
Pole diagrams showing four types of contoured LPO patterns of quartz c-axes (*grey*) and a-axes (*striped*) such as develop with increasing metamorphic grade in non-coaxial progressive deformation. The variation is due to a change in the dominant slip systems. Explanation in text

tributes mainly to c-axes in the periphery of the diagram, slip on prism planes to those in the centre, and slip on rhomb planes between both (Fig. 4.43a). Type II crossed-girdle c-axis patterns probably develop in constriction when rhomb slip is dominant over prism slip (Bouchez 1978; Schmid and Casey 1986).

In non-coaxial progressive deformation, domains of material line rotation are not of equal size as in coaxial progressive deformation (Sect. 2.7). As a result, one of the <a>-axes maxima is favoured and the c-axis patterns may be similar to those in Fig. 4.41 but one part will be better developed than the other. Consequently, the pattern of <a>- and c-axes obtains a monoclinic symmetry. For example, at high strain accumulated by simple shear at low to medium-grade metamorphic conditions, the Type I crossed girdle and double <a>-axes maxima are replaced by a single <a>-axes maximum parallel to the movement direction (the fabric attractor) and a single girdle of c-axes normal to the flow plane (Figs. 4.42, 4.43b; Sect. 2.9). The c-axes from the periphery to the centre of the girdle stem from c-axes of grains deformed by basal, rhomb and prism slip respectively (Fig. 4.43). At low temperature, basal <a> slip is most important and the girdles may have a strong cluster of c-axes in the periphery. With increasing temperature, prism <a> slip becomes more important (Wilson 1975; Bouchez 1977; Lister and Dornsiepen 1982; Law 1990) and the girdle tends to a maximum around the *Y*-axis (Figs. 4.42, 4.43b). At very high temperature and hydrous conditions, prism <c> slip operates (Lister and Dornsiepen 1982; Blumenfeld et al. 1985; Mainprice et al. 1986), and causes a c-axis maximum subparallel to the attractor (Figs. 4.42, 4.43), and <a> axes normal to it.

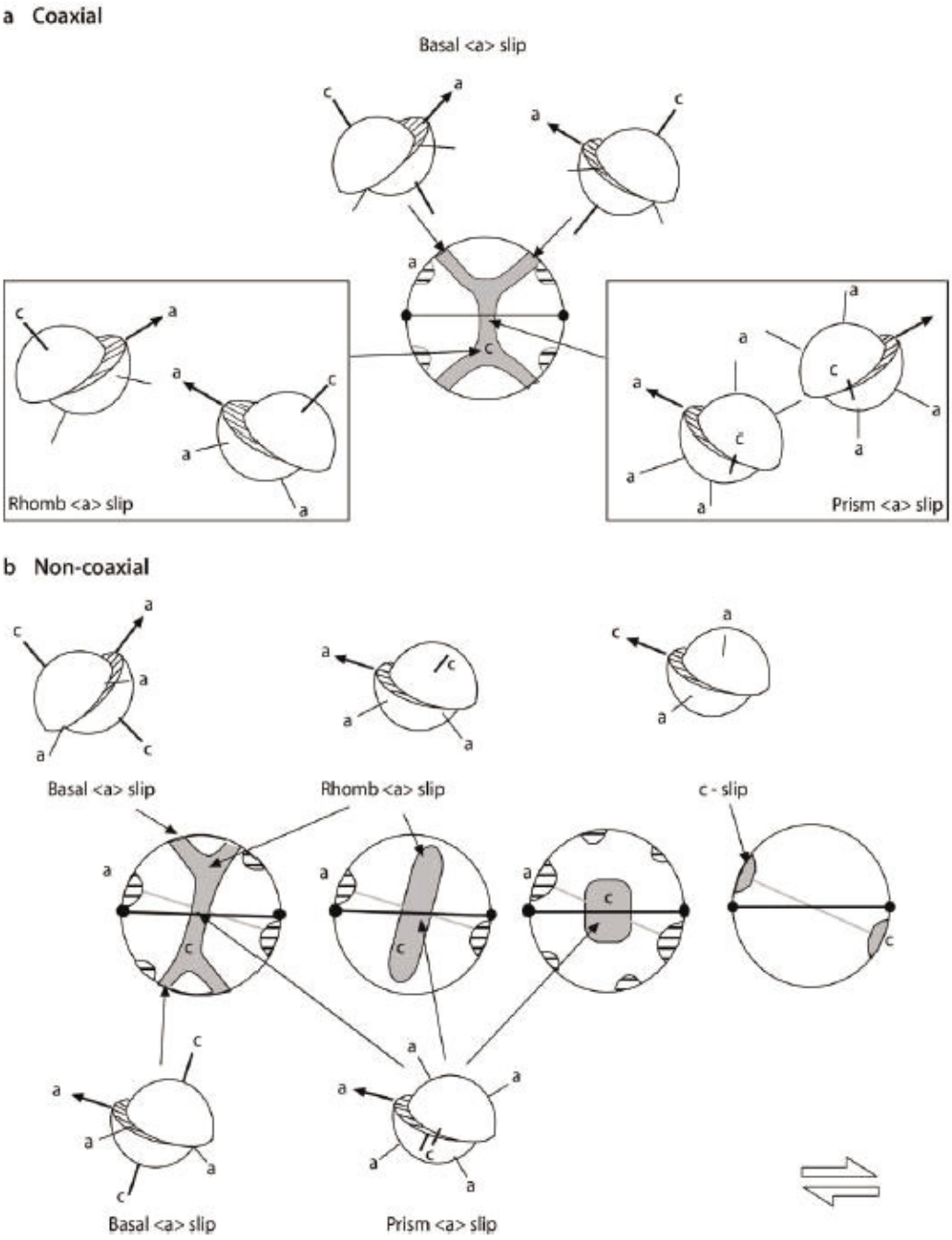

Fig. 4.43. a Illustration of the contribution of equidimensional quartz crystals with aligned <a>-axes and basal, rhomb or prism slip planes to a Type I crossed girdle pattern formed in coaxial progressive deformation. Ornamentation of contoured patterns of c- and a-axes in polar diagrams as in Fig. 4.42. **b** The same for several patterns that develop in non-coaxial progressive deformation. At *right* a pattern that developed by slip in direction of the c-axis

BIF Outcrop (low D)

S1	S2	Lic	F1	<--- Pole	F2	<--- Pole
335/70/E		58/082	320/72/E		022/89/E	
310/70/E		58/076	330/70/E		018/80/E	
338/60/E		72/070	335/78/E		022/82/E	
338/64/E		56/066	330/76/E		012/80/E	
320/58/E		50/082	342/70/E		028/90	
322/76/E		80/054	310/70/E		018/88/E	
334/80/E		78/072	320/60/E			
338/78/E			312/58/E			
328/82/E			308/62/E			
310/72/E			342/80/E			
320/78/E			330/80/E			
340/72/E			320/80/E			
332/78/E						

Meta Schist

S1	S2	Lc	F1	<--- Pole	F2	<--- Pole
152/62/E		50/024	001/80/W		300/40/E	60/010
130/60/E					308/60/E	20/020
140/80/E						
162/90						
146/78/E						
136/78/S						
154/82/W						
110/72/N						
342/62/E						
325/64/E						
318/62/E						
310/70/E						
350/58/E						
338/61/E						

Slatey Meta Peridotite

S1	S2	Lc	F1	<--- Pole	F2	<--- Pole	F3
334/72/E		326/18	352/66/E	68/346			
328/76/E			002/70/E	58/020			
346/80/E			328/80/E	60/312			
332/82/E							
326/80/E							
322/90							
334/78/E							

342/72/E							
332/90							

Meta Basalt L tectonite

S1	S2	Lc	CP	Lic	L1	L2	Lm
328/75/E				030/72/E	57/108		
340/72/E				025/65/E	60/110		
320/70/E				010/70/E	62/104		
330/74/E				028/68/E	54/092		
328/75/E				025/72/E	64/112		
342/68/E				032/70/E	66/111		
326/60/E				026/66/E	60/118		
334/72/E				018/74/E	55/098		
342/70/E							

L Tectonite (biotite lineation dominant) Southern most outcrop Warox 12

S1	S2	Lc	CP	Lic	L1	L2	Lm
355/58/E					60/070		
002/78/E					55/068		
060/70/S					65/047		
346/58/E					60/070		
006/60/E					68/065		
					70/116		
					58/080		
					52/090		
					55/074		

LLS Tectonite (biotite lineation dominant) Warox 11

Enclave	S1	Leco Dyke	Shear	L1	Qrtz Vein with Fe inclusions	
067/77/E	018/64/SE	105/70/N	→162	70/116	120/90	
	020/69/SE	088/68/N		60/090	Brittle Deformation	Obliangle
	010/66/SE	080/74/N		75/100	055/90	120/90
	355/70/E	100/72/N		72/096		
	002/74/E	100/65/N		62/102		
	012/65/E	082/62/N		62/098		
	334/62/E	150/70/N		73/112		
	024/54/SE	088/80/N		74/085		
	356/60/SE	087/75/N		68/115		
	158/62/E	100/72/N		64/112		
		100/65/N		68/108		
		120/70/N		70/085		
		128/68/N		70/061		
		122/72/E		62/116		
		150/72/N		50/268		
		157/68/E		50/056		
		180/70/E		48/068		
		190/72/E		56/090		
		192/80/E		62/089		
		190/72/E		68/100		
		178/82/E		60/088		
		156/78/E		64/062		
		294/55/S				

LS Tectonite (biotite foliation becoming dominant) Warox 38 & 39

S1	L1	Leco Dyke	Shear	Brittle Deformation	Oblique angle
338/52/E	70/105	130/50/E	070/82/S	030/90	120 deg
310/50/E	60/110	180/60/E	065/62/N	325/50/E	030/75/W
340/60/E	50/100	045/58/E			
038/82/E	55/102				
342/70/E	50/060				
314/50/E	60/068				
320/55/E	58/070				
334/58/E	54/062				
326/60/E	55/080				
344/58/E	45/086				
340/50/E	50/090				

SSL Tectonite (biotite foliation dominant) Warox 52 & 53

S1	L1	Leco Dyke	Shear
354/52/E	60/070		
356/55/E	62/075		
340/50/E	60/110		
339/60/E	61/080		
352/62/E	65/102		
360/50/E	58/095		
348/55/E	62/092		
345/58/E	64/107		
350/60/E	60/112		

SSL Tectonite (biotite foliation dominant) Warox 58 & 61

S1	L1	Leco Dyke	Fine Dyke	Med Dyke	Shear
338/48/E		078/80/S	170/50/E	118/85/N	062/82/SE
330/60/E				105/78/N	030/75/E
					358/70/E

Area of 3 distinct units over 300m. Warox 48

Area 1	338/60/E
Area 2	342/40/E
Area 3	324/50/E

RECORD 2015/4

TECTONITE TYPE: THEIR FORMATION AND SIGNIFICANCE, MAP PRODUCTION, FIELD RELATIONSHIPS AND PETROGRAPHY

This Record is published in digital format (PDF) and is available as a free download from the DMP website at <www.dmp.wa.gov.au/GSWApublications>.

Further details of geological products produced by the Geological Survey of Western Australia can be obtained by contacting:

Information Centre
Department of Mines and Petroleum
100 Plain Street
EAST PERTH WESTERN AUSTRALIA 6004
Phone: +61 8 9222 3459 Fax: +61 8 9222 3444
www.dmp.wa.gov.au/GSWApublications

Tomkins